THERMALLY INDUCED

CONFORMATIONAL TRANSITIONS

IN

MYOGLOBIN

BY

FAWWAZ H. JUMAYAN

submitted in partial fulfilment of the requirements

for the degree of Master of Science

in the Department of Chemistry

American University of Beirut

Beirut, Lebanon

June 1966

THERMALLY INDUCED

CONFORMATIONAL TRANSITIONS

IN

MYOGLOBIN

BY

FAWWAZ H. JUMAYAN

ACKNOWLEDGMENT

The author wishes to thank Dr. E. S. Awad for his guidance throughout this work and for his many helpful suggestions and ideas.

This work was supported in part by a grant from the National Institute of Health HE 04994 Bethesda, Md., U.S.A.

Figures 1 - 6 are taken from the literature for purposes of clarifying the presentation of this work.

ABSTRACT

The effect of heat on sperm whale ferrimyoglobin was studied spectrophotometrically in the temperature range 40 - 85°C (pH = 6.87, I = 0.100, (Mb) $\sim 10^{-5}$ M). Ultraviolet and visible difference spectra of thermally treated against native solutions were obtained (a) after re-equilibration at 25°C, and (b) at the elevated temperatures. The difference spectrum had a peak at 240 mμ and a plateau at 455 - 490 mμ, but the spectral profiles of the denatured states closely resembled the native form. Equilibrium values of the difference spectra were attained. The kinetics of the thermal transitions, followed at 280, 430 and 460 mμ, were complex, although the initial slopes were zero order. The Arrhenius plots for data taken at 280 and 430 mμ were linear, from which activation values were calculated. The transitions for 460 mμ did not obey the Arrhenius law. The variation of the equilibrium absorbance increments with temperature indicated two transitions for data taken at both 280 and 430 mμ and three transitions for 460 mμ. The van't Hoff plots were linear in each transition region, leading to the thermodynamic values.

The native molecule is shown to be very highly ordered with respect to the unfolded molecule, the high order being maintained largely by side-chain hydrogen bonds.

TABLE OF CONTENTS

	Page
CHAPTER I - INTRODUCTION	1
CHAPTER II - THEORETICAL ASPECTS OF THERMAL DENATURATION	5
A. Conformational Changes of Proteins	5
B. Factors that Maintain the Native Structure of Proteins	13
C. Kinetics and Thermodynamics	21
D. Review of Some Experimental Techniques	38
CHAPTER III - EXPERIMENTAL	44
1. Materials	44
2. Methods	45
CHAPTER IV - RESULTS	51
A. Heating and cooling Experiments	51
B. Spectral Recordings at Elevated Temperatures	65
C. Kinetics and Thermodynamics	77
CHAPTER V - DISCUSSION	100
A. Spectral Changes	100
B. Kinetic Behaviour	102
C. Thermodynamic Behaviour	105
LIST OF REFERENCES	111

LIST OF TABLES

Page

Table I - Absorbance Increments in the 240 - 300 mμ Region 52

Table II - Percentage Increments in Absorbance after 20 min. Heating, for Several Temperatures 55

Table III - Absorbance Increments in the 500 - 650 mμ Region 62

Table IV - Equilibrium Absorbance Increments at Several Wavelengths for Several Temperatures 74

Table V - Kinetic Data (for Arrhenius Plot) 85

Table VI - Activation Values at 280 and 430 mμ 88

Table VII - Thermodynamic Data (for van't Hoff plot) 94

Table VIII - Thermodynamic Values at 280, 430 and 460 mμ 99

Table IX - Theoretical Transition Parameters 107

LIST OF FIGURES

Page

Fig. 1 - Left and right-handed α-helices (Pauling, 1960) 8

Fig. 2 - Atomic model of whale myoglobin (Kendrew et al, 1961) .. 11

Fig. 3 - Several hydrogen bonding situations (Laskowski and Scheraga, 1954) 16

Fig. 4 - A model for thermal denaturation (Scheraga, 1960) 24

Fig. 5 - Dependence of k_F on pH and temperature for the denaturation of ricin (Levy and Bengalia, 1950) 27

Fig. 6 - Reciprocal scattering envelope of native and thermally denatured collagen 42

Fig. 7 - Diagram of the rapid-heating device 48

Fig. 8 - Absorbance as a function of temperature for the chemical system of Chapter III, Part C. 50

Fig. 9 - Difference spectra (240 - 300 mμ) taken at room temperature 56

Fig. 10 - Spectra (240 - 300 mμ) of native and thermally denatured solutions 57

Fig. 11 - Spectra (400 - 430 mμ) of native and thermally denatured solutions 59

Fig. 12 - Difference spectra (500 - 650 mμ) taken at room temperature 60

Fig. 13 - Spectra (500 - 650 mμ) of native and thermally denatured solutions 64

Page

Fig. 14 - Difference spectra (230 - 350 mμ) taken at the elevated temperature 66

Fig. 15 - Difference spectra (350 - 550 mμ) taken at the elevated temperature 67

Fig. 16 - Difference spectra (550 - 750 mμ) taken at the elevated temperature 68

Fig. 17 - Progress curves at 460 mμ (Part B experimental recordings) 69

Fig. 18 - Equilibrium difference spectra (230 - 350 mμ) 70

Fig. 19 - Equilibrium difference spectra (350 - 550 mμ) 71

Fig. 20 - Equilibrium difference spectra (550 - 750 mμ) 72

Fig. 21 - Plot of ΔA_{eq} as a function of temperature at 240 and 460 mμ 73

Fig. 22 - Plot of ($\Delta A_{eq}/A$) 100 as function of wavelength 76

Fig. 23 - Progress curves at 460 mμ (Part C experimental recordings) 78

Fig. 24 - Plot of the logarithm of the initial rate against the logarithm of myoglobin concentration 80

Fig. 25 - Initial slopes as a function of temperatures for data taken at 280, 430 and 460 mμ 81

Fig. 26 - Plot of log k_F versus 1/T for the transitions as followed at 280 mμ 82

Fig. 27 - Plot of log k_F versus 1/T for the transitions as followed at 430 mμ 83

Page

Fig. 28 - Plot of log k_F versus 1/T for the transitions as followed at 460 mμ 84

Fig. 29 - Dependence of ΔA_{eq} on temperature for the transitions followed at 280 mμ 90

Fig. 30 - Dependence of ΔA_{eq} on temperature for the transitions followed at 430 mμ 91

Fig. 31 - Dependence of ΔA_{eq} on temperature for the transitions followed at 460 mμ 92

Fig. 32 - Plot of log K_{eq} versus 1/T for the transitions followed at 280, 430 and 460 mμ 98

LIST OF SYMBOLS

A	Absorbance
ΔA	Absorbance increment
A_{eq}	Equilibrium absorbance
ΔA_{eq}	Equilibrium absorbance increment
$\Delta A_{t_{(n)}}$	Equilibrium absorbance increment for the nth transition at temperature t
$\Delta A_{t_{\infty}{}_{(n)}}$	Equilibrium absorbance increment for the nth transition at infinite temperature
C_D	Concentration of denatured species
C_N	Concentration of native species
ΔF^{o}_{obs}	Observed free energy change
ΔF^{o}_{unf}	Standard free energy change for unfolding
ΔF^{o}_{b}	Standard free energy change for unfolding of the helical backbone
ΔF^{o}_{h}	Standard free energy change for unfolding of side-chain hydrogen bonds
$\Delta F^{o}_{H\phi}$	Standard free energy change for unfolding of side-chain hydrophobic bonds
ΔF^{o}_{res}	Standard free energy change per residue
ΔH^{o}_{obs}	Observed standard enthalpy change
ΔH^{o}_{unf}	Standard enthalpy of unfolding

ΔH^0_h	Standard enthalpy change for the unfolding of side-chain hydrogen bonds
ΔH^0_{res}	Standard enthalpy change per residue
I	Ionic strength (M)
k_F	Forward rate constant for denaturation
K_n	Equilibrium constant for the nth transition
Mb	Myoglobin molecule
ΔS^0_{obs}	Net standard entropy change.
ΔS^0_{unf}	Standard entropy of unfolding
ΔS^0_h	Standard entropy of unfolding of side-chain hydrogen bonds
ΔS^0_{res}	Standard entropy change per residue
ΔS^0_x	Standard entropy change due to cross-links
ΔS^0_{el}	Difference in entropy between isotropic coils and coils in solution
T_{tr}	Transition temperature
α	Fraction of molecules denatured

CHAPTER I

INTRODUCTION

The term protein denaturation will be used to denote a process, or sequence of processes, in which the native molecule undergoes a transition from an ordered to a disordered state. The transition is essentially conformational, involving spatial rearrangement of polypeptide chains, without any concomitant rupture of covalent bonds. Whereas the most perfectly ordered state is helical, the disordered state looks very much like a randomly coiled polymer. Hence, an alternate definition of denaturation would be a helix to random coil transformation.

Having defined denaturation as a conformational transition, we next need to consider the nature of the various forces that cooperatively maintain the native conformation, bearing in mind that it is the collapse of these forces that induces the transition. Since the ordered native conformation is improbable on account of the negative entropy requirement, then clearly these stabilizing forces must be quite significant. It is by now established that hydrogen bonds and hydrophobic bonds are by far the most generous contributors and will therefore be expected to be very influential in determining the rate and position of equilibrium of the transition. Indeed, the study of denaturation is capable of giving information about the strength,

number, and location of such bonds, thereby revealing certain intimate aspects of protein structure.

We are led to look at the properties of a protein that undergo a change upon denaturation and the experimental techniques used to detect them. Neurath et al (1944), Putnam (1953), and Kauzmann (1959) list a number of these properties which, for convenience, may be divided into two classes. The first class deals with the external envelope of the protein molecule and may be appropriately called shape properties. These may be studied by various hydrodynamic and radiation scattering techniques. The second class involves more specific changes, such as exposure of certain chromophoric groups or loss of biological activity. For this reason, the term short range properties is applied. It is important to realize that a comprehensive study of denaturation requires observing many of these properties, since each is capable of yielding information of a specific type. We shall examine the particular usefulness of some techniques in a later section.

One of the most informative and convenient techniques in following denaturation is by observing the changes in optical density. In their highly compact native configurations, proteins normally absorb less than in the flexible open chains and much less than the individual amino-acids. This behaviour may be readily explained on the basis that, in the native state, several chromophoric functional groups are either trapped by their involvement in hydrogen bonding or masked inside the helix. Upon denaturation, these groups become more exposed and hydrogen bonds rupture so that their absorbance approaches that of the completely

free state. Furthermore, since the native molecule is ordinarily compact, one cannot ignore the possibility of existence of certain interactions that influence the spectral pattern, for example the π-bond overlap between adjoining aromatic groups, which may even lead to the creation of an essentially new electronic species with an absorbance spectrum characterizing the whole molecule (Michaelson, 1958). Denaturation is very likely to weaken such interactions or, at least, modify them in some way, thereby producing differences in the absorptive behaviour.

Proteins, in general, have only marginal stability. It is perhaps for this reason that one encounters a great diversity of denaturing agents. These appear to act by competing for stabilizing bonds, such as hydrogen bonds, or by providing sufficient energy to rupture them. Their action is therefore ordinarily cooperative. For example, thermal denaturation can be greatly accelerated by increasing the concentration of hydrogen ions. Some of these agents, according to the classification of Neurath *et al.* (1944), are:

1. Physical agents:

a) Heat (b) freezing (c) sound waves (d) surface forces (e) pressure (f) grinding (g) ultraviolet irradiation (h) ionizing irradiation (i) shaking.

2. Chemical agents:

a) Hydrogen and Hydroxyl ions (b) organic solvents (acetone, alcohols, etc..) (c) organic solutes, e.g. amides and related compounds (urea, formamide, guanidium ion, etc..) (d) detergents.

3. Biological agents:

Enzymes.

To a molecular biologist, the phenomenon of denaturation is of interest because, by yielding detailed information about protein structure, it can aid him in correlating chemical structure with biochemical function. To a physical chemist, the phenomenon merits study for its own sake. This is because of the unusual and often intriguing chemical behaviour that accompanies denaturation, for example extremely high energies and entropies of activation and marked sensitivity of reaction order and rate to temperature, pH, and not infrequently protein and water concentrations. Furthermore, the transition from the native to the denatured state is usually quite abrupt.

It is the purpose of this study to report on the influence of heat on myoglobin, using the increase in optical density as a criterion for following the thermal denaturation. The results are then discussed in terms of the known aspects of myoglobin structure.

CHAPTER II

THEORETICAL ASPECTS OF THERMAL DENATURATION

In this chapter the phenomenon of thermal denaturation will be examined in terms of structure and the forces that maintain it. Next, the kinetics and thermodynamics of thermal transitions will be dealt with in some detail. Finally, a few examples of practical and theoretical interest will be cited from the literature.

A. Conformational Changes of Proteins

It has been said that a general theory of protein denaturation is essentially a general theory of protein structure. This is because denaturation is accompanied by numerous measurable changes, each capable of elucidating some kind of structural detail. It is therefore necessary to outline the major features of the structure of native proteins and the modifications that can be brought about by denaturation.

Linderstrøm-Lang (1952) has proposed three types of structure in proteins:

1. Primary Structure is the nature and organization of covalent bonds and therefore may be expressed simply by the structural chemical formula of classical Organic Chemistry. The peptide linkage is one outstanding feature of this structure. In general, the bonds involved here are stronger than 40 Kcal. per mole. The C-N bond strength is

about 60 Kcal. per mole. Ordinary denaturing agents are too mild to break such bonds and hence no loss in the molecular weight of the protein is normally observed in denaturation. McLaren and Pearson (1949) have demonstrated that ultraviolet and ionizing radiation break, or at least weaken, primary bonds; but then the structure of the native protein has enough compactness to preclude the possibility of re-organization or reaction at the broken sites.

Elliott (1952) has established an important source of weakness in the primary structure of proteins containing serine and threonine residues. Here, at pH about 3, acyl shifts of the type

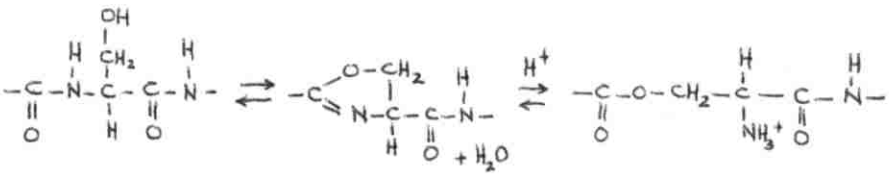

were observed in model compounds. This internal rearrangement increases the chain length by one bond and introduces an easily hydrolyzable ester linkage. Similar N → S shifts are possible but seem to be unfavoured energetically (Lumry and Eyring, 1954).

Covalent cross-links between peptide chains enhance the stability of the gross native structure. These links may be naturally occuring (e.g. disulphide bonds) or artificially introduced (e.g. the methylene bridges between amino groups introduced by tanning with formaldehyde). In most denaturation reactions, these linkages remain intact and limit, therefore, the number of configurations available for the random coil.

2. Secondary Structure arises by virtue of the folding of peptide

chains in the form of an α-helix maintained largely by hydrogen bonds. These bonds are produced by the sharing of hydrogen atoms between the nitrogen and carboxyl oxygen of the same or different polypeptide chains. The α-helices may be right handed or left-handed. A characteristic feature of the α-helix is its very low degree of flexibility. Fig. 1., taken from Pauling (1960), illustrates well the foregoing statements. There are 3.6 aminoacid residues per 360° turn and a 5.4 Å pitch. Consequently, the rise per residue is 1.5 Å and the rotation per residue is 100°. A distance of 5.1 Å separates tipped planes of the helix. The C_{α} carbon atoms are at a distance of 2 - 3 Å from the axis. The hydrogen bonds, 2.8 Å in length, nearly linear, and parallel to the axis, hold the structure together. Five complete turns yield an integral number ($5 \times 3.6 = 18$) of residues and therefore an identical repeat occurs every $5 \times 5.4 = 27$ Å along the helical axis. (Pauling 1960).

If the helix is extended, the rise per aminoacid residue will be 3.6 Å, as compared to 1.5 Å in the native form. If, according to Scheraga (1961), L_m is defined as the maximum length the fibre can have and L_{α} as the length in the α-helix, then $L_{\alpha}/L_m = 0.41$. Flory (1956) derived from statistical mechanical theory, the following expression for the length of a random coil, L_{RC}

$$L_{RC}/L_m = 1/\sqrt{n'} \qquad (1)$$

where n' is the number of statistical elements in the equivalent statistical chain. Scheraga (1961), making certain appropriate assumptions, replaced n' by $n/2$, where n is the number of aminoacid residues. He obtained

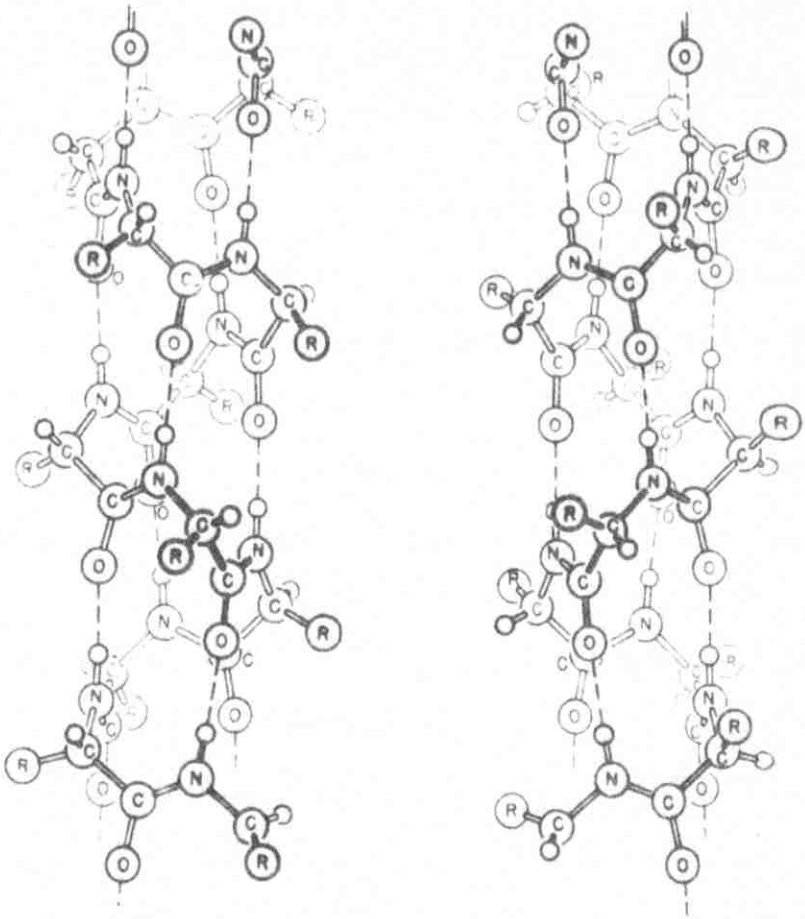

Fig. 1 - Left- and right-handed α-helices composed of L-aminoacids. The right-handed version to the right is theoretically more stable and has been found to occur naturally. (Pauling, 1960).

$$L_{RC}/L_m = 1.4/\sqrt{n} \qquad (2)$$

and, since $L_m = L_\alpha/0.41$

$$L_{RC}/L_\alpha = 3.4/\sqrt{n} \qquad (3)$$

By use of these equations one may calculate the percentage shrinkage in any given helix upon its transformation to a random coil.

3. Tertiary Structure refers to the spatial arrangement of the secondary structures. It is largely maintained by side-chain hydrogen and hydrophobic bonds, but backbone hydrogen bonds may participate as well. Covalent cross-links between adjoining polypeptide chains, such as the disulphide bond between two half-cystine residues, increase the degree of stability of the tertiary structure.

The tertiary structure is susceptible to examination by established methods in physical chemistry, such as X-ray diffraction and electron microscopy. There are two important connections between the secondary and tertiary structures: they mutually stabilize each other (Foss, 1961). Furthermore, a knowledge of the nature of side-chain interactions is of considerable aid in determining the secondary structure (Scheraga, 1961). If such specific interactions can be demonstrated experimentally, certain postulated structures may be rejected in favour of others.

The following two examples illustrate the tertiary structure. In collagen the three polypeptide chains intertwine in a slowly winding triple helix (Crick and Kendrew, 1957). In hemoglobin, the four polypeptide chains lie in an irregular tetrahedral array, with the four heme groups in separate pockets near the apices.

Denaturation normally involves the collapse of the organized secondary and tertiary structures in favour of more random configurations. However, in the thermal denaturation of lysozyme (Foss, 1961), this collapse takes place in two distinct steps: the first, corresponding to the tertiary structure; the second, to the secondary structure.

Structure of the Myoglobin Molecule.

We now turn to examine the primary, secondary, and tertiary structures of myoglobin in its native state. Then, an attempt will be made to outline the probable conformational changes that accompany the thermal transition to the denatured state.

The structure of myoglobin is by now well-characterized. The protein has a molecular weight of 17,800, consists of a single polypeptide chain of 153 aminoacid residues (Edmundson, 1965) and an iron containing heme group. Kendrew et al (1958) reported the first successful three dimensional X-ray pattern of the molecule. A 6 Å resolution was achieved by deducing the phases of 400 reflections with spacings greater than 6 Å in the protein, and four isomorphous replacement derivatives. Later (Kendrew et al, 1961) this resolution was carried down to 2 Å and the phases of 10,000 reflections were deduced. This study gave the first direct view into the detailed protein structure (Fig. 2). The existence of α-helices was demonstrated by the presence of hollow cylindrical tubes in the straight portions of the chain. These tubes are helical, with an axial repeat of 5.4 Å, identical with that expected of an α-helix. A closer study reveals that all straight chains are right-handed α-helices. Of the 153 aminoacid residues, 118 are in helical

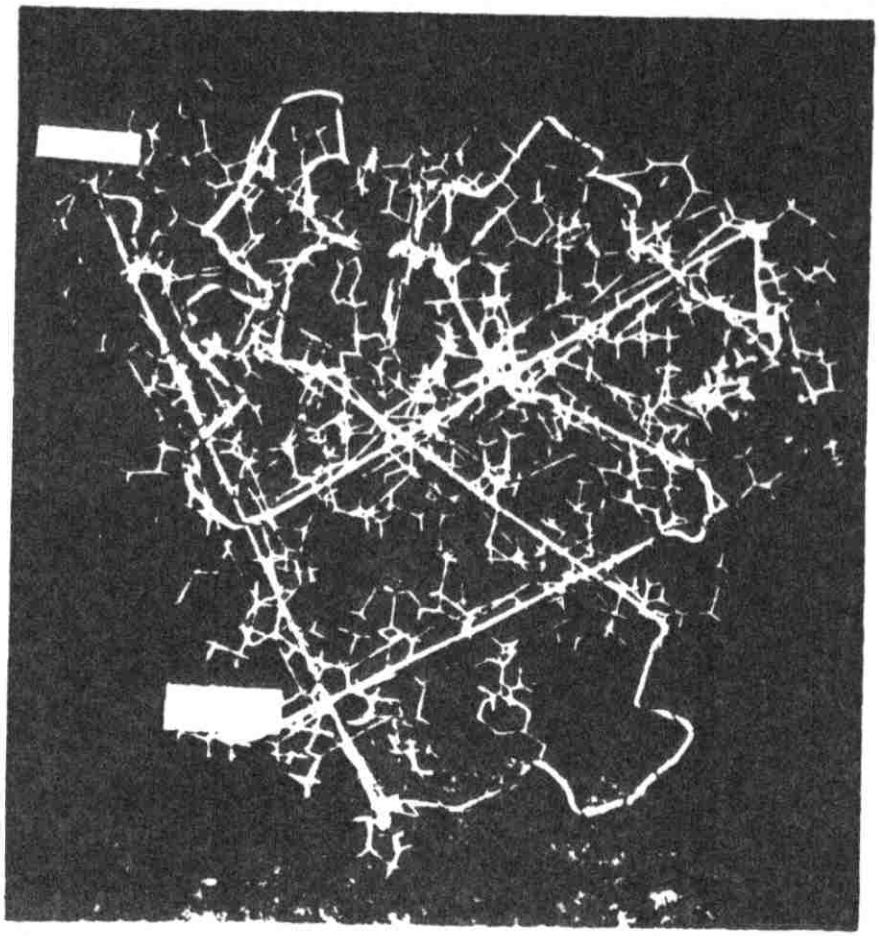

Fig. 2 - Atomic model of whale myoglobin at 2.0Å resolution. The course of peptide chains is marked by a thread. The straight segments represent right-handed α-helices. (Kendrew et al., 1961).

regions. There are eight such regions labelled alphabetically from A to H, containing 16, 16, 7, 10, 10, 19, 9 and 24 aminoacid residues. There are also eight non-helical regions, seven being interposed between helical regions and one at the carboxyl end of the chain. All helices are straight but helix E has a slight kink in the middle. All four proline residues are located at corners. Although covalent bond lengths are of the order of 1.5 Å, the 2 Å X-ray pattern has permitted the identification of many side-chain residues.

The study of Kendrew further revealed that the polar side-chain aminoacid residues are mainly directed toward the outside of the molecule, the non-polar toward the inside (from Braunitzer et al.(1964). The polar groups seem to interact with corresponding polar groups of the chain and of the solvent. According to Kendrew's estimate, the non-polar interactions between hydrophobic aminoacid residues are much greater than the polar interactions and therefore would appear to be of greater importance in stabilizing the structure. The molecule is very tightly packed, and it appears that there are fewer than 5 molecules of water trapped in the interior (Braunitzer et al., 1964). The structure in solution would therefore be expected to closely approximate that in the solid.

The heme group, located in a crevice 5 Å deep near the surface, is attached to a histidine residue oriented perpendicular to the porphyrin ring. The sixth coordination position is believed to be occupied by a water molecule. Polar propionic acid groups of the porphyrin lie near the exterior of the molecule, while non-polar vinyl groups are burried in the interior. The inner part of the heme group is surrounded by non-

polar side-chains and a number of aromatic side-chains lie in the surrounding volume. The heme group is therefore largely maintained by hydrophobic bonds.

In the thermal transition of the native myoglobin molecule to a more random configuration, several types of spectral perturbations may be expected to occur both in the ultraviolet and visible regions. The absorption spectrum of myoglobin between 250 and 310 mu is due to contributions from 6 phenylalanyl, 3 tyrosyl and 2 tryptophyl residues. Since these are aromatic side-groups they are, according to the previous discussion, more likely to be situated in the internal hydrophobic environment of the molecule where they can interact with each other and with other hydrophobic side-chains. Since hydrophobic interactions modify the spectrum of these groups (Wetlaufer, 1961) and considering that the random configuration is one in which most of the sites come into close contact with the polar solvent, a difference in absorbance may be expected on this account. Furthermore, a significant rise in absorbance is expected due to the unmasking of these groups in the coiled form. A similar line of argument may be applied to predict changes in the visible spectrum of heme.

B. Factors that Maintain the Native Conformations of Proteins

It was previously mentioned that the highly ordered conformations of native proteins are maintained by forces stronger than the natural tendency toward disorder. In this section, estimates of the strengths of these forces will be presented together with a description of some of their properties.

1. Hydrogen Bonds

Hydrogen bonding in proteins is essentially of two types: backbone hydrogen bonds between peptide linkages and side-chain hydrogen bonds. Whereas the first type serves to maintain the secondary structure, the second is involved in stabilizing the tertiary structure. Schellman (1955a), reported thermodynamic data for the formation of a peptide hydrogen bond in aqueous urea solutions. His assumptions were that deviations from ideality in this system are entirely due to the formation of aggregated species of urea and that aggregation is a result of hydrogen bonding between the amide and carbonyl groups. For the reaction

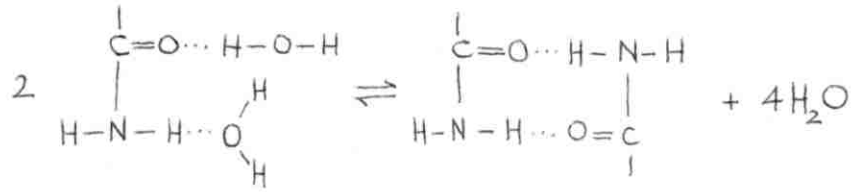

$K = 4.1 \times 10^{-2}$, $\Delta F = 1890$ cal/mole, $\Delta H = -2090$ cal/mole, and $\Delta S = -13.4$ e.u. These results led to the conclusion (Schellman, 1955b) that "hydrogen bonds, taken by themselves, give marginal stability to ordered structures, which may be enhanced or disrupted by interactions of side chains." Doubting the validity of Schellman's assumptions, Klotz (1960) investigated hydrogen bonding in aqueous N-methyl acetamide systems. He concluded that peptide hydrogen bonds are present only at very high concentrations of the amide. As the concentration of water is progressively increased, these bonds begin to rupture because of the stronger hydrogen bonding capacity of water. Intramolecular hydrogen bonds in

amides are, accordingly, intrinsically unstable. Despite all that, enough evidence for the formation of extensive hydrogen bonding in proteins in solution was obtained from the analysis of X-ray diffraction data and the presence of α-helical configurations (Rich and Crick, 1955). This suggests that other types of interactions are present and that they contribute cooperatively to maintain the native conformation.

Side-chain hydrogen bonds, especially OH....O bonds appear to have a larger negative heat of formation than backbone hydrogen bonds. Arguments supporting a value of -6,000 cal. per mole for the heat of formation of a side-chain hydrogen bond are presented by Laskowski and Scheraga (1961). The same authors (1956) have attempted to estimate the strengths of several types of side-chain hydrogen bonds. They considered four situations: 1) single bonds, (2) double bonds, (3) cooperative bonds, (4) competitive bonds. Both single and double bonds may be either heterologous or homologous. In heterologous bonds the participating groups are classicaly distinct whereas in homologous bonds they are chemically identical, the donor differing from the acceptor by the presence of an additional proton. Fig. 3, illustrates these types of bonding. The helix is an extreme type of cooperative bonding.

The strength of a hydrogen bond may be expressed in terms of the equilibrium constants K_{ij}, K_{lm} and K_{rs} for the formation of single, double and cooperative bonds, respectively. These are given by:

$$K_{ij} = \frac{P\ (DH \ldots\ldots A)}{P\ (DH, A)} \qquad (4)$$

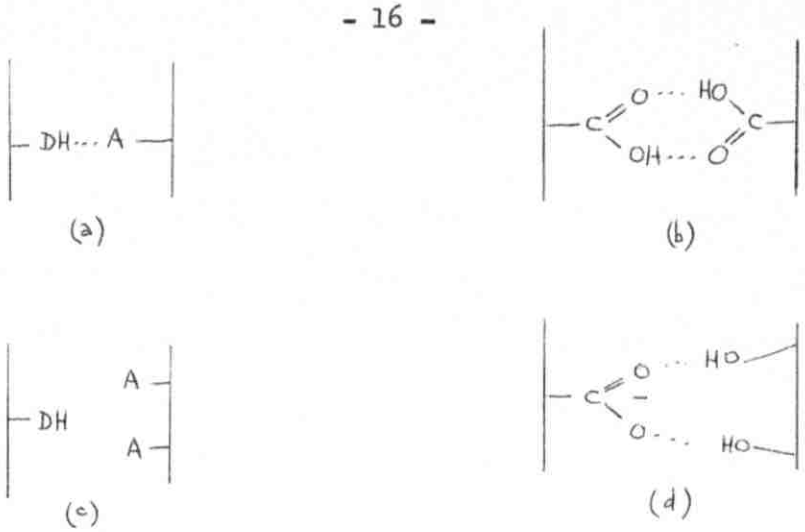

Fig. 3 - Several types of hydrogen bonding situations.
a) single heterologous bond (b) double homologous bond
c) competition (d) cooperation. (Laskowski and Scheraga, 1954).

$$K_{lm} = \frac{P\left(\begin{matrix} C(=O)\cdots O(H) \\ OH \cdots O=C \end{matrix}\right)}{P\left(C(=O)OH\ ,\ HO\,C(=O)\right)} \qquad (5)$$

$$K_{rs} = \frac{P\,(D_1H \cdots A \cdots HD_2)}{P\,(D_1H,\ A\ ,\ D_2H)} \qquad (6)$$

Rough estimates of the relative magnitudes of these constants yield

$K_{ij} \sim 1$, $K_{rs} \sim 10$, and $K_{lm} \sim 100$.

2. Hydrophobic Bonds

Hydrophobic bonds arise from the tendency of the apolar side-chains of proteins to cluster together and avoid the water phase. About 40% of the aminoacids in myoglobin contain apolar side-groups. Since such groups have a low affinity for water, then a conformation that brings a large number of them together will be more stable than another which requires their separation, other things being equal (Kauzmann, 1959). It is therefore expected that hydrophobic bonds in proteins, to a large measure in myoglobin, should play an important role in stabilizing the native configuration.

The nature of these bonds is essentially a theoretical question. Put in the words of Klotz (1960), it is "a question of which type of interaction observed in simple systems is an appropriate model for the interpretation of the interactions observed in macromolecular species." Up to the present date, no thermodynamic parameters are available for the formation of a hydrophobic bond between two nonpolar, side-chain groups in a protein. Most of the current interest centers around the thermodynamics of mixing of nonpolar solutes with water (Klotz, 1958, 1960; Kauzmann, 1959). Kauzmann has attempted to estimate some of the thermodynamic properties of hydrophobic bonds from literature values for the transfer of hydrocarbons, such as CH_4, C_2H_6 or C_6H_6 from an apolar solvent to water. His results may be summarized as follows:

1. The transfer of an apolar molecule from organic solvent to water is associated with a favorable energy change, ΔH being between 0 and -2 Kcal. per mole. Therefore, the stability of a hydrophobic bond increases with decreasing temperature.

2. The entropy of mixing is extremely unfavourable, ΔS is approximately -20 e.u. Hydrophobic bonds are therefore stabilized largely by entropy effects.

3. The free energy change in the transfer from water to a non-polar environment is exergonic to the extent of about 3 to 5 Kcal. per mole of groups at room temperature.

The large negative entropy change observed was first interpreted by Frank and Evans (1945). They postulated that when a non-polar molecule is present in water, the water molecules in the vicinity must arrange themselves into a quasi-crystalline structure in which there is less randomness and somewhat better hydrogen bonding than in ordinary liquid water at the same temperature. They called these structures 'icebergs'. These may, or may not, be similar to the structure of ice. That such 'icebergs' do exist was supported by the work of Frank and Wen (1957). These authors observed that the apparent molal heat capacity of tetra (n-butyl) ammonium bromide is much higher than expected from additivity rules. Their interpretation was that the extra heat is needed to melt the icebergs. Crystalline hydrates of this amine were later characterized by X-ray diffraction (McMullan and Jefrey, 1959).

There is some evidence in favour of the existence of icebergs in proteins. Klotz (1960) attributed the inaccessibility of some -SH groups in proteins to their participation with neighbouring side-chains in the formation of icebergs. Thus when the -SH group is titrated with Ag^+, the movement of the latter would be greatly hindered as compared to its movement in water. Schellman (1955) made some calculations on a 30

residue poly-D, L-alanine polypeptide, known to exist in the helical form in aqueous solutions. He concluded that this polypeptide should not exist in the helical form unless some added stability were acquired from another source. This source was assumed to be hydrophobic interactions between the side-chain methyl groups. Recently, Hartman (1966) from infrared and proton magnetic resonance studies, concluded that the stability of the secondary structures of ribonuclease is much more than expected. Another stabilizing factor must therefore be present. This factor is probably hydrophobic bonding.

From the foregoing, it would be expected that hydrophobic bonds would decrease the entropy and enthalpy of denaturation, as compared to the entropy and enthalpy that would be expected in the presence of hydrogen bonds alone.

3. Ionic Bonds

The electrostatic attraction between the positively charged amino and guanido groups and the negatively charged carboxyl groups may contribute to the stability of native proteins. Tanford (1954) measured the effect of ammonium and guanidium ions on the pH of acetate buffer and from the shifts in pH estimated the association constant for the reaction

$$NH_4^+ + {}^-OOCH_3 = NH_4^+{}^-OOCCH_3; \qquad K = 0.5.$$

Within the protein, where the dielectric constant should be less than in bulk water, this association constant ought to be larger. Kauzmann (1959) doubts the existence of ionic bonds on the grounds that added electrolytes do not act as denaturants. However, an indirect support

for their existence is obtained by the observation that, in the binding of organic molecules by proteins, the replacement of a charged substituent by an analogous uncharged one markedly decreases the extent of reaction (Klotz, 1946). The thermodynamic properties of ionic bonds are illustrated by the following example (Rossini, 1952):

$$\text{Acetate} + H_3O^+ \longrightarrow \text{acetic acid} + H_2O;\ \Delta H = 400 \text{ cal},\ \Delta S = 30.1 \text{ e.u.},\ \Delta V = 11 \text{ ml}.$$

Kauzmann (1959) attributes the large entropy effect to the disordering of water in the vicinity of the charged groups. His interpretation is that when these groups are separated, their electric fields compress and orient the surrounding water molecules; but when they are very close to each other the electric fields no longer penetrate extensively through water, so that much of the compression and orientation is relaxed.

4. Stabilization by Electron Delocalization

It has been suggested by Evans and Gegley (1949) that when the polypeptide chain is folded in certain ways electron delocalization is possible across the hydrogen bonds that join the peptide groups. They described the delocalization by means of the resonating forms

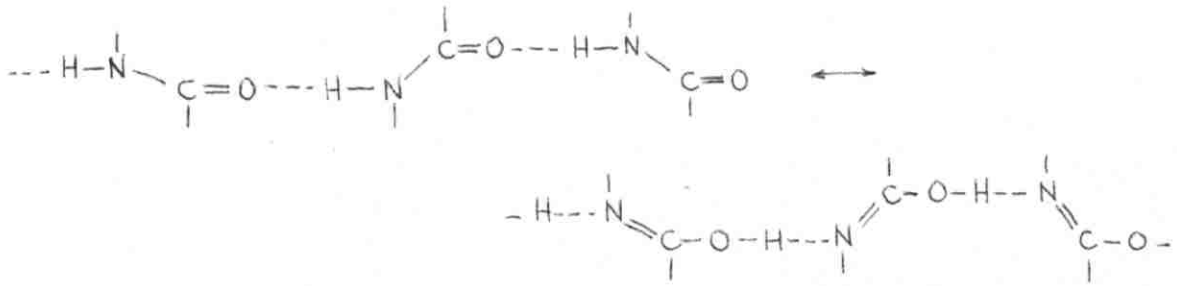

where the peptide groups may belong to the same or different polypeptide

chains. Using a molecular orbital approach, these authors have estimated the delocalization energies to lie between 500 and 1000 cal. per linear peptide link. However, the magnitude of average stabilization per peptide group is dependent on the number of peptide groups that are hydrogen bonded to one another, becoming larger as the number of groups is increased (Evans and Gegley, 1949). In an α-helix the axes of pi orbitals in a given peptide link are rotated by 65.4^{0} with respect to the axes of pi orbitals on the two peptide chains to which it is hydrogen bonded, so that the delocalization energy is reduced by a factor of $\cos 65.4 = 0.418$ (Kauzmann, 1959). This decrease should contribute slightly to the sharpening of the helix-coil transition (Hill, 1959).

C. Kinetics and Thermodynamics

1. Kinetics

Thermally induced helix-coil transitions are characterized by an abnormal kinetic behaviour. Very high entropies and enthalpies of activation are commonly encountered. Furthermore, the transition order may depend, frequently in a complex manner, on such factors as pH, temperature, and even protein concentration. Whereas the rates of ordinary chemical reactions double or triple with a 10^{0} rise in temperature, those of thermal denaturation may increase up to 600 fold within $2 - 3^{0}$ only. Such deviations from ordinary behaviour have attracted the attention of physical chemists and presented them with many challenging problems.

Some kinetic studies on specific denaturation reactions were performed by Laidler (1951), Gibbs et al. (1952), Haurowitz et al. (1952), Simpson and Kauzmann (1953), Kauzmann and Simpson (1953), Schellman et al. (1953), Frensdorff et al. (1953), Loeb and Scheraga (1961), Hermans and Scheraga (1961), Scott and Scheraga (1963).

In the present treatment, the kinetic behaviour will be approached by considering two theories: the transition state theory and the theory of order-disorder transitions.

a) Application of the Transition State Theory: In this theory the equilibrium constant K^* for the formation of the activated complex is expressed in terms of the free energy of activation in the standard state, ΔF^*.

$$\Delta F^* = -RT \ln K^* \qquad (7)$$

Since $\Delta F^* = \Delta H^* - T\,\Delta S^*$, where ΔH^* and ΔS^* are the enthalpy and entropy of activation respectively, then

$$K^* = e^{\frac{\Delta S^*}{R}} \; e^{-\frac{\Delta H^*}{RT}} \qquad (8)$$

The forward rate constant k_F, is related to K^* by the following equation

$$k_F = \frac{kT}{h} K^* \qquad (9)$$

where T is the absolute temperature, k is Boltzmann's constant, and h Planck's constant. The factor KT/h, is a universal frequency for the decomposition of the activated complex. A consequence of this theory is that both ΔH^* and ΔS^* affect the reaction rate.

Scheraga (1960) has presented a model for thermal denaturation,

shown in fig. 4, in which he treats the phenomenon as a crystalline to amorphous phase transition. The native protein is regarded as completely crystalline (Form C) and the denatured protein as completely amorphous (Form A). Form I is an intermediate in which all side-chain hydrogen bonds, are broken but backbone hydrogen bonds and covalent cross-links remain unaffected. The process of activation involves the simultaneous rupture of a critical number of side-chain hydrogen bonds. For practical purposes Scheraga regards the activated state simply as Form I. He envisages activation to take place in two steps:

1. As the temperature is increased, a stress is introduced in the native protein solution, and the molecules equilibrate instantaneously with the new environment. This equilibration may occur in several ways, for example, by ionization, rupture or formation of hydrogen bonds, binding of inorganic ions, etc.

2. Among the newly-equilibrated native molecules, there exists a small fraction of molecules of Form I, whose concentration is designated as C^*. This process takes a finite time, since C^* is very small and is replenished only when some molecules pass over the activation barrier.

In the native and activated states the helices are assumed to be held in rigid positions. After passing through the activation barrier, these helices aquire an ability to assume different positions relative to one another. Subsequent passage to the randomly coiled state proceeds at a rate depending on the free energy of activation for unwinding the free helix.

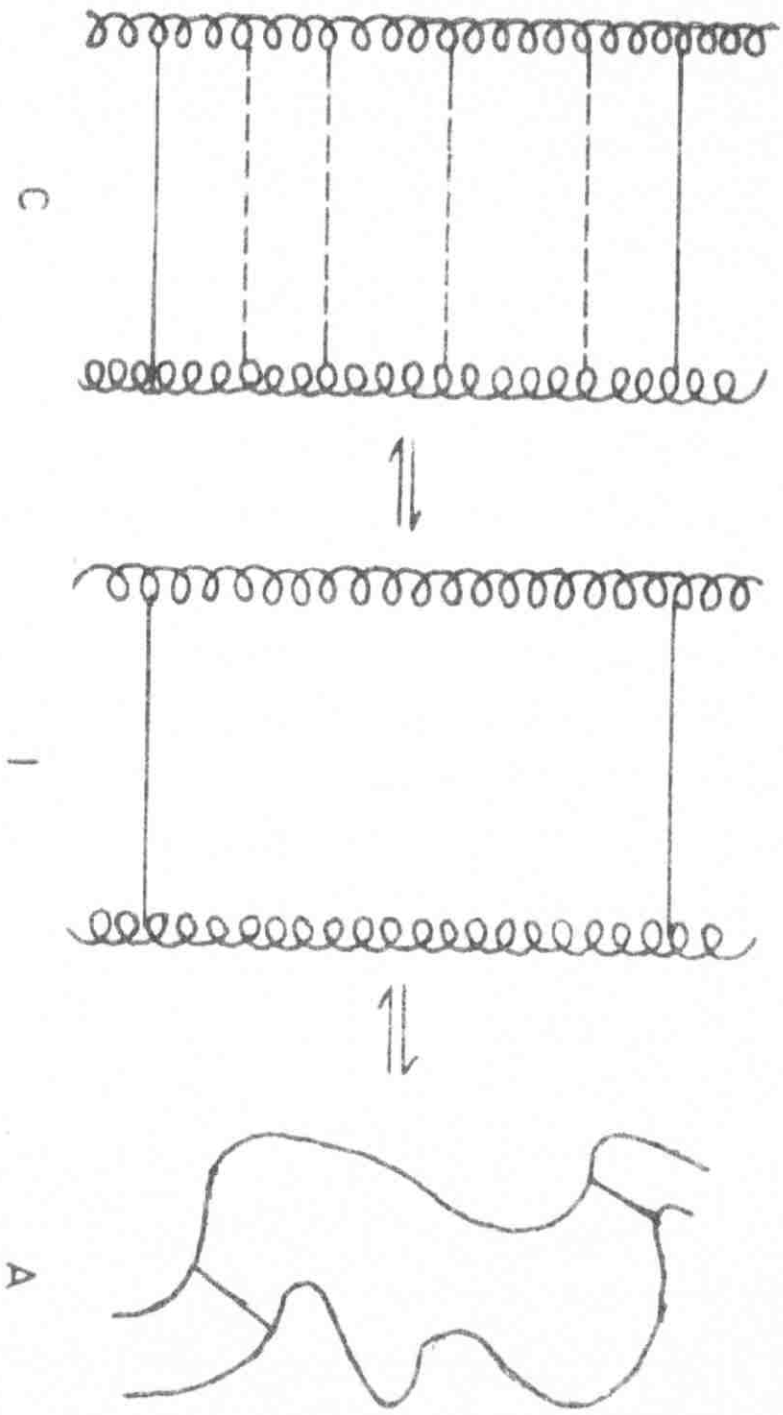

Fig. 4 - A model for thermal denaturation. Forms C, I, A are crystalline intermediate, and amorphous phases, respectively. (Scheraga, 1960).

By using equation (6)

$$\frac{dC_D}{dt} = -\frac{dC_N}{dt} = \left(\frac{kT}{h}\right) C^* \qquad (10)$$

where C_D and C_N are the concentrations of denatured and native protein, respectively.

Now C^* will be expressed in terms of the several types of hydrogen bonding formation constants introduced earlier in the chapter. If X_{ij}, X_{lm}, X_{rs} are taken as the fraction of molecules involved in single, double and cooperative bonds, respectively, then, at a pH intermediate between the pK's of the donor and acceptor groups (Laskowski and Scheraga, 1956)

$$X_{ij} = K_{ij}/(1 + K_{ij}); \quad X_{lm} = K_{lm}/(1 + K_{lm}); \quad X_{rs} = K_{rs}/(1 + K_{rs})$$

X_{ij}, X_{lm}, X_{rs} may be taken as the probabilities of existence of these three hydrogen bonded species. The probabilities for their absence are therefore given by $(1 - X_{ij})$, $(1 - X_{lm})$, and $(1 - X_{rs})$. If it is assumed that these species are independent, then the probability that all of them do not exist is given by the product of the individual probabilities for their absence. According to the model, this latter term is given by the fraction of activated species. Thus

$$C^* = C_N \overline{\prod} (1 - X_{ij}) \overline{\prod} (1 - X_{lm}) \overline{\prod} (1 - X_{rs}) \qquad (11)$$

and $$k_F = \frac{kT}{h} \overline{\prod} (1 - X_{ij}) \overline{\prod} (1 - X_{lm}) \overline{\prod} (1 - X_{rs}) \qquad (12)$$

where the products are taken over all kinds of hydrogen bonds.

Since X_{ij}, X_{rs}, X_{lm} are dependent on temperature and pH, the forward rate constants for denaturation should be dependent on the same variables.

Such a dependence is well illustrated in fig. 5, taken from Levy and Bengalia (1950). In this plot it is observed that in some pH regions the rate of denaturation is insensitive to pH. In these regions it may therefore be assumed that the X_{ij}'s, X_{rs}'s and K_{lm}'s are independent of pH.

If we limit ourselves to considering stabilization by one type of hydrogen bond, say X_{ij}, then since $X_{ij} = K_{ij}/(1 + K_{ij})$

$$k_F = \frac{kT}{h} \prod \frac{1}{1 + K_{ij}} \tag{13}$$

Furthermore, it can be shown (Laskowski and Scheraga, 1956) that

$$\Delta F^* = RT \sum \ln (1 + K_{ij}) \tag{14}$$

$$\Delta H^* = - \sum \frac{K_{ij}}{1 + K_{ij}} \cdot \Delta H^0_{ij} \tag{15}$$

$$\Delta S^* = -nR \sum \ln (1 + K_{ij}) - \frac{1}{T} \sum \frac{nK_{ij}}{1 + K_{ij}} \cdot \Delta H^0_{ij} \tag{16}$$

where ΔH^0_{ij} is the standard enthalpy of formation of the ijth hydrogen bond. Since K_{ij} is approximately 1 (page 16), these equations predict large positive values for ΔF^*, ΔH^* and ΔS^*.

According to Flory (1961), the helix-coil transition takes place in a sequence of steps, each consisting of the conversion of one unit at the junction between helical and random coil sequence of units.

$$H_n \underset{k_-}{\overset{k_i}{\rightleftharpoons}} H_{n-1}C_1 \underset{k_-}{\overset{k_+}{\rightleftharpoons}} H_{n-2} \underset{k_-}{\overset{k_+}{\rightleftharpoons}} \cdots\cdots H_1C_{n-1} \underset{k_i^*}{\overset{k_+}{\rightleftharpoons}} C_n$$

where $H_{n-i}C_i$ denotes the species comprising a sequence of $(n - i)$ helical

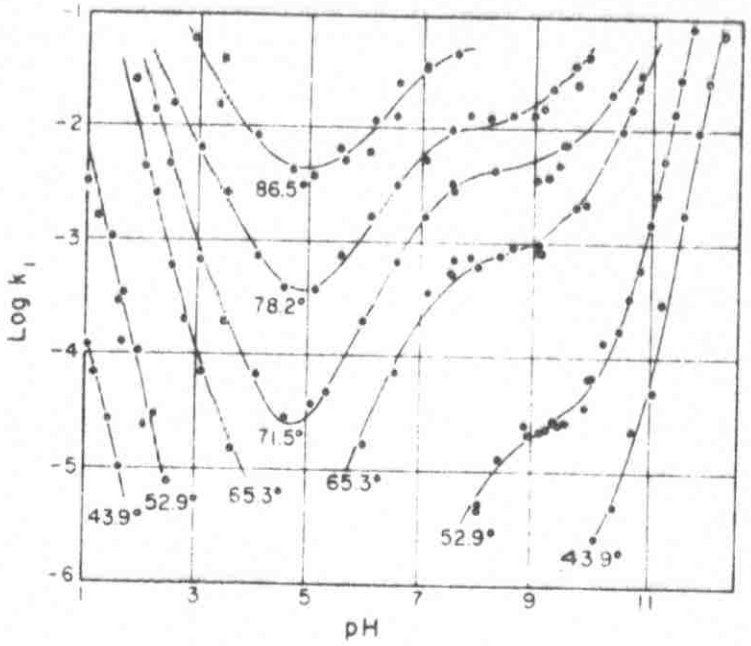

Fig. 5 - Dependence of the first order rate constant, k_1, on pH and temperature for the denaturation of ricin (Levy and Bengalia, 1950).

units adjoining a sequence of i disordered units. The rate constant for initiation is k_i, that for propagation is k_+, and the reverse rate constant is k_-. k_i is the rate constant for initiation of a random coil and k_i^* is that for the introduction of an incipient helix in a random coil chain. The rate of transformation may be equated to the rate of initiation multiplied by the expectation that the initially generated sequence will eventually envelope the whole molecule. The entire process may be likened to a one dimensional diffusion which is subject to a bias depending on the temperature relative to the melting temperature (page 37). The problem was treated by Flory (1961), using the solution to the gambler's ruin problem (Upensky, 1937). The situation may be illustrated as follows: If a gambler sets out with one stake and his opponent with n-1 stakes, then the probability y of ultimate success is determined by the ratio r of the probability of a win to the probability of a loss. In our case $r = \frac{k_+}{k_-}$ and

$$y = \left[\frac{r^n}{r^n - 1} \right] \left(1 - r^{-1} \right) \qquad (17)$$

If conditions were such that as the transformation is favoured, then $r > 1$. At the melting temperature $r = 1$ and near the melting temperature it is close to unity. If n is sufficiently large and at $r > 1$ we have

$$y = 1 - r^{-1} = r - 1$$

and the rate becomes

$$- \frac{dC_N}{dt} = k_i C_N \left[r^n / (r^n - 1) \right] \left(1 - r^{-1} \right) = k_i (r - 1) C_N \qquad (18)$$

Near the melting temperature, it can be shown that

$$-\frac{dC_N}{dt} = k_i C_N \frac{(\Delta H_u)}{RT^2} \cdot \Delta T \qquad (19)$$

where $\Delta T = T - T_m$ and ΔH_u is the enthalpy change per unit. In the immediate vicinity of T_m, the temperature coefficient will be dominated by ΔT, the change in k_i with temperature being less important.

b) Application of the Theory of Order - Disorder Transitions: Order - disorder phenomena belong to the class of cooperative phenomena. The theory was first applied to the study of simple alloys where various amounts of metal B were added to metal A. It was observed that long range order is still maintained as B atoms occupy definite positions in the crystal lattice of A. As the temperature is increased, sufficient energy is acquired by some atoms which makes them interchange positions in the super-lattice. The process is cooperative in the sense that a small fraction of atoms in the 'wrong' positions are enough to destroy the long range order within a narrow temperature range. A detailed description of this theory is given by Block (1956).

Colvin (1953) extended this theory to proteins, in an effort to interpret the unusual aspects of thermal denaturation. He made the assumptions that proteins have definite elements of structure, that they are large enough to be considered as microcrystals and that these crystals are well-ordered at low temperature. If these assumptions are valid, then the transformation of protein from a helical to a coiled configuration

requires an initial formation of very small coiled segments whose free energy of formation is given by

$$\Delta F_i = Ai^{2/3} + Bi + Ci \qquad (20)$$

where A is a positive constant, B is the bulk free energy difference between the completely helical and completely coiled states for a given temperature, C is a coefficient representing the increase in free energy and i is the number of elements in the coil. ΔF_i is related to the equilibrium number of incipient coils by the equation

$$\frac{n_i}{n} = e^{-\Delta F_i/kT} \qquad (21)$$

where n_i and n are the equilibrium number of species in the denatured and native states, respectively. Below the melting temperature, all terms in equation(20) are positive and all coiled modifications are stable. At the melting temperature B is zero but the formation of an 'embryo' coil still requires an increase in free energy. As the temperature increases B becomes negative and soon counter balances the effects of A and C, and coiled 'nuclei' begin to grow spontaneously. As a result, the rate of formation of these nuclei has an abnormally high temperature coefficient at the equilibrium point and long range order falls sharply to zero (completely coiled configuration) within 2 - 3^0.

In addition to interpreting the high temperature coefficient, this theory also successfully interprets the effects of pH and water on the rate. From equation (21), the transition rate should be an extremely sensitive

function of ΔF_i, which is in turn a strong function of electrostatic interactions in the helical form. In general, these will be least and therefore the helical form most stable, near the isoelectric point of the protein. Furthermore, rates of denaturation should increase very much in the presence of strong acid or alkali. Water, acting as a diluent, lowers the 'crystallization' temperature of the ordered form and therefore accelerates the transformation to the disordered form.

The striking features of this theory is that it requires degrees of denaturation and that a molecule undergoing the transition does not have to pass through an activated state.

2. Thermodynamics

For ease of presentation, the thermodynamic properties of thermal denaturation will be discussed individually. However, this division cannot be strictly followed as these properties are mutually interdependent.

a) Equilibrium Constants and Enthalpy: For the process

$$\text{Helix} \rightleftharpoons \text{Random coil}$$

the equilibrium constant, K, is given by (Flory, 1961)

$$K = (\omega_a / \omega_c)^x \qquad (22)$$

where ω_a and ω_c are the partition functions of the amorphous (random coil) and crystalline (helix) phases, respectively, and x is

the number of units in the chain. This equation applied to the case where the species involved are either entirely helical or randomly coiled throughout. When x is very large, the thermally induced helix-coil transition may be so sharp as to resemble a phase transition (Schellman, 1958). There are two important consequences of this behaviour. Provided x is large enough, the equilibrium constant changes very rapidly with temperature and the enthalpy change is large. When the chains are very long, it becomes improbable that the molecule exists either in a helical or a randomly coiled form. More elaborate theories are given by Peller (1959) and by Zimm and Bragg (1958, 1959).

To be able to attach any real significance to an enthalpy value, the initial and final states of the system must be well known. The native state of a protein is well characterized. However, a description of the denatured state, due to the many available conformations, has to be often provided by indirect means depending on the method of study.

The change in enthalpy may be determined calorimetrically (Kistiakowsky and Roberts, 1940); Conn et al., 1940; Buzzel and Sturtevant, 1951) or by measuring the temperature dependence of the equilibrium constant between helical and randomly coiled states. The van't Hoff equation

$$\frac{d \ln K}{d\left(\frac{1}{T}\right)} = \frac{\Delta H}{RT^2} \qquad (23)$$

is used for the latter purpose. Most measurements indicate that ΔH is typically of the order of 100 Kcal per mole, or more (Sturtevant, 1954).

Following the model of fig. 4, the total standard enthalpy change, ΔH^{0}_{obs}, is made up of two terms

$$\Delta H^{0}_{obs} = \Delta H^{0}_{unf} + \Delta H^{0}_{h} \qquad (24)$$

where ΔH^{0}_{unf} and ΔH^{0}_{h} are standard enthalpy changes for the $I \rightarrow A$ and $C \rightarrow I$ transformations, respectively. Since the side-chain hydrogen bonds, which stabilize Form C with respect to Form I, are sensitive to changes in pH, it is to be expected that ΔH^{0}_{h}, and consequently ΔH^{0}_{obs}, will also show a dependence on pH (Scheraga, 1960). Such a dependence is supported by several experimental results (Buzzel and Sturtevant, 1952; Loeb and Scheraga, 1961; Scott and Scheraga, 1963).

If, again, thermal denaturation is regarded as a crystalline to amorphous phase transition, then the crystallinity must disappear above a characteristic temperature at a given force. Flory (1956) derived a Clayperon-type equation which may be applied to the situation where the two phases coexist in equilibrium.

$$\left(\frac{\partial(f/T)}{\partial\left(\frac{1}{T}\right)}\right)_{p} = \frac{\Delta H}{\Delta L} \qquad (25)$$

where f is the tensile force acting in the direction of fibre length, L. ΔH and ΔL are the latest changes in enthalpy and length, respectively. p is the pressure.

b) <u>Entropy</u>: The entropy change accompanying denaturation may be obtained directly from the enthalpy change, using the relation

$$\frac{\Delta S}{R} = \ln K + \Delta H / RT \qquad (26)$$

The denatured protein commonly has a larger entropy than the native protein by several hundred entropy units. Available values are tabulated by Kauzmann (1954) and by Lumry and Eyring (1954).

Returning to the model of fig. 4, the net standard entropy change, ΔS^0_{obs}, is given by

$$\Delta S^0_{obs} = \Delta S^0_{unf} + \Delta S^0_h \qquad (27)$$

where ΔS^0_{unf} and ΔS^0_h refer to the $I \longrightarrow A$ and $C \longrightarrow I$ transformations, respectively.

Schellman (1955) formulated the following expression for the entropy change per residue, ΔS^0_{res}, for the unfolding of an infinitely long helix to an isotropic random coil.

$$\Delta S^0_{res} = \frac{(n-4)\ \Delta H^0_{res} - \Delta F^0_{unf}}{T\ (n-1)} \qquad (28)$$

in which n is the number of aminoacid residues.

If the random coil contains cross-links, then ΔS^0_{res} is reduced by an amount ΔS^0_x, given by (Flory, 1956)

$$\Delta S^0_x = - Rv \left[(3/4) \ln n' + 9/4 \right] \qquad (29)$$

where v is the number of polypeptide chains and n' is the number of statistical elements between cross-links. Furthermore, at the melting temperature, the amorphous chains are under a force sufficiently large to make the lengths of the amorphous and crystalline chains equal. This

requires that ΔS^{o}_{res} be further reduced by an amount ΔS^{o}_{el} given by (Flory, 1956)

$$\Delta S^{o}_{el} = -\frac{3Rv}{2}\left[n' \left(\frac{L^c}{L^m} \right)^2 - 1 \right] \qquad (30)$$

where L^c and L^m are the chain lengths in the crystalline and amorphous phases, respectively.

Kauzmann (1954) employed the Boltzmann relation

$$\Delta S = R \ln (C_2 / C_1) \qquad (31)$$

to account for the large entropy values of denaturation. ΔS is the entropy change which results when one mole of a substance undergoes a change from a state in which its molecules can have C_1 configurations to a state in which they can have C_2 configurations. For the rigid native protein C_1 may be taken as unity. If in the denatured molecule there are n single bonds each capable of twisting about p positions, then $C_2 = p^n$ and equation (31) becomes

$$\Delta S = nR \ln p \qquad (32)$$

In proteins n is very large and $p \longrightarrow 2$ in the most flexible coil, so that ΔS values may range between 200 and 2000 e.u.

c) <u>Free Energy and Transition Temperature</u>: The observed free energy change during denaturation, ΔF^{o}_{obs} is also given by

$$\Delta F^{o}_{obs} = \Delta F^{o}_{unf} + \Delta F^{o}_{h} \qquad (33)$$

where ΔF^{o}_{h}, the free energy change accompanying the rupture of side-

chain hydrogen bonds, is given by (Scheraga, 1960[a])

$$\Delta F^{0}_{h} = -RT \sum \ln (1 - X_{ij}) \qquad (34)$$

for single bonds of the ij type (see discussion on hydrogen bonds). Schellman (1955) ascribes ΔF^{0}_{unf} to several contributions

$$\Delta F^{0}_{unf} = \Delta F^{0}_{b} + \Delta F^{0}_{x} + \Delta F^{0}_{h} + \Delta F^{0}_{H\emptyset} + \Delta F_{comb} + \Delta F^{0}_{elec} + \ldots \qquad (35)$$

where

ΔF^{0}_{b} is the free energy to unfold the helix in the absence of side-chain interactions,

ΔF^{0}_{x} arises from covalent cross-links between helices in the crystalline form,

ΔF^{0}_{h} and $\Delta F^{0}_{H\emptyset}$ are contributions from side-chain hydrogen and hydrophobic bonds,

ΔF_{comb} is the free energy change for the combination of the randomly coiled chain with the solvent,

ΔF^{0}_{elec} is the free energy change arising from the difference in electrostatic free energy between the helix and the random coil.

Furthermore, ΔF^{0}_{unf} is related to ΔH^{0}_{res} and ΔS^{0}_{res} by equation (28).

If α is the fraction of molecules in the randomly coiled state at any given temperature, then (Schellman, 1955)

$$\alpha = 1 + \left[\exp \left(F^{0}_{obs} / RT \right) \right]^{-1} \qquad (36)$$

The melting temperature (transition temperature) is defined as that

temperature at which $\Delta F^0_{obs} = 0$, i.e., when $\alpha = \frac{1}{2}$. The sharpness of the transition depends on several factors such as cooperation between helices, number of aminoacid residues, relative strength of side-chain hydrogen bonds, nature of the solvent etc. (Zimm and Bragg, 1959; Flory, 1961). This sharpness parameter may be defined as $d\alpha / dt$ at T_{tr} (Schellman, 1955) and can be shown to be given by (Scheraga et al., 1961)

$$\left(\frac{d\alpha}{dt}\right)_{T_{tr}} = \frac{(n-4)\ \Delta H^0_{res} + \Delta H^0_h}{4\ RT^2_{tr}} \qquad (37)$$

The following relationship between the transition temperatures in the absence and presence of denaturants was derived by Peller (1956)

$$T^0_{tr} - T_{tr} \cong \frac{R\ (T_0)^2}{\Delta H} \cdot 2\ K\ c \qquad (38)$$

where T^0_{tr} and T_{tr} are transition temperatures in the absence and presence of a denaturant respectively, K is the average equilibrium constant for denaturant binding to the exposed sites after the configurational collapse, ΔH is the heat of binding for the same process, and c is the protein concentration. Peller has pointed out the interesting similarity between this equation for the transition point depression and the usual expression for the freezing point depression. This supports the assumption of the order-disorder transition theory (see Kinetics section) that the native molecule would correspond to a microcrystal in the solid phase and the denatured molecule to one in the liquid phase.

D. Review of Some Experimental Techniques

It is not within the scope of this work to discuss all the experimental techniques available for detecting the process of thermal denaturation or the various types of results obtained. However, some techniques of wide applicability together with some interesting results will be presented as examples.

1. The Thermal Transition of Ribonuclease in Urea Solutions (Foss and Schellman, 1959).

The temperature dependence of levorotation of ribonuclease for several concentrations of urea was determined. The transition temperatures were shown to fall markedly with increasing urea concentrations. Whereas $T_{tr} = 65^{\circ}C$ in the absence of urea, it is approximately $20^{\circ}C$ for 8 M urea. This was attributed to the cooperative effect of heat and urea in disrupting hydrogen bonds. Interestingly, an inverted transition was observed at lower temperatures, the fraction of denatured molecules at $25^{\circ}C$ being less than that at 10° for 8 M urea. This effect considerably increases with increasing urea concentrations. The interpretation proposed was as follows: if urea were more strongly bound than water it would decrease the heat of unfolding. On the other hand, whenever it is adsorbed it loses a good deal of its freedom and therefore there will be a decrease in entropy favoring the native state. It is this critical balance which leads to the inverted transition. The situation may be visualized by considering the following situation

$$\Delta F_{unf} = \Delta H_{unf(s)} + r\Delta \langle H \rangle - T \Delta S_{unf(s)} + r\Delta \langle S \rangle \quad (39)$$

in which $\Delta H_{unf(s)}$ is the enthalpy of unfolding in the pure solvent, r is the number of bound urea molecules, $\Delta\langle H\rangle$ and $\Delta\langle S\rangle$ are average values for the heats and entropies of urea binding. If it is assumed that r decreases linearly with temperature, a quadratic with a maximum in ΔF_{unf} is obtained. This maximum leads to the inverted transition.

2. Influence of pH on the Thermal Transition in Ribonuclease (Scott and Scheraga, 1963).

The kinetics of thermal denaturation of ribonuclease was studied by a spectrophotometric stopped-flow apparatus. The technique allows a reaction to be followed within a few milliseconds after mixing of the reactants. This apparatus consists of two thermostated reservoirs and a lucite mixing chamber mounted on a spectrophotometer. Solutions of ribonuclease and acid were thermally equilibrated before mixing. The signal from the photomultiplier of the spectrophotometer was amplified and recorded as millivolts against time on an oscillograph chart. The kinetics were studied in the pH range 0.9 - 3.26 at 287 mμ.

The rate data were complex but resolvable into two steps representable by the empirical equation

$$D_{287} = D_0^1 \, e^{-\lambda_1 t} + D_0^2 \, e^{-\lambda_2 t} \qquad (40)$$

where D_{287} is the optical density at 287 mμ, $D_0^1 + D_0^2$ is the value of D_{287} at zero time, and λ_1 and λ_2 are slopes of log D_{287} vs. time for the two resolved transitions.

Neither the Arrhenius nor the van't Hoff plots were linear. The

first behaviour was accounted for qualitatively using the solution to the gambler's ruin problem (see Kinetics section). The problem of non-linear van't Hoff plots was solved by resolving the transition into two component transitions, taking the requirement of symmetry into account and checking for uniqueness of resolution. Their results indicated that there are two cores on the native molecule that denature independently.

3. The Thermally Induced Transition in Fibrin (Loeb and Scheraga, 1963).

The thermal transition in fibrin films and fibres was observed by following the changes in three properties: the length at zero force, the retractive force at constant length, and the optical birefringence. These properties were observed to undergo sharp changes at a well-defined temperature which depended on the diluent with which the sample was in equilibrium. The pH dependence of the transition temperature was accounted for in the manner previously described.

4. The Thermal Transition in Lysozyme (Foss, 1961).

The thermal transition in lysozyme was followed spectrophotometrically and polarimetrically. Whereas the optical density is sensitive to the changes in the environment of chromophoric groups, the optical rotation is sensitive to structure. Frequently, optical density and rotation changes are parallel, but in this particular case they were not. The transition temperature obtained spectrophotometrically was significantly lower than that obtained polarimetrically. The explanation offered was that the chromophoric groups become exposed upon the collapse of the

tertiary structure before any changes in the secondary structure, responsible for the optical rotation changes, can occur.

5. The Thermal Denaturation of Collagen (Boedtker and Doty, 1956).

The thermal denaturation of collagen, to yield gelatin, was followed by light scattering. The Zimm plots for native and denatured species are shown in fig. 6. Collagen consists of three polypeptide chains, wound in a slowly rising triple helix. Heating for 5 minutes at 40^{0} unwinds the triple helix and yields three single polypeptide chains in its place. In the figure the straighter line of the open circles, obtained after heating, exhibits almost three times the intercept, corresponding to nearly one-third the molecular weight of the initial material. The lesser slope of the denatured collagen indicates a lesser spatial extent, and the lack of curvature is typical of a random coil conformation.

6. Differential Thermal Analysis (DTA) Method (Steim, 1965).

In this technique differential thermocouples are employed to measure the difference in temperature between a protein and a solvent buffer known to be thermally stable. Both examples are contained in the same cell and the temperature of the cell is raised linearly with time. Since the heating rate of the solvent is constant, any endothermic or exothermic reaction in the system should give rise to a minimum or maximum, respectively, in the thermogram ($\triangle$T vs. T). A minimum is usually obtained in the case of proteins (since denaturation is endothermic) corresponding to the transition temperature. In the case of murimadase thermal denaturation, the thermogram revealed fine aspects of the transition.

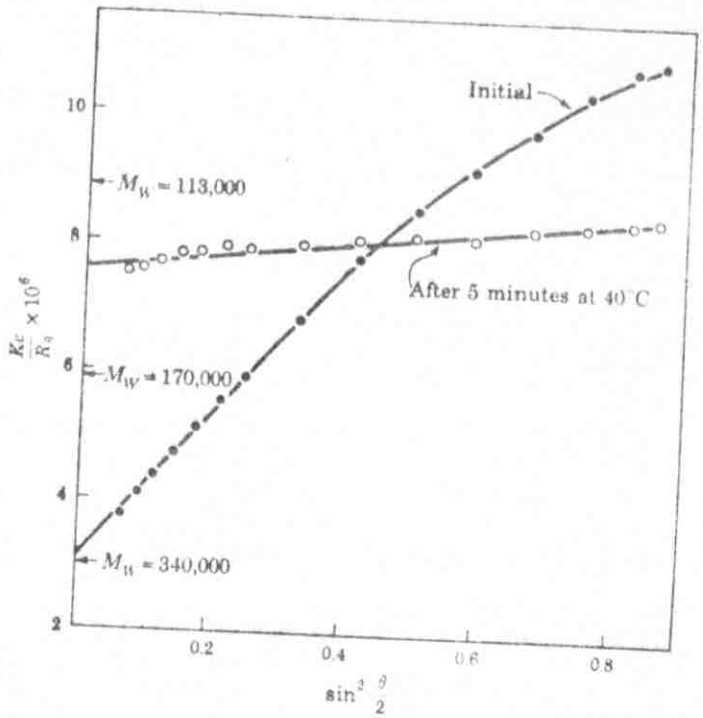

Fig. 6 - Reciprocal scattering envelope of native (solid circles) and thermally denatured (open circles) collagen at 2.6×10^{-4} g/cc. (Boedtker and Doty, 1956).

This method is easy, rapid, and capable of providing kinetic as well as thermodynamic data.

Several other methods for following thermal denaturation are also available. For example, H - D and H - T exchange (Scheraga, 1961), changes in small ion binding (Dechev, 1961), changes in the amount of titrable groups (Steinhardt and Zaiser, 1955), and changes in the electrophoretic pattern (Ribeiro and Villela, 1957).

Very little work has been reported in the literature concerning studies on conformational changes of myoglobin in solution.

Breslow and Jurd (1961) investigated the reactivity of sperm whale ferrimyoglobin towards hydrogen ions and p-nitrophenyl acetate. The titration curve of myoglobin makes a sharp break near pH 4.5 with a considerable uptake of hydrogen ions in the range down to pH 4. Their results led to the conclusion that approximately six imidazole groups are freely reactive in the native protein. Most probably these lie near, or very close to the surface. There are also six masked imidazole groups that are liberated on acid denaturation.

Peiffer and Leonis (1964) have attempted to assess the importance of hydrophobic bonding in myoglobin. They studied the thermal behaviour of the protein in aqueous and non-polar media. Their conclusions were that hydrophobic bonds and the heme-linkage play an important role in

stabilizing the native structure of the protein.

Harrison and Blout (1965) used optical rotatory dispersion to study conformational changes in myoglobin and apomyoglobin. They were able to carry with complete reversibility the following operations: removal of heme and urea denaturation. Whereas the removal of heme decreased the helical content by 20%, urea denaturation resulted in a complete transformation to a randomly coiled configuration. They concluded that the heme groups is of importance in determining the native structure.

CHAPTER III

EXPERIMENTAL

1. Materials

Buffer: Phosphate buffer solutions (0.050 M) were used in all experiments. These were 0.025 M in potassium dihydrogen phosphate and 0.025 M in disodium hydrogen phosphate (May and Baker Ltd., Dagenham, England). The pH measured at 25^{0} was 6.86 and the calculated ionic strength is 0.100.

Myoglobin: Sperm whale skeletal muscle ferrimyoglobin (1 x cryst., lypholized, salt-free, batch 2) was purchased from Saravac Laboratories, Pty. Ltd., England, and used without further purification. Stock solutions were prepared by dissolving approximately 0.3 g myoglobin in 20 ml buffer, then filtering through Whatmann No. 42 filter paper. Dilutions were made depending on the spectral region to be examined, the concentrations being 3 mg/ml for the visible and 0.7 mg/ml for the ultraviolet. The exact concentrations were measured spectrophotometrically at 423 mμ against buffer after the addition of a few crystals of potassium cyanide to 3 ml of the myoglobin solution. The extinction coefficient of the myoglobin cyanide complex at this wavelength is 110 x 10^{3} (Hanania et al., 1965). Solutions were stored at

4°C and used within three days of preparation. All myoglobin solutions had a pH of 6.87 (± 0.002).

2.Methods

pH Measurements: All pH measurements were made with a Radiometer pH-meter 4, by means of a glass electrode.

Part A: Heating and Cooling Experiments: Several aliquots, about 8 ml each, of the myoglobin solution were placed in a thermostated bath (Wilkins Anderson Co.) at a given temperature for definite time intervals. After heating, the sample was brought back to room temperature by equilibrating it in a 25°C bath. With the lower temperatures, a 10 minute equilibration time was enough whereas about 40 - 50 minutes were necessary for the higher temperatures. Runs above 65°C were not feasible with the more concentrated solutions (used to study the visible region) as the protein begins to aggregate within 20 minutes of heating. The absorption spectra of the heated and cooled solutions were then measured against the unheated solution in the spectral regions of 240 - 300, 400 - 430, and 500 - 650 mμ. These measurements were made with a Zeiss PM QII spectrophotometer.

Part B: Spectra of Denatured States: The Perkin-Elmer spectrophotometer was used to record difference spectra of denatured against native myoglobin solutions. Recordings were obtained at three sets of wavelength regions: 230 - 350, 350 - 550, and 550 - 750 mμ. Thermostated 10 mm cells (Scientific Cell Company, N.Y.) were

used to contain the sample and reference solutions. Both were initially filled with the native myoglobin solution. Water was then circulated through the sample cell from a constant temperature bath by means of a pump. The spectrophotometer scanning motor and the pump were switched on simultaneously. Two speeds for the scanning motor were possible: fast, covering either U.V. or visible regions in 2 minutes and slow, covering the same regions in 8 minutes. Whenever the recorder pen reached the end of a particular wavelength region, the scanning motor was switched off and the pen brought back to the initial position - the whole operation being timed to 15 seconds. The scanning was interrupted when an equilibrium absorbance value was attained. Runs were performed in the temperature range 45 - 75°C. Temperatures were measured at the end of each run by immersing a thermometer directly in the spectrophotometer cell.

Part C: Kinetic Method: Kinetic and equilibrium runs were conducted at three wavelengths: 280, 430 and 460 mμ. The Zeiss spectrophotometer together with a Sargent recording attachment (Model MR) were used. The cells were thermostated as in part B. Prior to any run, the transmittance scale was adjusted to either 80 or 100% with reference to native myoglobin. The adjustment was made on both the Zeiss indicating instrument and the recorder.
In the preliminary experiments, the procedure was similar to that described in part B, with the exception that time-transmittance recordings were obtained. However, it was soon realized

that the initial portions of the kinetic curves were inaccurate. This is because, especially at the higher temperatures, the time required to attain thermal equilibrium in the cell is about three minutes. Results obtained in this manner are only of qualitative value.

A rapid-heating device was constructed, which allowed about 2 ml myoglobin solution at 25°C to reach thermal equilibrium at 80°C within 30 seconds. A diagram of this device is shown in Fig. 7. A fluorocarbon tube about 1 mm in diameter, 2.5 meter long was wound around a glass tube jacked by a tube 5 cm. diameter and 30 cm long and thermally insulated on the outside by styrofoam. Water from a thermostated bath was circulated through the jacket of the heating device in series with the spectrophotometric cell. The heating device was mounted on a stand directly above the cell compartment of the spectrophotometer. A typical run is as follows: (1) Water at the desired temperature is circulated through the system until thermal equilibrium is attained. (2) About 1.8 ml myoglobin solution are injected by means of the syringe shown in Fig. 7, where it passes through the coil and reaches the cell within 15 sec. (3) After 30 sec. of starting the injection, the recorder is operated and transmmittance-time curves obtained.

Runs were made in the temperature range 40 - 85°C..

To verify that thermal equilibrium is attained within 30 sec. after injection, a chemical system whose absorbance varies

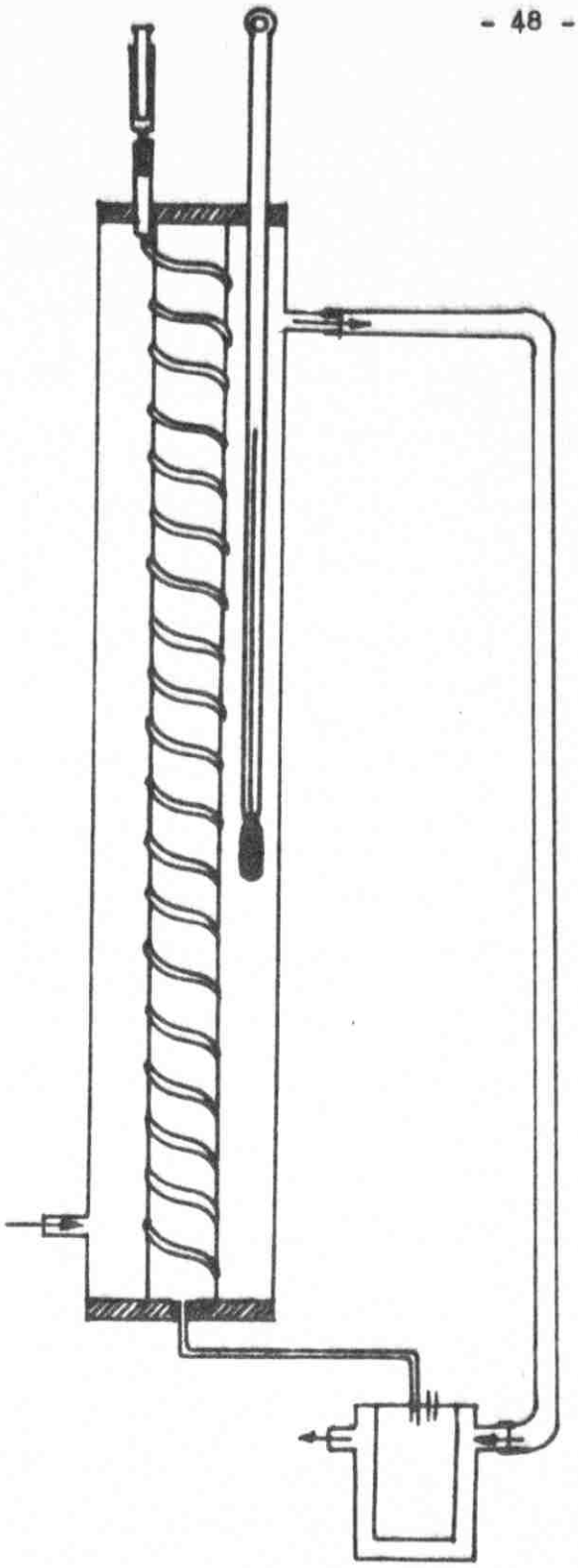

Fig. 7 - Rapid-heating device. See page 47 for details.

considerably with temperature was prepared in the following manner: 3.0 ml of 0.01% ethanolic phenolphthalein solution was added to 100 ml. of 0.100 M aqueous glycine solution. 10 ml absolute ethanol were then added to avoid precipitation of phenolphthalein. About 3 ml of 1 N NaOH was then added to bring the pH up to 9.71, close to the basic pK of glycine. The visible spectrum of this system indicated a sharp peak at 556 mμ. The absorbance-temperature data at 556 mμ are plotted in Fig. 8. The absorbance varies linearly from 1.87 at 20°C to 1.00 at 68° C. The same procedure (steps 1 - 3) of the previous paragraph for myoglobin was followed. The time from injection to thermal equilibrium, as detected by the recorder was 25 seconds at 75°C. It was therefore concluded that 30 seconds were enough for myoglobin to attain thermal equilibrium, at the high temperatures used in this experiment.

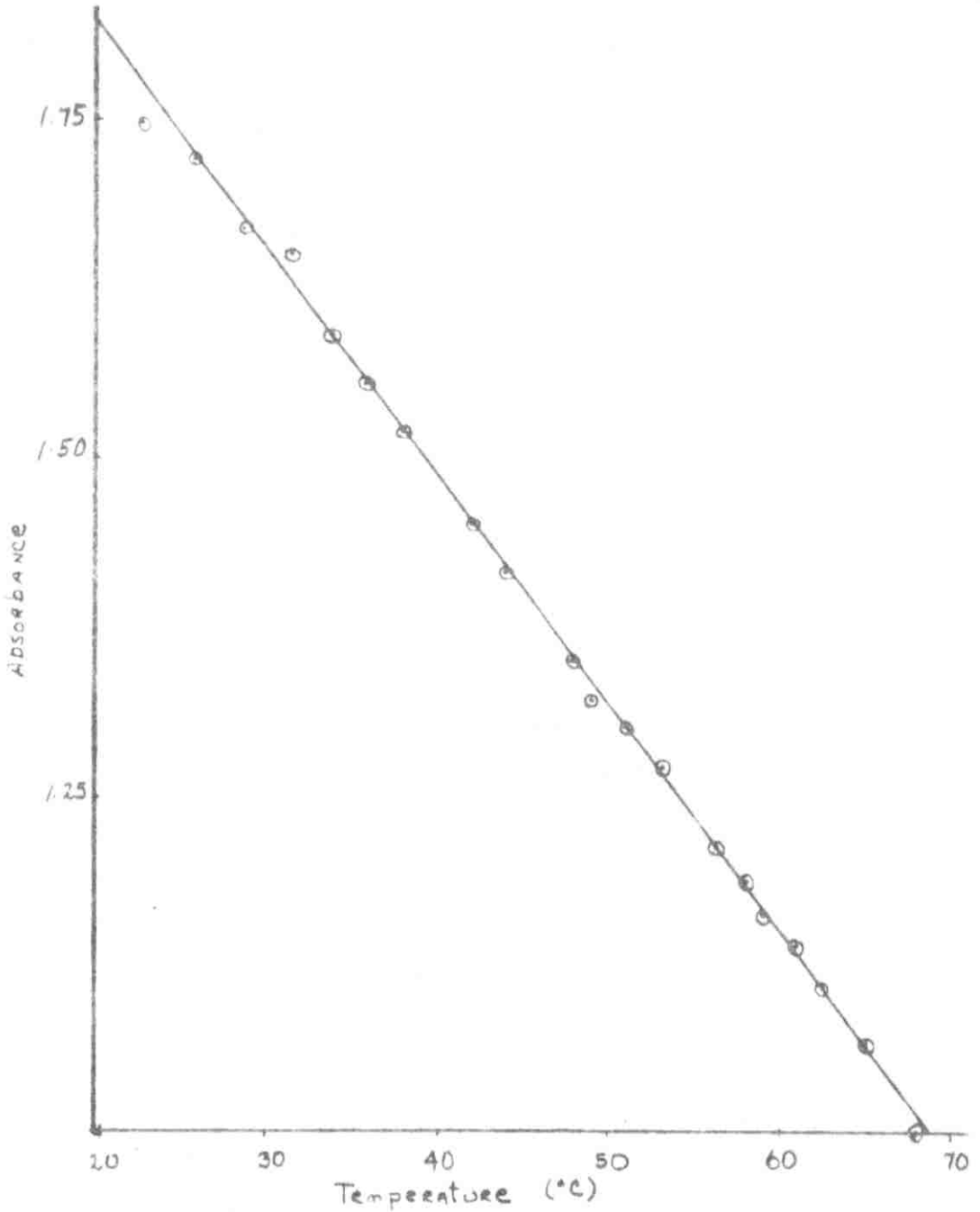

Fig. 8 - Absorbance as a function of temperature for the chemical system used in Part C. Composition of system is given in page 49.

CHAPTER IV

RESULTS

A. Heating and Cooling Experiments

1. Heating to Temperatures below 50°C: Following a two-hour heating period at temperatures below 50°C and then cooling to 25°C, no alterations in the ultraviolet and visible spectra of myoglobin solutions were detected.

2. Heating to Temperatures between 50 and 70°C.: Significant increments in absorbance, in both the ultraviolet and visible regions, were observed after heating the myolgobin solutions to temperatures above 50°C and then cooling to 25°C. For a given temperature, the absorbance increment, $\triangle A$, increases with time of heating (Figs.9, 12). Table I illustrates this point clearly. Furthermore, the magnitude of $\triangle A$ is an extremely sensitive function of temperature (Table II). For example, heating for 20 minutes at 55°C produced a 2.7% rise in absorbance at 250 mμ, whereas heating for the same period at 70°C produced a 118% rise. That this effect is not entirely kinetic is demonstrated by re-examination of Table I. Here, it is apparent that even after prolonged heating at the lower temperatures, $\triangle A$ is still relatively small.

It should be noted that $\triangle A$ does not continue to rise with increasing time of exposure to the elevated temperature. This effect is apparently due to aggregation of the denatured species. The process

TABLE I

Absorbance increments in the 240 - 300 mμ Region

pH = 6.87

I = 0.100

Temp. of measurement = 25°C.

Absorbancies of native myoglobin vs buffer are included for comparison.

Set a. Temp. 55.0°C, (Mb) = 1.8×10^{-5} M

λ	A	△A ± 0.005 Heating period (min.)		
mμ	(native)	20	50	80
240	0.737	0.020	0.050	0.057
250	0.450	0.018	0.050	0.057
260	0.497	0.013	0.043	0.048
270	0.585	0.010	0.036	0.039
280	0.624	0.007	0.028	0.031
290	0.525	0.004	0.027	0.030
300	0.298	0.006	0.029	0.031

(Table I ctd.)

Set b. Temp. 60.0°C, (Mb) = 2.2×10^{-5} M

λ mμ	A (native)	ΔA ± 0.005 Heating period (min.) 10	20	40	50	70	90
241	0.915	0.151	0.207	0.240	0.306	0.327	0.322
250	0.558	0.136	0.190	0.224	0.288	0.308	0.312
260	0.612	0.119	0.166	0.203	0.260	0.278	0.283
270	0.718	0.104	0.146	0.180	0.233	0.250	0.259
280	0.765	0.092	0.133	0.163	0.215	0.230	0.240
290	0.645	0.083	0.125	0.155	0.206	0.223	0.233
300	0.367	0.080	0.120	0.152	0.202	0.221	0.231

Set c. Temp. 65.0°C, (Mb) = 2.34×10^{-5} M

λ mμ	A (native)	ΔA ± 0.005 Heating period (min.) 5	10	20	30	40
241	0.981	0.220	0.388	0.456	0.482	0.585
250	0.607	0.194	0.347	0.425	0.454	0.555
260	0.665	0.164	0.305	0.381	0.413	0.504
270	0.779	0.141	0.269	0.344	0.375	0.456
280	0.828	0.124	0.243	0.314	0.343	0.415
290	0.697	0.116	0.233	0.295	0.331	0.395
300	0.400	0.114	0.225	0.286	0.325	0.387

(Table I ctd.)

Set d. Temp. 70.0°C, (Mb) = 1.2×10^{-5} M

λ mμ	A (native)	A ± 0.005 Heating period (min) 5	10	15	20	30
240	0.488	0.210	0.323	0.366	0.388	0.426
250	0.309	0.176	0.291	0.339	0.365	0.401
260	0.334	0.154	0.256	0.302	0.331	0.365
270	0.386	0.133	0.228	0.275	0.303	0.335
280	0.407	0.117	0.208	0.254	0.282	0.314
290	0.344	0.109	0.196	0.243	0.271	0.303
300	0.202	0.102	0.189	0.237	0.265	0.295

of aggregation is very sensitive to temperature and myoglobin concentrations. Whereas heating for 6 hours below 55°C did not result in any precipitation of myoglobin, heating for 30 minutes at 70°C followed by re-equilibration at 25°C resulted in the formation of aggregates. Furthermore, precipitation sets in more rapidly for solutions of higher myoglobin concentrations.

a) The Ultraviolet Region: Difference spectra in the 240 - 300 mμ region, for several periods of heating at 60°C., are shown in Fig. 9. From this figure, it is apparent that $\triangle A$ is largest at 240 mμ, the wavelength of maximum extinction of the peptide bond. The value of $\triangle A$ decreases steadily from 240 to 300 mμ.

TABLE II

Percentage Increments in Absorbance

after 20 min. heating, for several temperatures

(c.f. Table I)

λ mμ	$(\Delta A/A) \times 100$			
	Heating temperatures			
	55°C	60°C	65°C	70°C
241	2.7	22.6	46.5	79.5
250	4.0	34.0	70.0	118
260	2.6	27.1	57.3	99.1
270	1.7	20.3	44.1	78.5
280	1.1	17.4	37.9	69.3
290	0.8	19.4	42.3	78.8
300	2.0	32.7	71.5	131

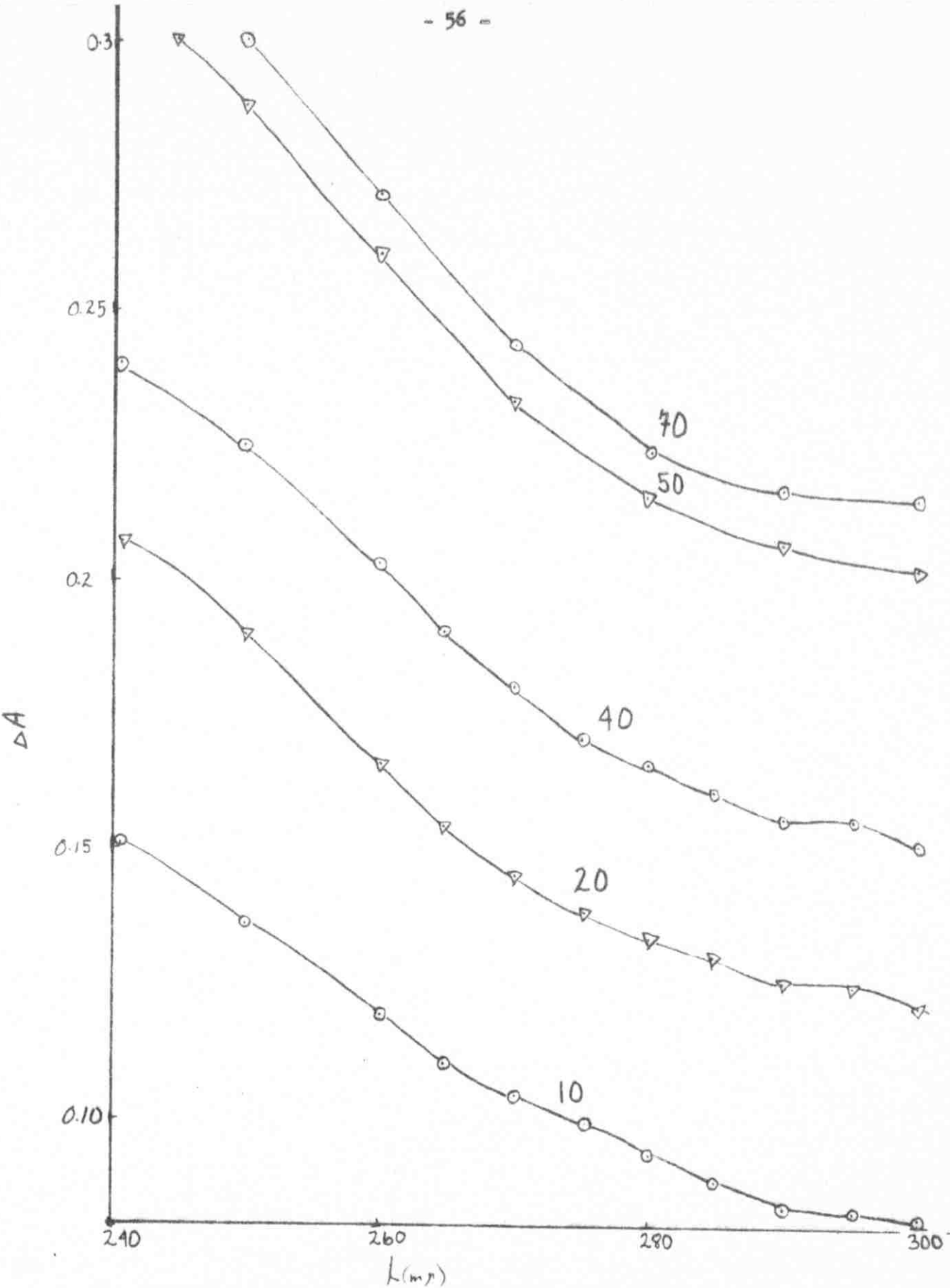

Fig. 9 - Difference spectra of native and thermally denatured myoglobin solutions. Temp. of heating = 60.0°C., Temp. of measurement = 25.0°C (Mb) = 2.17×10^{-5} M, pH = 6.87, I = 0.100. Periods of heating (min.) are indicated.

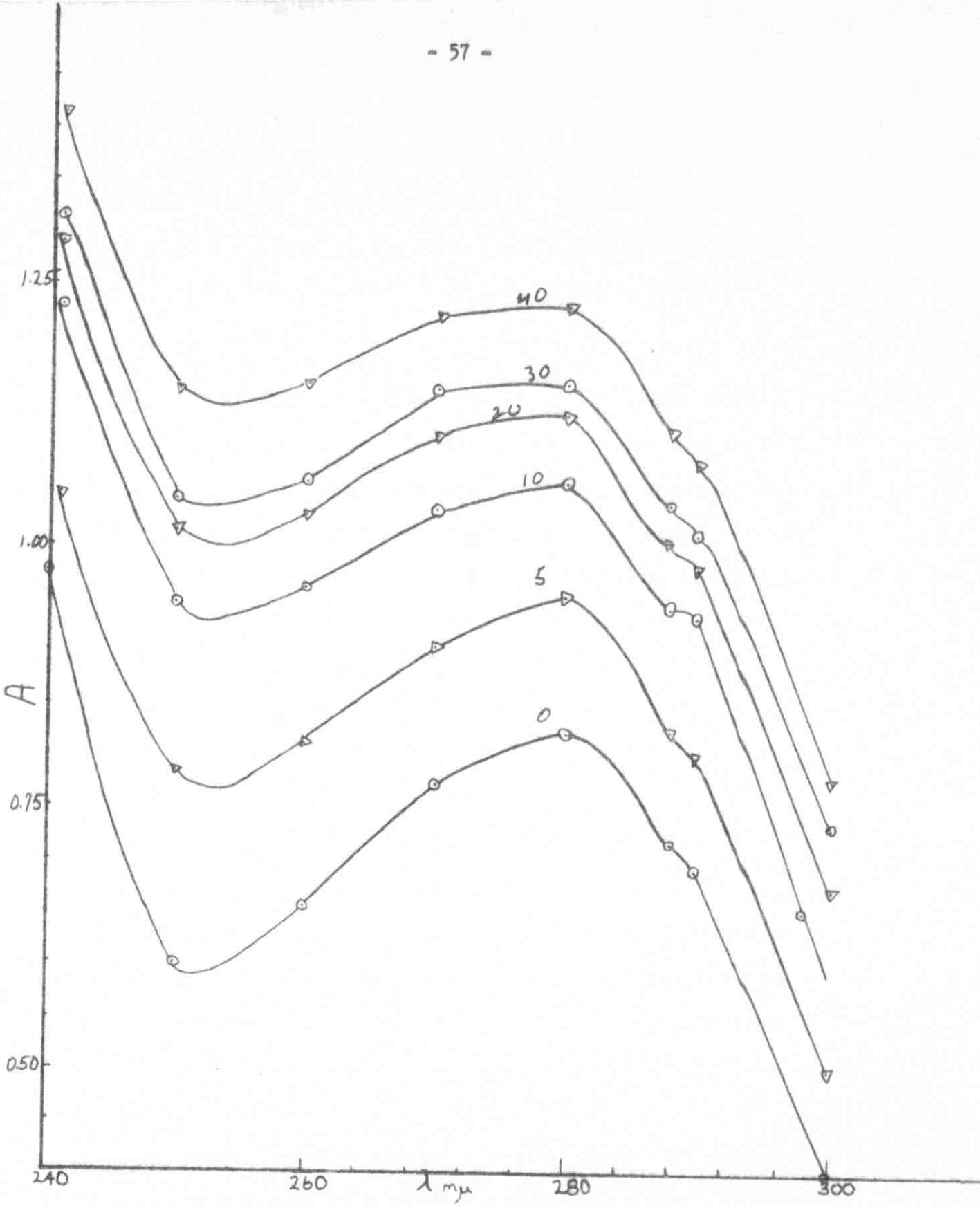

Fig. 10 - Spectra of native and thermally denatured myoglobin solutions. Temp. of heating = 65.0 °C, Temp. of measurement = 25.0 °C. (Mb) = 2.34 x 10^{-5} M, pH = 6.87, I = 0.100. Periods of heating (min.) are indicated.

Moreover, the spectra of native and denatured species do not differ significantly in profile (Fig. 10). Only minor alterations are observed, for example, the 280 mμ peak broadens and shifts slightly to lower wavelengths as the temperature is increased.

b) The Visible Region

1. The 400 - 430 mμ Region: The wavelength of maximum extinction of the heme group is 409 mμ. No significant changes were observed between 400 and 430 mμ. As a result of a one hour heating period at 65°C., followed by re-equilibration at 25°C., a 5% decrease in absorbance was detected at 409 mμ (Fig. 11). Although the myoglobin concentration used here was very small, some aggregation might have caused this effect. It might also have been due to reversible denaturation in which the heme group 'sits'in a deeper, more probable position within the molecule. Results obtained by direct measurement at the elevated temperature (part B) strongly suggest that thermal denaturation, as followed in this spectral region, is reversible.

2. The 500 - 600 mμ Region: Difference spectra in this region at 65°C. are shown in Fig. 12. Absorbance increments at 60 and 65°C. are given in Table III. The results indicate that ΔA is largest at 500 mμ and decreases progressively up to 650 mμ. The significant features in the difference spectrum are two shoulders around 540 mμ and 560 mμ, and a peak at 600 mμ.

As in the ultraviolet region, the profiles of the spectra of denatured species closely resemble each other and those of the native

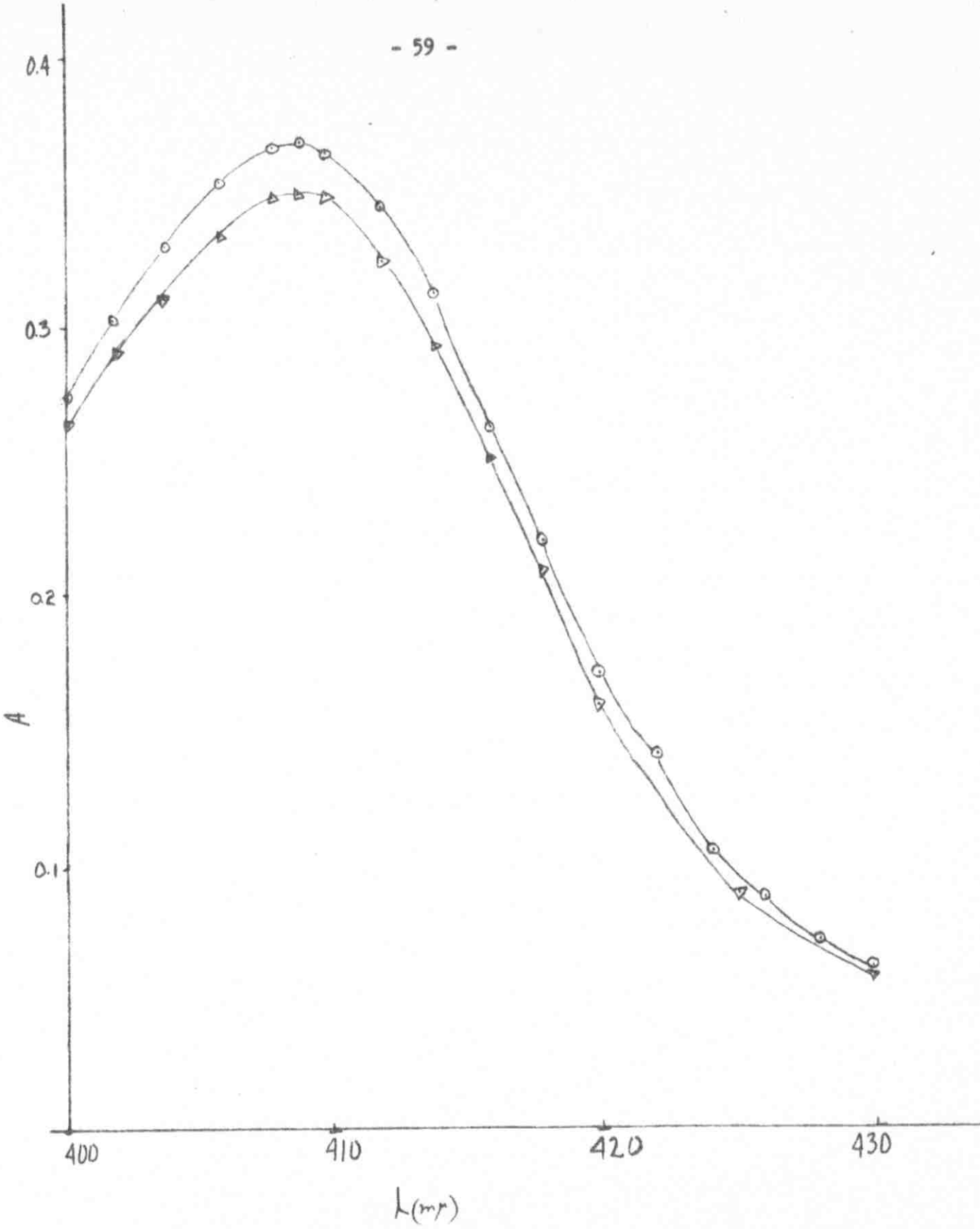

Fig. 11 - Spectra of native and thermally denatured myoglobin solutions in the region of absorption maximum of heme. Temp. of heating = 65.0°C. Temp. of measurement = 25.0°C., period of heating = 1 hr. (Mb) = 2.40×10^{-6} M, pH = 6.87, I = 0.100.

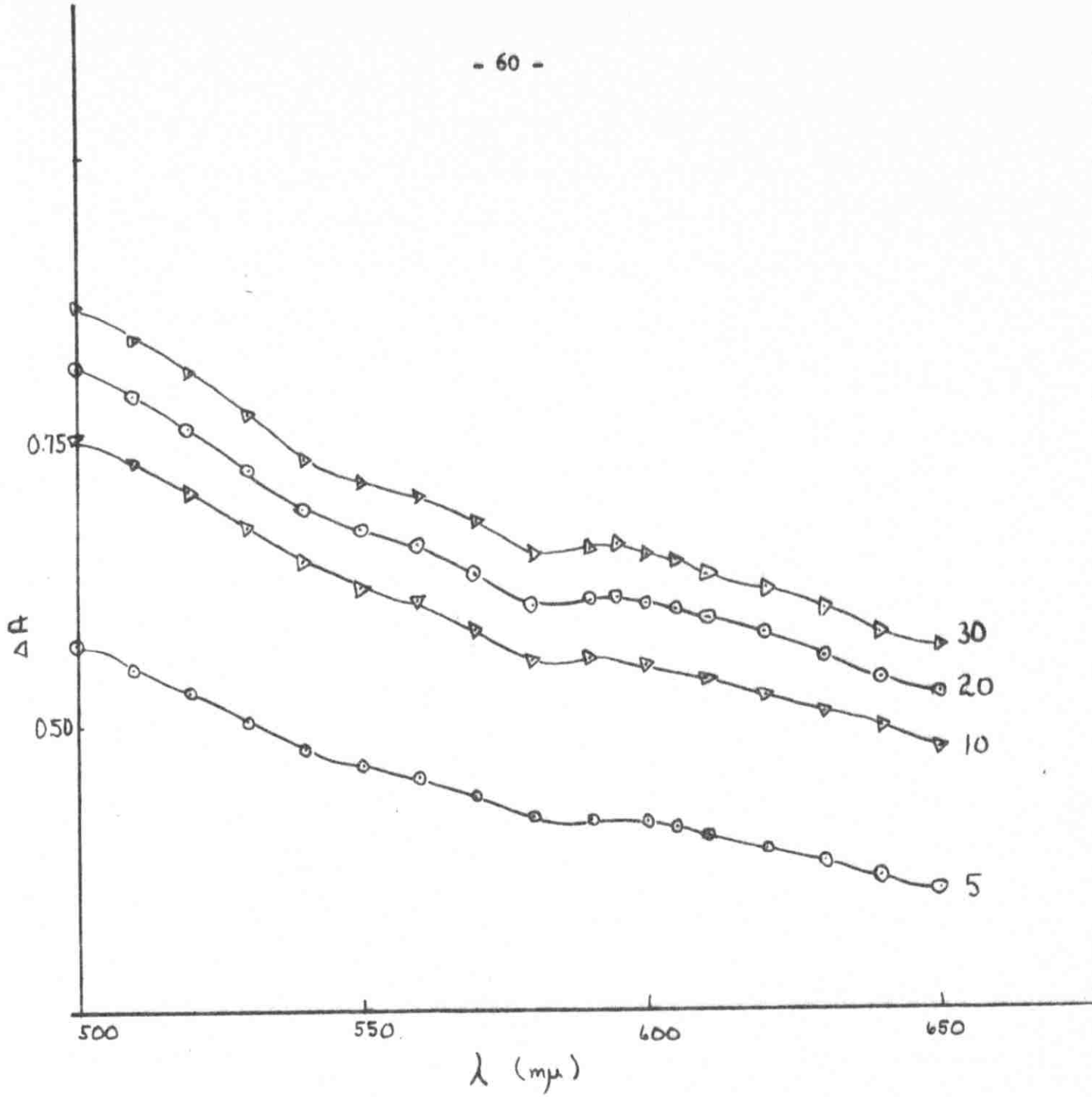

Fig. 12 - Difference spectra of native and thermally denatured myoglobin solutions. Temp. of heating = 65.0°C. Temp. of measurement = 25.0°C. (Mb) = 9.12×10^{-5} M, pH = 6.87, I = 0.100. Periods of heating (min.) are indicated.

species (Fig. 13). The following minor differences may be noted:

a) The 580 mμ peak broadens progressively as the time of exposure to the elevated temperature is increased.

b) A blue shift is observed with the 640 mμ peak under the same conditions.

TABLE III

Absorbance Increments in the 500 - 650 mμ region

(Mb) = 9.1×10^{-5} M, pH = 6.87, I = 0.100

Temp. of measurement = 25°C.

Absorbancies of native myoglobin vs buffer are included for comparison.

Set a. Temp. 65.0°C.

λ mμ	A (native)	ΔA ± 0.005			
		Heating period (min.)			
		5	10	20	30
505	0.860	0.286	0.490	0.642	0.651
520	0.734	0.269	0.454	0.598	0.599
545	0.528	0.231	0.382	0.521	0.518
560	0.360	0.226	0.377	0.502	0.509
580	0.344	0.204	0.335	0.458	0.462
600	0.288	0.212	0.343	0.466	0.470
630	0.333	0.197	0.320	0.436	0.441
650	0.195	0.183	-	0.416	0.412
700	0.103	0.168	0.258	0.366	0.367

(Table III ctd.)

Set b. Temp. 65.0°C.

λ mμ	A (native)	ΔA ± 0.005 Heating period (min.) 5	10	20	30
505	0.860	0.562	0.741	0.804	0.857
520	0.734	0.531	0.708	0.762	0.812
545	0.528	0.472	0.633	0.678	0.721
560	0.360	0.455	0.610	0.660	0.703
580	0.344	0.418	0.558	0.604	0.649
600	0.288	0.415	0.555	0.607	0.651
630	0.333	0.379	0.511	0.560	0.602
650	0.195	0.354	0.481	0.528	0.570
700	0.103	0.317	0.456	0.494	0.567

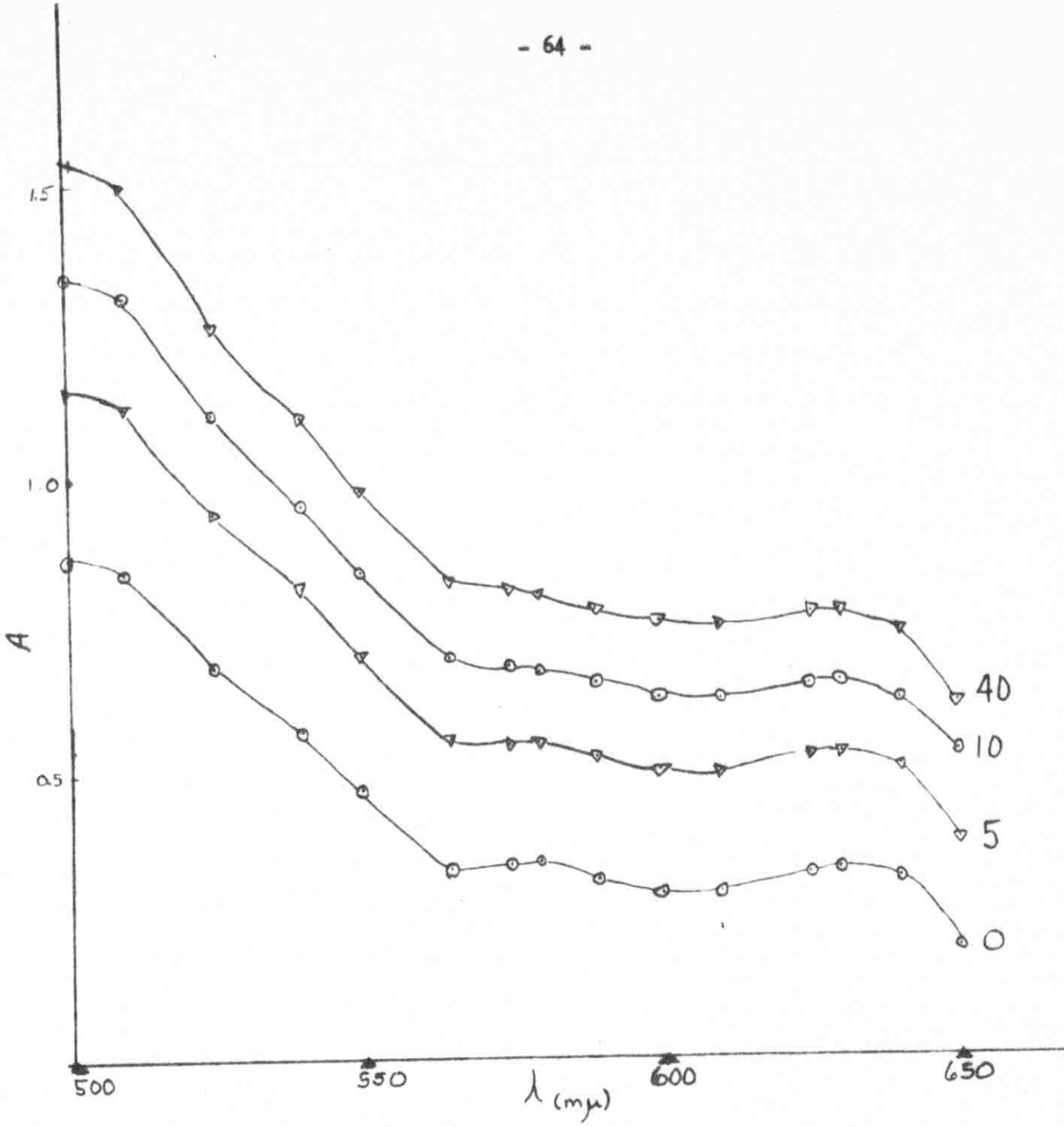

Fig. 13 - Spectra of native and thermally denatured myoglobin solutions. Temp. of heating = 60.0°C., Temp. of measurement = 25.0°C. (Mb) = 9.12×10^{-5} M, pH = 6.87, I = 0.100. Periods of heating (min.) are indicated.

B. Spectral Recordings at Elevated Temperatures

The heating process and the process of scanning the spectrum were made to take place simultaneously. Three spectral regions were studied separately: 230 - 350 mμ, 350 - 550 mμ, and 550 - 750 mμ, in the temperature range 45 - 73°C. (Below 230 mμ recordings were rendered difficult by the weak power imput of the spectrophotometer lamp). Typical difference spectra, representing the three regions, are shown in Figs. 14, 15 and 16. In these figures, every curve is separated from the preceding or following one by a constant time interval. This allows for following the kinetics of the denaturation process by plotting $\triangle A$ against time, for any wavelength desired. Such a plot is shown in Fig. 17.

Following the lapse of a definite heating period, an equilibrium difference spectrum was obtained for each temperature. These spectra are presented in Figs. 18, 19 and 20. They allow for thermodynamic treatment of the process by plotting $\triangle A_{(equilibrium)}$ against temperature. Such plots are shown in Fig. 21. Table IV gives $\triangle A_{(equilibrium)}$ as a function of wavelength, for several temperatures. The percentage increments in the equilibrium values of absorbance, at 73°C. are plotted in Fig. 22 for the spectral region 250 - 650 mμ.

The two major features of the difference spectra are a peak at 240 mμ and a plateau at 455 - 490 mμ. Other features are a shoulder at 260 mμ and three small peaks at 505, 590, and 645 mμ.

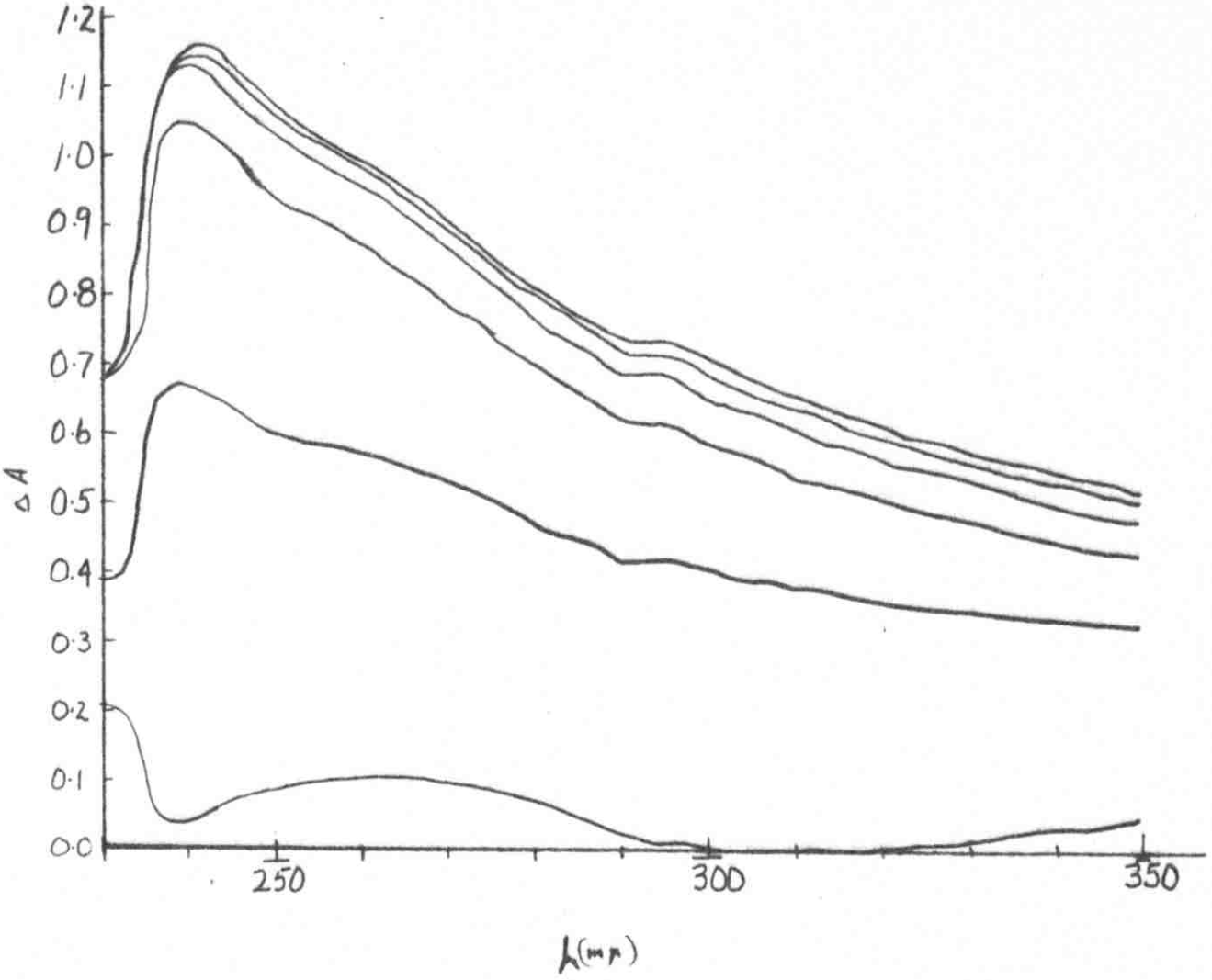

Fig. 14 - Difference spectra of native and thermally denatured myoglobin solutions. Temp. of heating and measurement = 67.8°C. (Mb) = 4.05 x 10^{-5} M, pH = 6.87, I = 0.100. A point on one curve precedesthe corresponding point (same wavelength) on the succeeding curve by 87 sec.

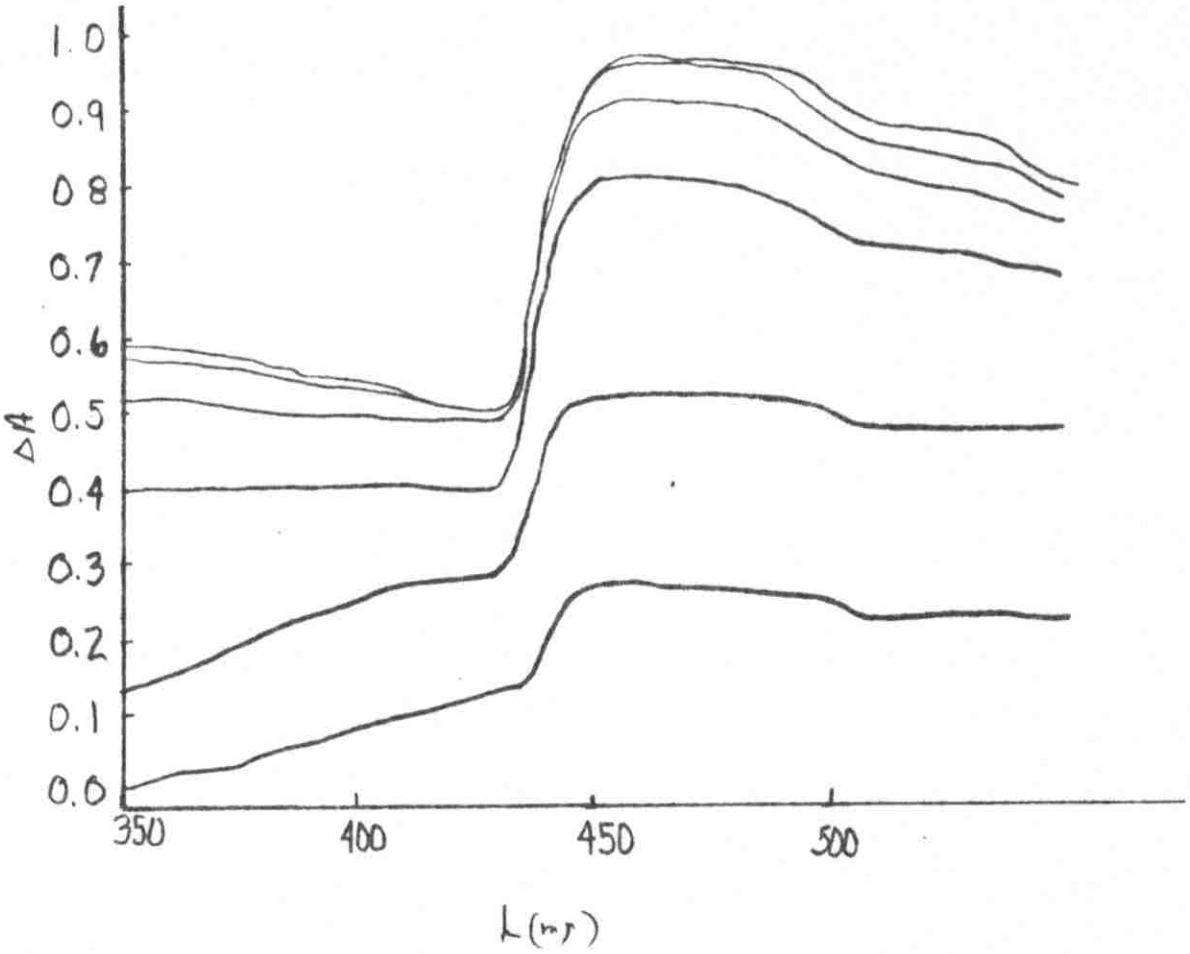

Fig. 15 - Difference spectra of native and thermally denatured myoglobin solutions. Temp. of heating and measurement = 65.4°C., (Mb) = 1.17×10^{-4} M, pH = 6.87, I = 0.100. A point on one curve precedes the corresponding point (same wavelength) on the succeeding curve by 87 sec.

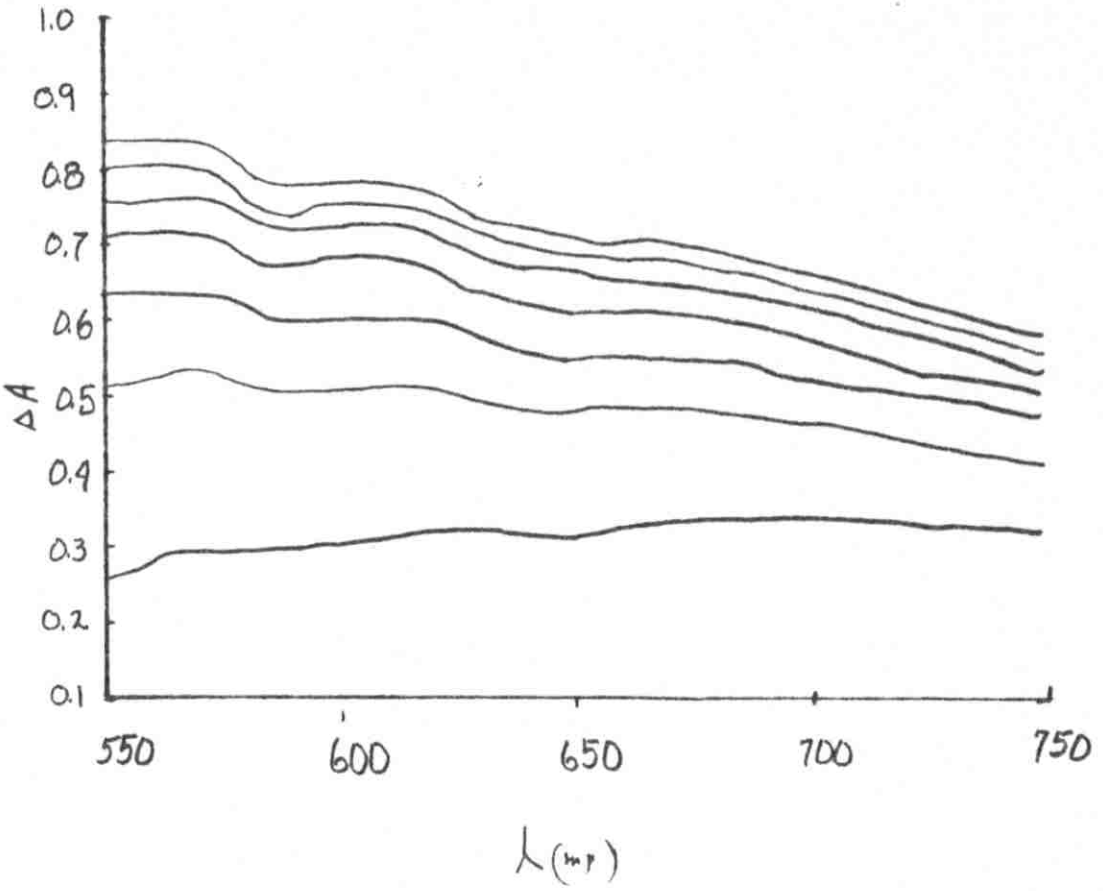

Fig. 16 - Differences spectra of native and thermally denatured myoglobin solutions. Temp. of heating and measurement = 65.4°C., (Mb) = 1.11×10^{-4} M, pH = 6.87, I = 0.100. A point on one curve precedes the corresponding point (same wavelength) on the succeeding curve by 87 sec.

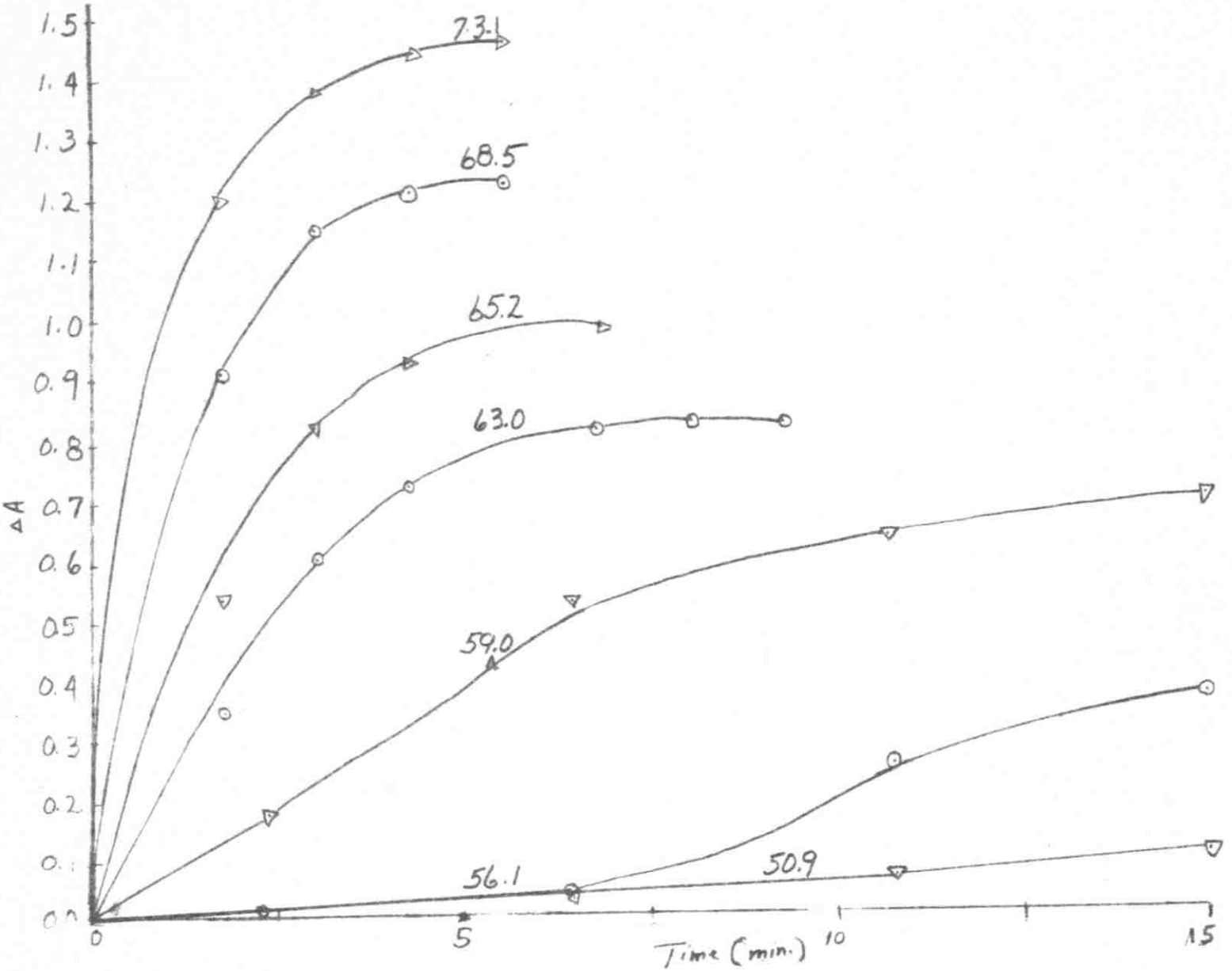

Fig. 17 - Progress curves at 460 mμ (taken from recordings of part B). Temperatures (°C.) are indicated. (Mb) = 1.20×10^{-4} M, pH = 6.87, I = 0.100.

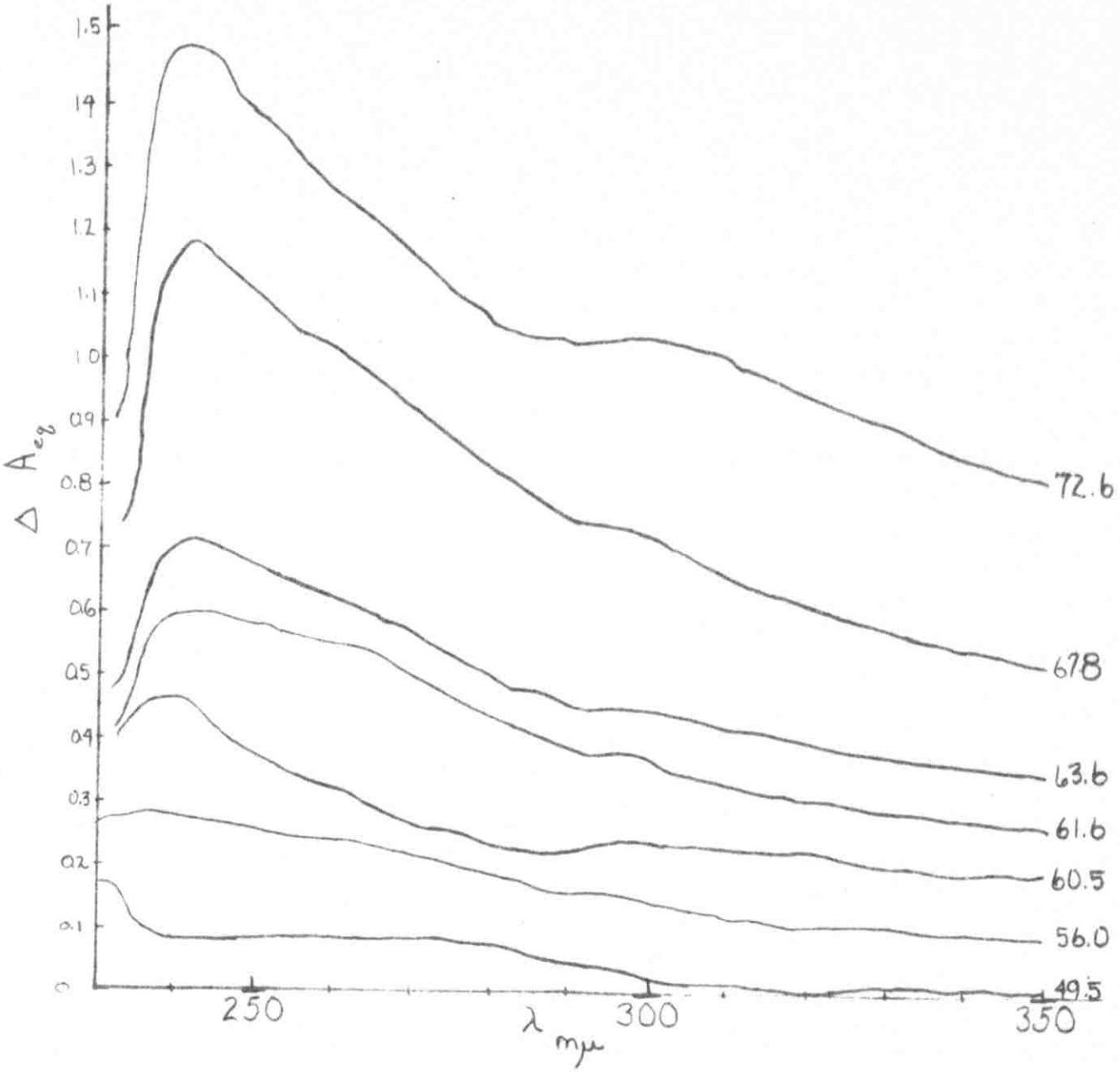

Fig. 18 - Equilibrium difference spectra. (Mb) = 4.05×10^{-5} M, pH = 6.87, I = 0.100. Temperatures at which equilibrium was achieved are indicated.

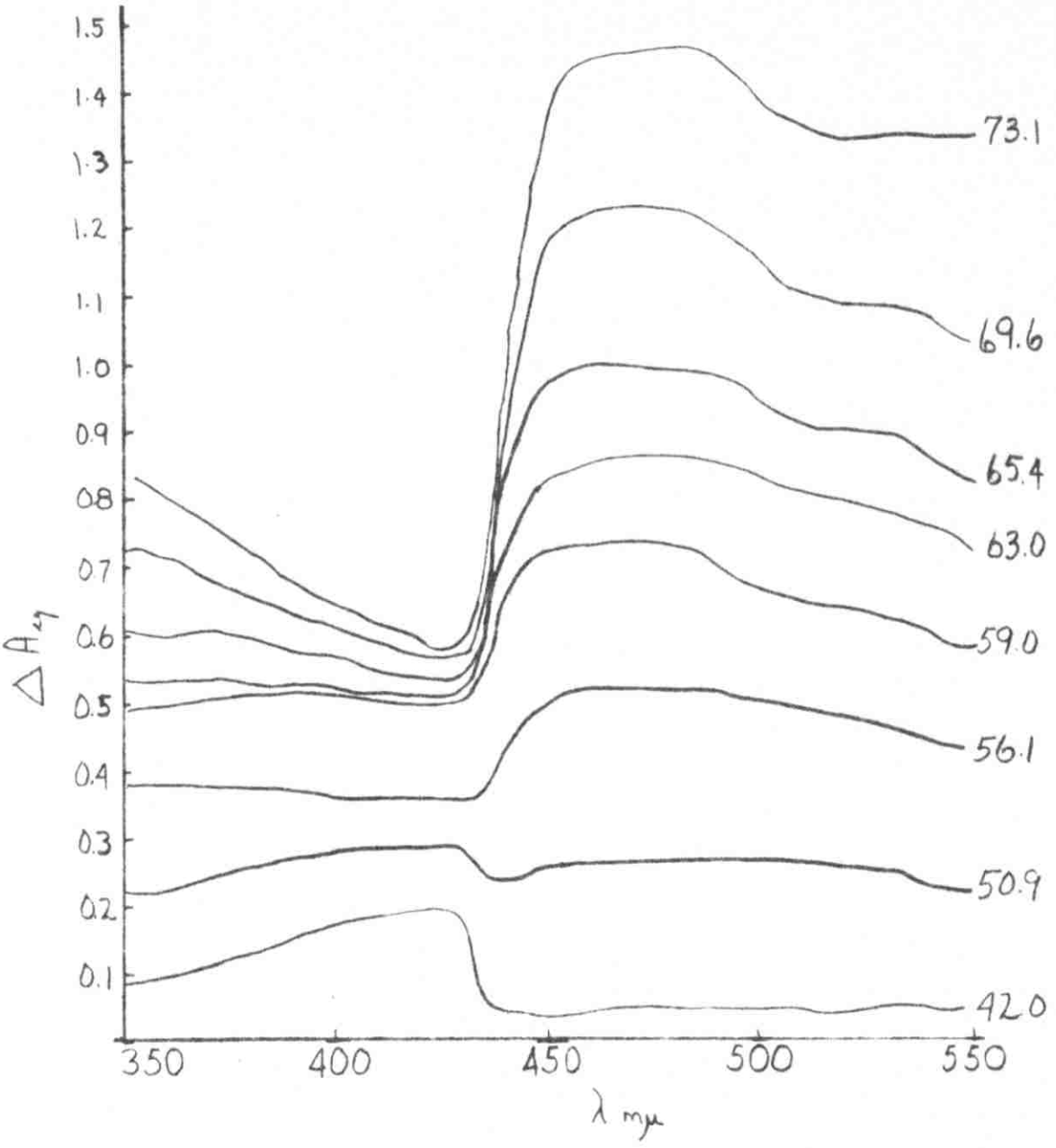

Fig. 19 - Equilibrium difference spectra. (Mb) = 1.17×10^{-4} M, pH = 6.87, I = 0.100. Temperatures at which equilibrium was achieved are indicated. (°C)

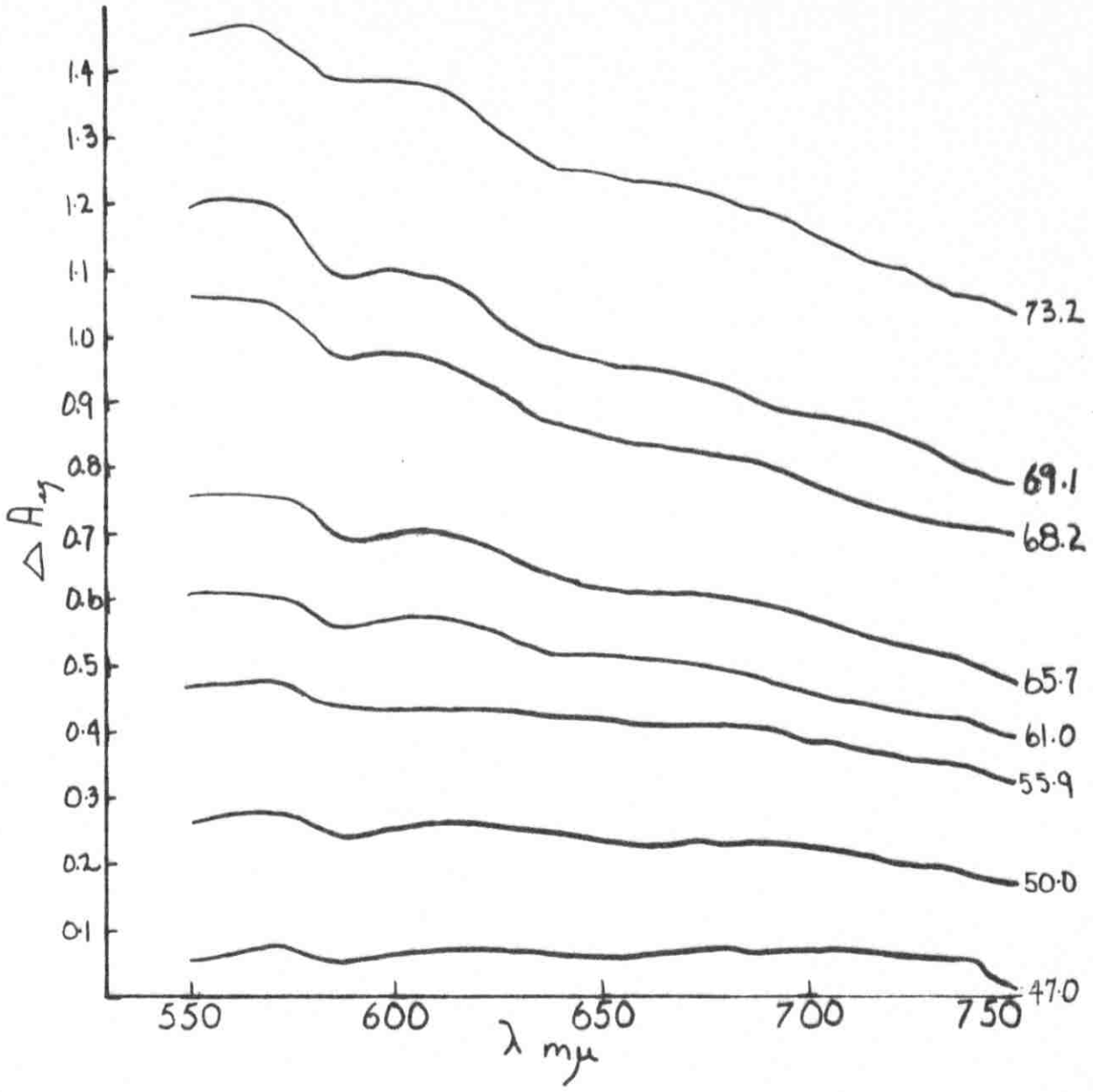

Fig. 20 - Equilibrium difference spectra. (Mb) = 1.11×10^{-4} M, pH = 6.87, I = 0.100. Temperatures at which equilibrium was achieved are indicated. (°C)

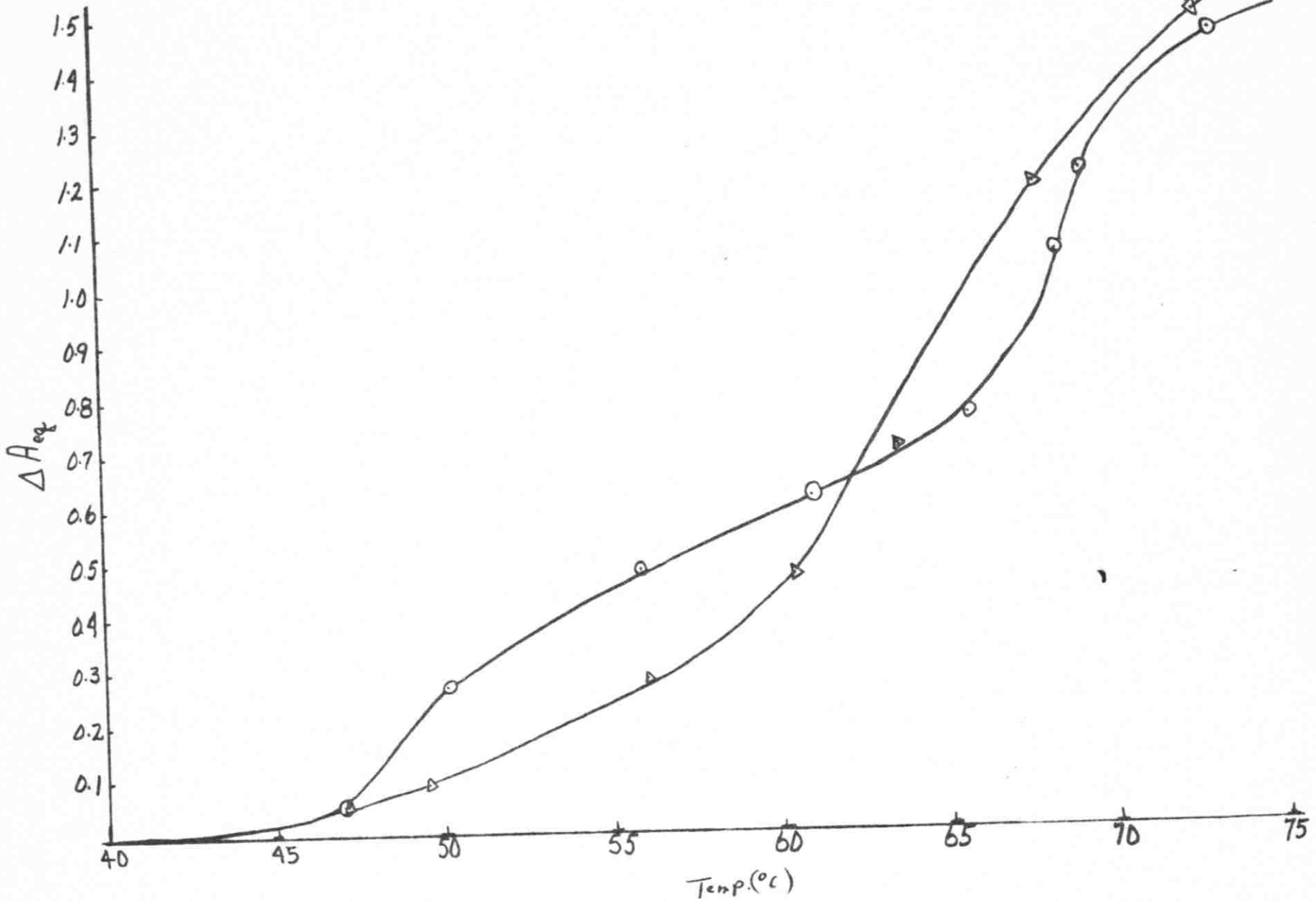

Fig. 21 - Equilibrium absorbance increments as a function of temperature. ⊙ at 460 mμ, ▲ at 240 mμ, pH = 6.87, I = 0.100, (Mb) at 460 mμ = 1.17×10^{-4} M, (Mb) at 240 mμ = 4.05×10^{-5} M.

TABLE IV

Equilibrium Absorbance Increments at Several Wavelengths For Several Temperatures

pH = 6.87, I = 0.100

Absorbancies of native myoglobin vs buffer are included for comparison.

Set a. (Mb) = 4.05×10^{-5} M, (240 - 350 mμ).

λ	A	$A_{eq} \pm 0.005$						
		Heating temperature (°C)						
mμ	(native)	49.5	56.0	60.5	61.6	63.6	67.8	72.6
240	1.49	0.090	0.280	0.465	0.600	0.705	1.17	1.49
250	1.01	0.085	0.255	0.375	0.580	0.670	1.09	1.38
260	1.08	0.085	0.240	0.325	0.550	0.620	1.02	1.26
270	1.25	0.085	0.220	0.265	0.505	0.570	0.920	1.16
280	1.33	0.080	0.190	0.240	0.540	0.500	0.830	1.06
290	1.16	0.050	0.160	0.225	0.485	0.455	0.755	1.03
300	0.670	0.025	0.150	0.240	0.470	0.445	0.720	1.03
310	0.525	0.015	0.120	0.230	0.430	0.420	0.760	1.00
320	0.550	0.010	0.115	0.230	0.410	0.400	0.715	0.945
330	0.680	0.015	0.110	0.210	0.390	0.480	0.680	0.900
340	0.865	0.010	0.100	0.190	0.380	0.465	0.650	0.850
350	1.07	0.010	0.095	0.190	0.370	0.450	0.620	0.815

(Table IV ctd.)

Set b. (Mb) = 1.2×10^{-4} M, (350 - 550 mμ).

λ	A	$\Delta A_{eq} \pm 0.005$							
		Heating temperature (°C)							
mu	(native)	47.0	50.9	56.1	59.0	63.0	65.4	69.6	73.1
350	3.18	0.085	0.220	0.380	0.490	0.530	0.610	0.830	0.845
375	4.77	0.120	0.250	0.365	0.510	0.520	0.600	0.665	0.740
400	12.7	0.180	0.280	0.360	0.515	0.520	0.565	0.610	0.645
425	6.36	0.195	0.290	0.355	0.490	0.510	0.525	0.565	0.580
450	1.15	0.040	0.260	0.500	0.520	0.825	0.965	1.17	1.34
475	0.925	0.045	0.260	0.520	0.735	0.860	0.990	1.23	1.46
500	1.08	0.045	0.260	0.500	0.665	0.830	0.945	1.15	1.39
525	0.970	0.045	0.250	0.465	0.630	0.790	0.895	1.08	1.33
550	0.700	0.045	0.220	0.420	0.580	0.720	0.825	1.03	1.33

Set c. (Mb) = 1.1×10^{-4} M, (550 - 750 mμ).

λ		$\Delta A_{eq} \pm 0.005$							
		Heating temperature (°C)							
mμ	(native)	47.0	50.0	55.9	61.0	65.7	68.2	69.1	73.2
550	0.700	0.055	0.260	0.470	0.610	0.760	1.06	1.20	1.45
600	0.415	0.070	0.260	0.435	0.570	0.705	0.975	1.10	1.38
650	0.385	0.060	0.230	0.415	0.510	0.720	0.850	0.960	1.24
700	0.065	0.070	0.225	0.380	0.455	0.670	0.775	0.880	1.15
750	0.060	0.010	0.165	0.320	0.385	0.570	0.695	0.780	1.03

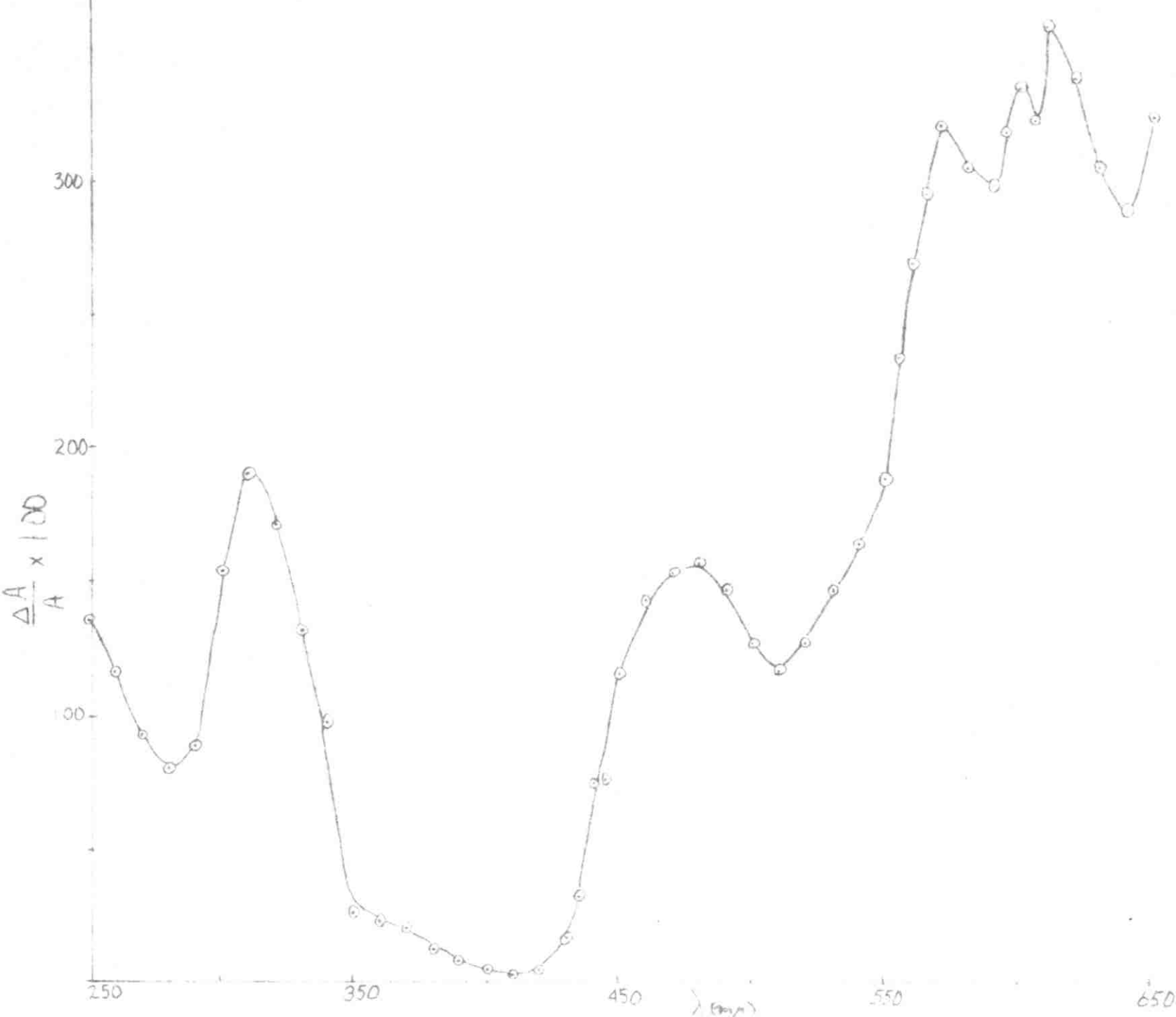

Fig. 22 - Equilibrium percentage increments in absorbance as a function of wavelength. Terms of heating

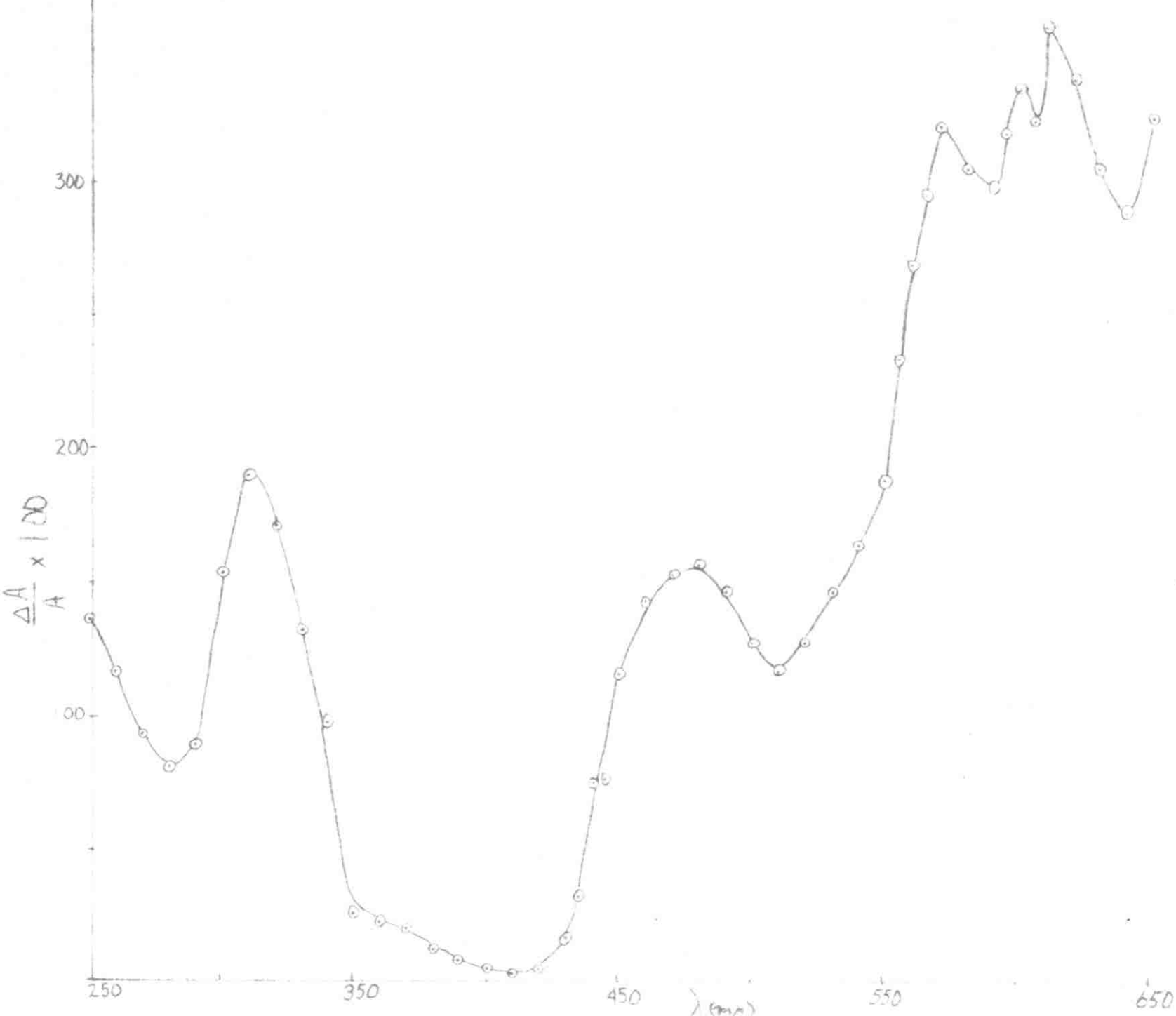

Fig. 22 - Equilibrium percentage increments in absorbance as a function of wavelength. Temps. of heating

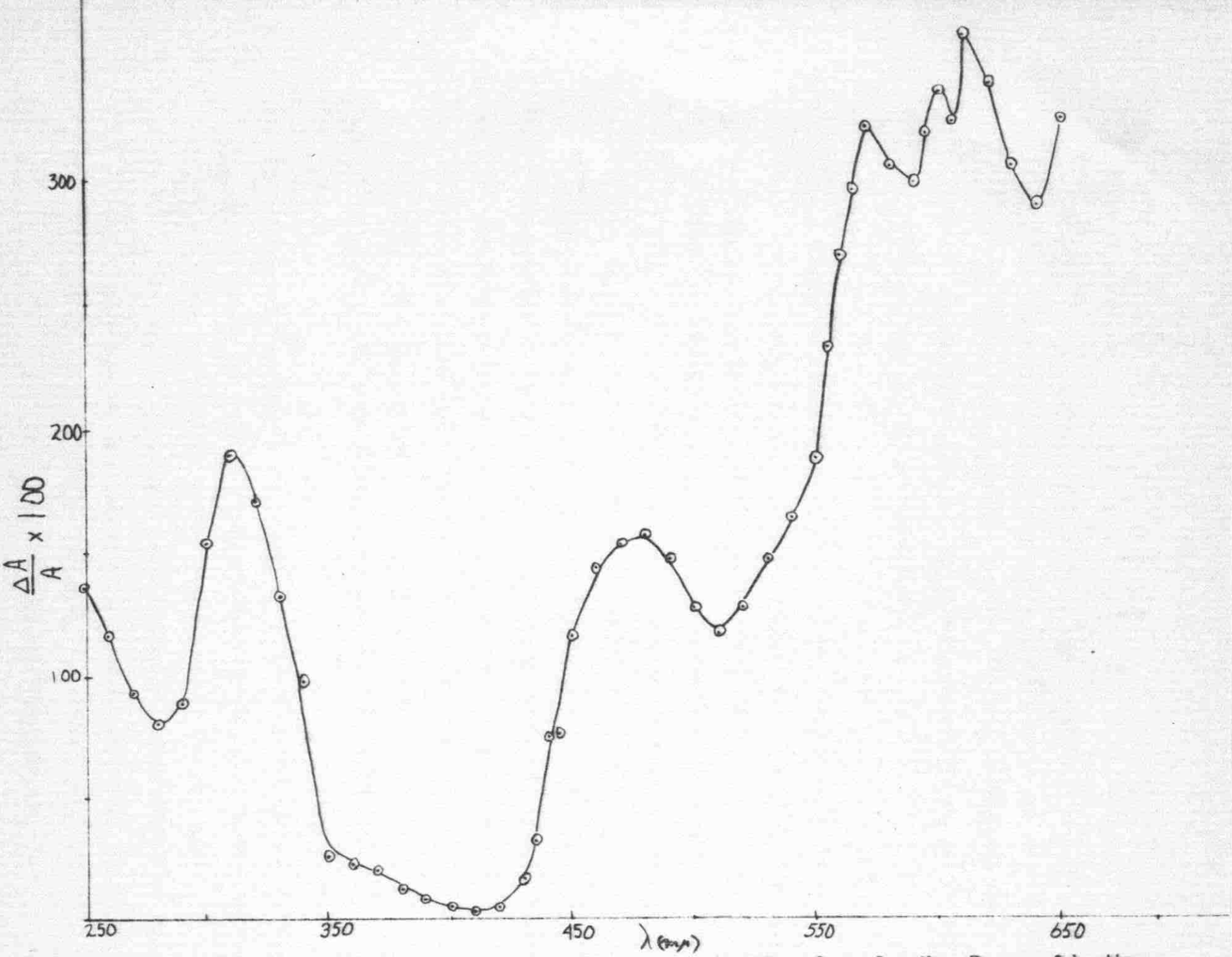

Fig. 22 - Equilibrium percentage increments in absorbance as a function of wavelength. Temps. of heating and measurements - 71.6°C. above 350 mμ, 72.6°C below 350 mμ.

C. Kinetics and Thermodynamics

Kinetic and thermodynamic data were obtained at 280, 430 and 460 mμ. As in part B, thermostated cells were used (see Chapter III, C). Runs were made at approximately 2° intervals in the temperature range 45 - 85°C., and were carried through until an equilibrium value was attained. The recordings were given as percentage transmittance against time. These were then converted to ΔA against time.

1. Preliminary Results: These were obtained by circulating water from a constant temperature bath directly through the cell containing the native myoglobin solution. Three steps were observed at 280 mμ, two at 240 mμ, and only one at 460 mμ. The first steps at 240 and 280 mμ were associated with positive ΔA values. The second step at 280 mμ exhibited a tendency to revert to the absorbance of the native solution, i.e., a negative ΔA value relative to the first step. The last steps at 240 and 280 mμ, together with the step at 460 mμ, were normal progress curves with positive ΔA values.

2. Results with the Rapid-heating Device: This device allows for following the slow progress curves, as the initial fast steps are apparently complete within the 30 sec. interval required to attain thermal equilibrium in the system.

a) Kinetic Results: The kinetics were complex but the initial slopes indicated a zero order transition. A family of progress curves at 460 mμ is shown in Fig. 23. Attempts to analyze further portions of the progress curves were rendered difficult, as it was found that the transition order varies with temperature as well as

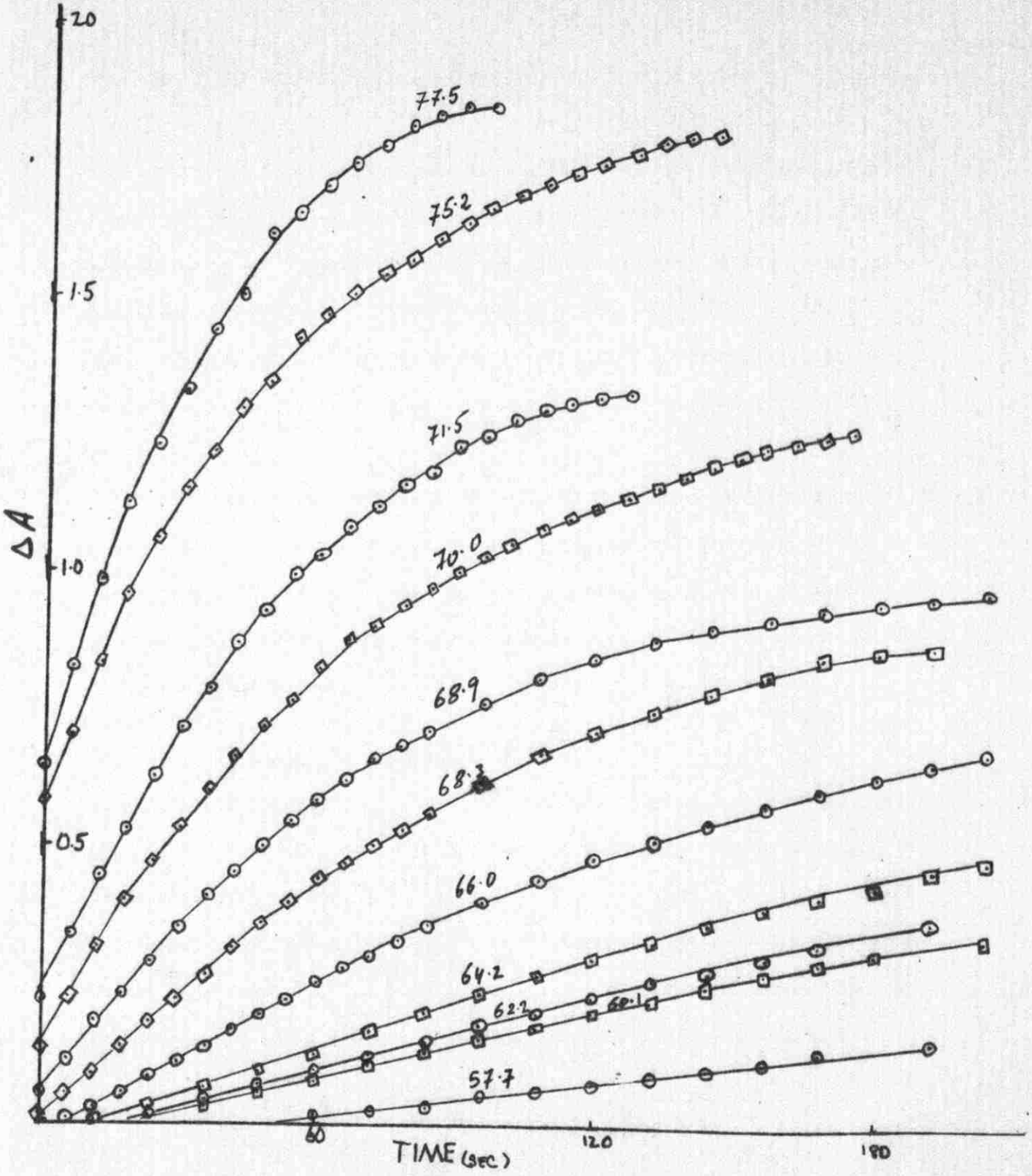

Fig. 23 - Progress curves at 460 mu (taken from recordings of part Q). Temperatures (°C.) are indicated. (Mb) = 1.17×10^{-4} M, pH = 6.87, I = 0.100.

with time. All kinetic calculations were therefore based on the initial slopes.

The transition order with respect to myoglobin concentration was determined as follows. Several myoglobin solutions, of concentrations between 1.2×10^{-4} M and 4.9×10^{-5} M were prepared. Kinetic runs were performed at 71.0°C. and 460 mμ. A plot of the logarithm of the initial slope against the logarithm of myoglobin concentration yielded a straight line with slope 1.39, corresponding to the transition order (Fig. 24).

The forward rate constant, k_F, was calculated by dividing the initial slope by the myoglobin concentration raised to the 1.39th power (Table V). Plots of the initial slope as a function of temperature are shown in Fig. 25. The activation energy, E^*, was obtained from the Arrhenius equation.

$$\log k_F = \log A - E^*/2.303\ RT$$

by plotting k_F against 1/T. These plots were fairly linear at 280 and 430 mμ, but wide deviations from linearity were observed at 460 mμ (Figs. 26, 27, and 28).

The activation values ΔS^*, ΔF^*, and K^* were calculated according to equations (7, 8, and 9; page 22). Values are found in Table VI. The frequency factor A was calculated from ΔS^*, using the equation

$$A = \frac{RT}{Nh}\ e^{\Delta S^*/R}$$

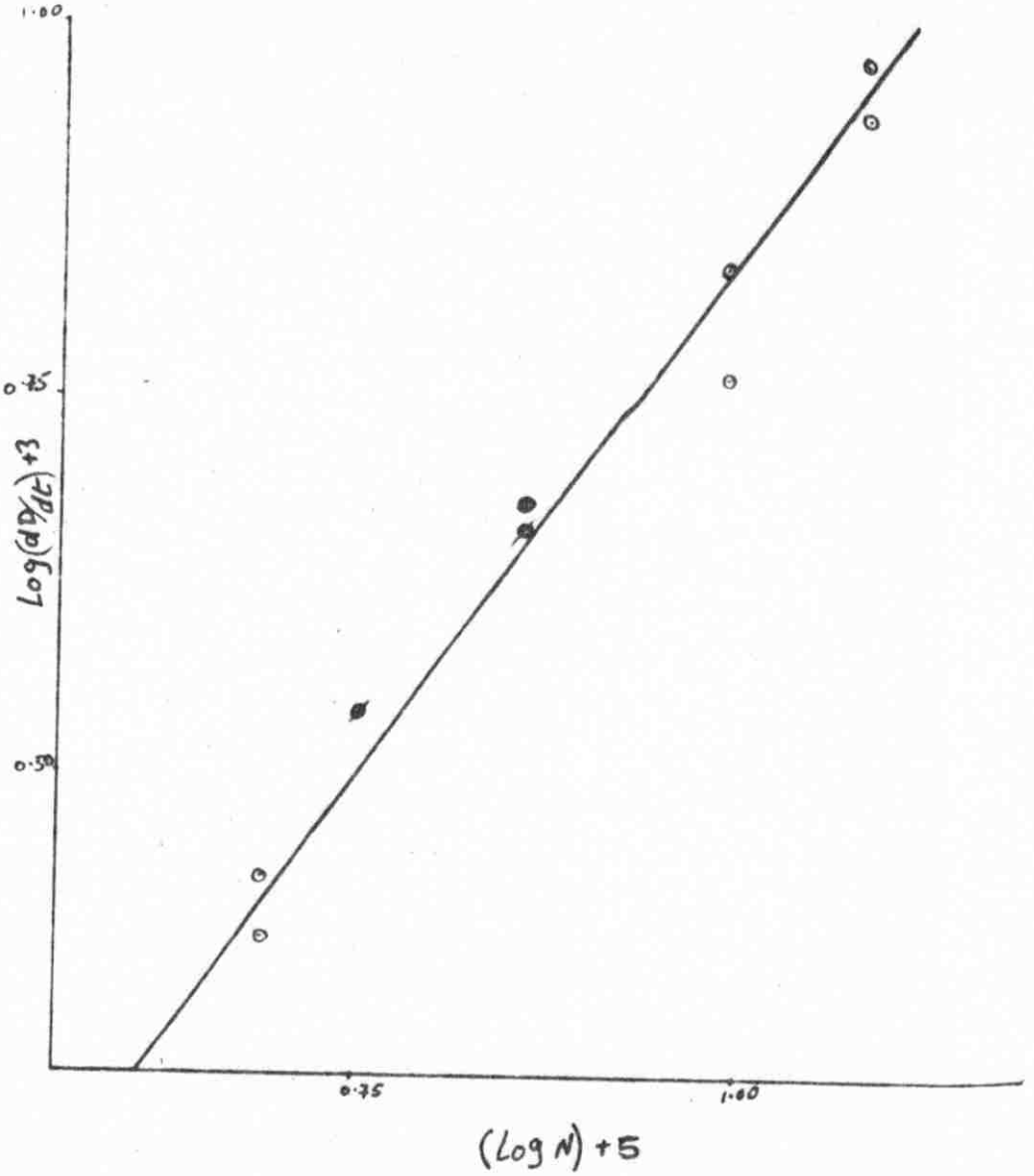

Fig. 24 - Plot of the logarithm of the initial rate against the logarithm of myoglobin concentration. Temperature of experiment = 71.0°C. (Mb) = 1.2×10^{-4} M to 4.9×10^{-5} M, wavelength = 460 mμ, pH = 6.87, I = 0.100.

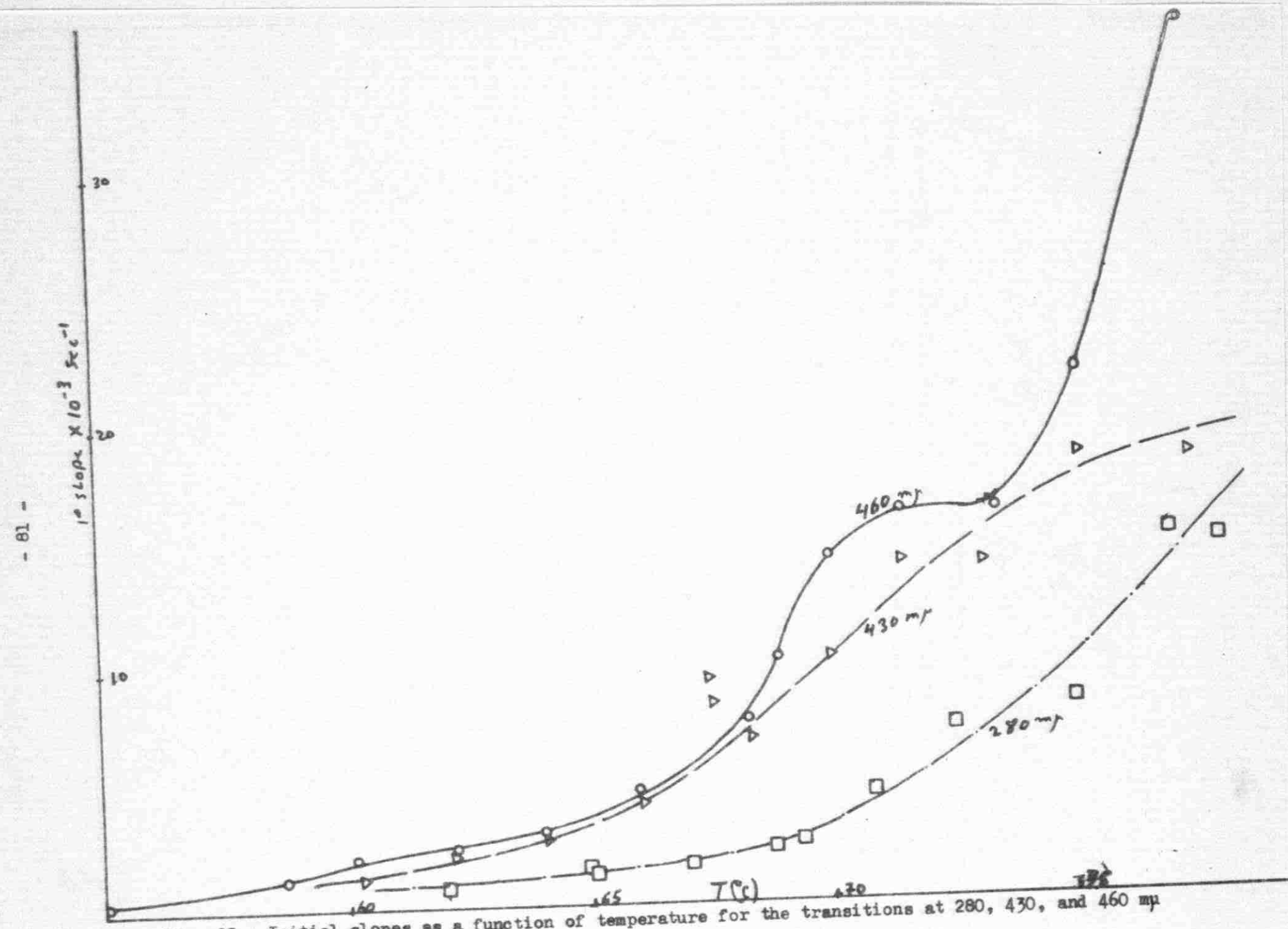

Fig. 25 - Initial slopes as a function of temperature for the transitions at 280, 430, and 460 mμ (c.f. Table V).

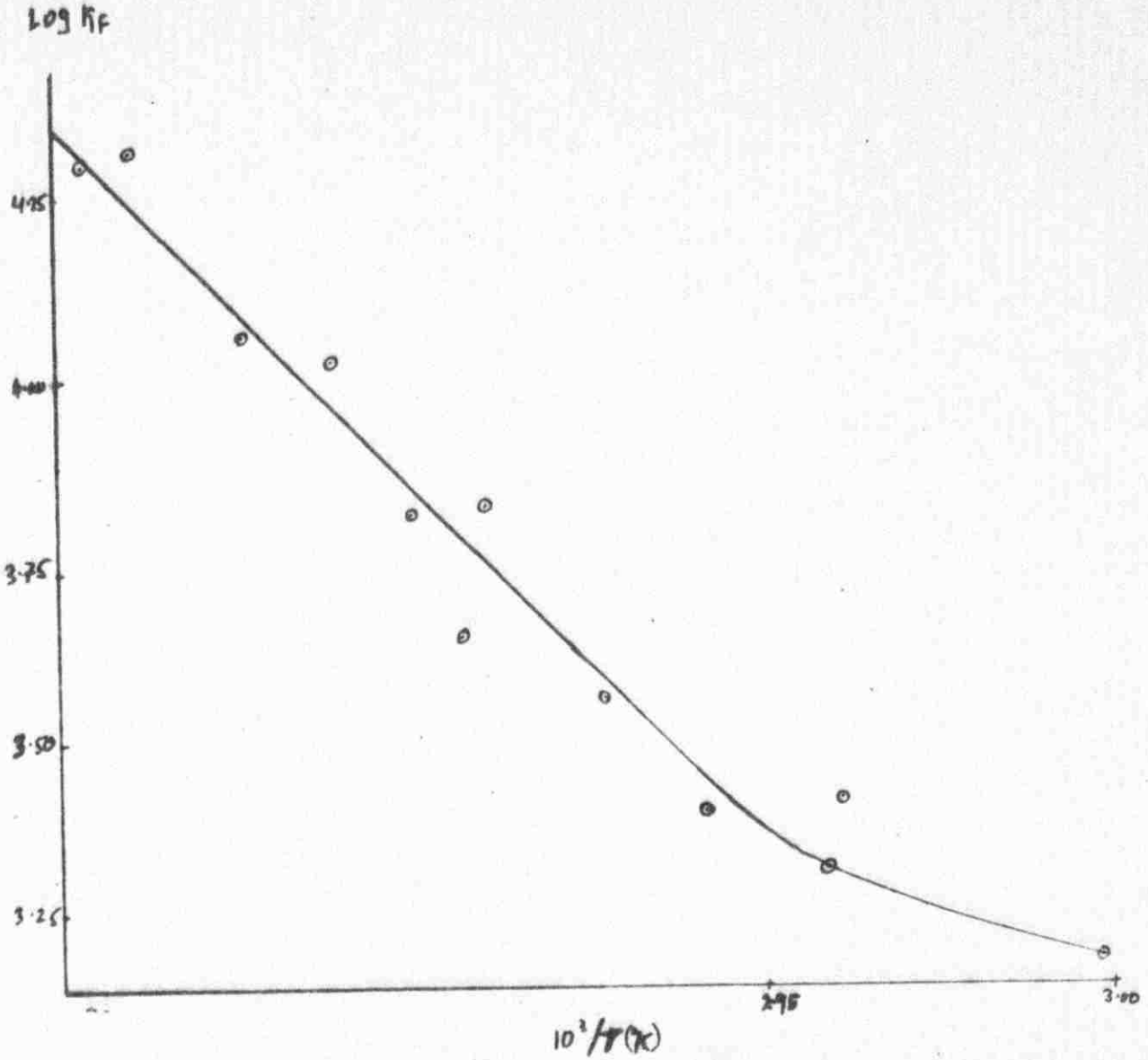

Fig. 26 - Plot of the logarithm of the forward rate constant, k_F, against the reciprocal of the absolute temperature for the transition at 280 mμ (c.f. Table Va).

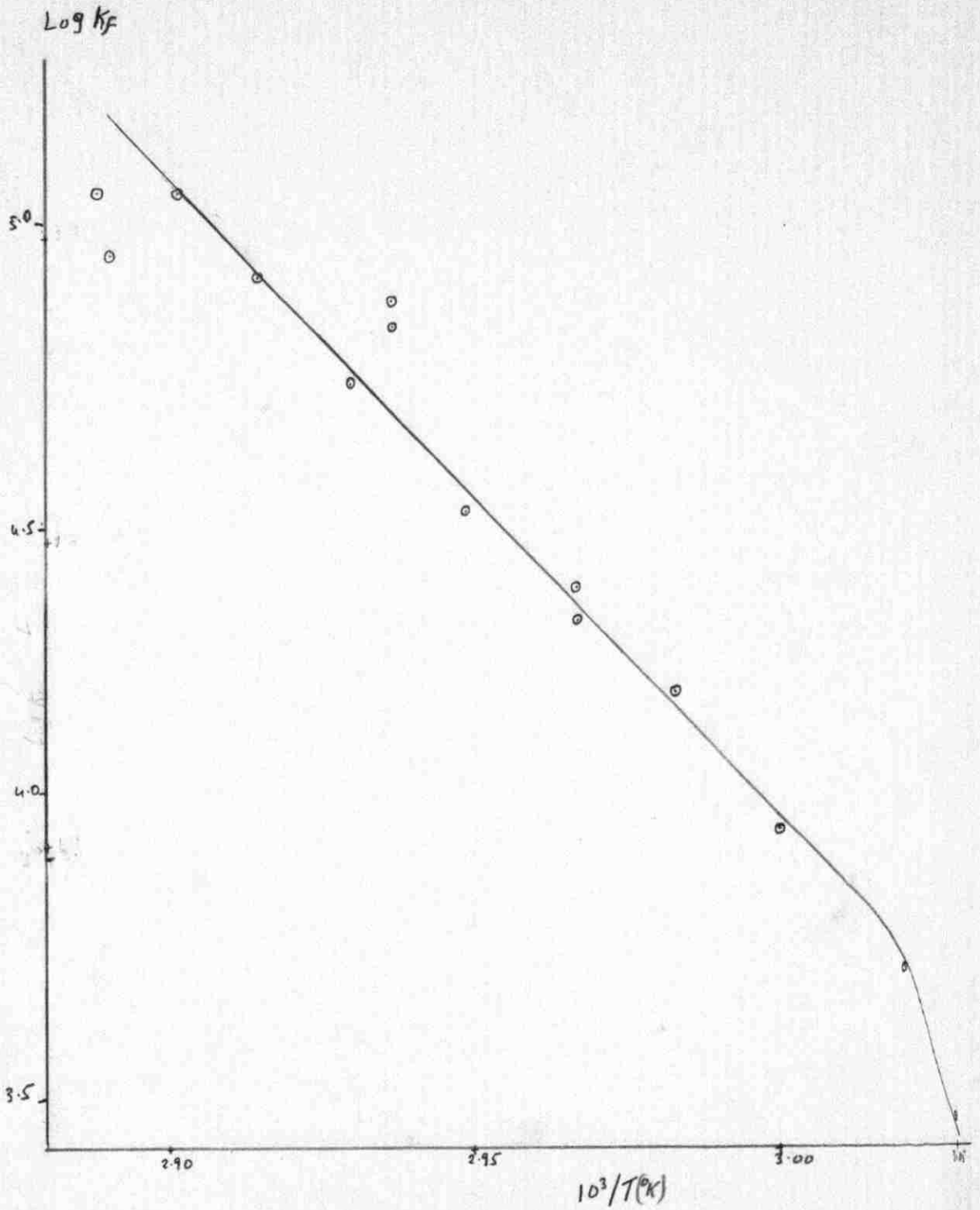

Fig. 27 - Plot of the logarithm of the forward rate constant, k_f, against the reciprocal of the absolute temperature for the transition at 430 mμ (c.f. Table Vb).

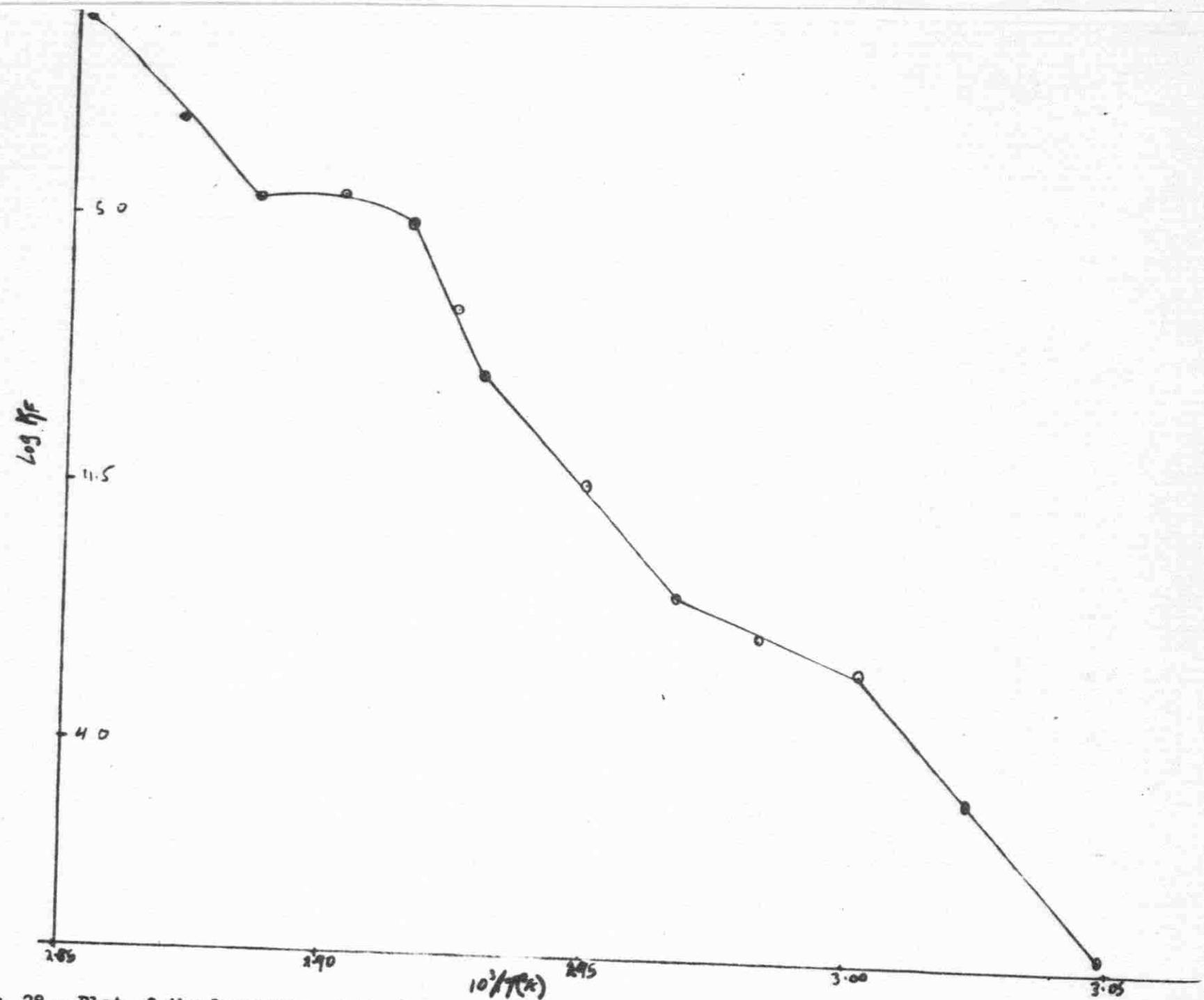

Fig. 28 - Plot of the logarithm of the forward rate constant, k_p, against the reciprocal of the absolute temperature for the transition at 460 mu (c.f. Table Vc).

TABLE V

KINETIC DATA

(for Arrhenius plot)

pH = 6.87

I = 0.100

Set a - λ = 280 mμ, (Mb) = 3.57×10^{-5} M.

T (°C.)	$10^3/T(^\circ K)$	Initial slope x 10^3 (sec^{-1})	k_F x 10^{-3} (sec^{-1})	log k_F
60.5	2.998	0.970	1.55	3.190
62.0	2.985	0.730	1.37	3.137
64.8	2.960	1.67	2.67	3.426
65.0	2.958	1.31	2.09	3.320
67.0	2.941	1.60	2.55	3.406
68.7	2.926	2.34	3.73	3.572
69.3	2.921	2.48	3.96	2.598
70.7	2.909	4.50	7.18	3.856
70.8	2.908	2.14	3.41	3.533
71.0	2.906	2.89	4.61	3.664
72.0	2.898	4.35	6.95	3.842
73.5	2.886	7.37	11.7	4.068
75.0	2.873	8.00	12.8	4.107
77.1	2.856	15.0	23.9	4.378
78.0	2.849	14.4	23.0	4.362

Table V ctd.

Set b - λ = 430 mμ , (Mb) = 1.17×10^{-4} M

T (°C.)	$10^3/T(^\circ K)$	Initial slope x 10^3 (sec^{-1})	$k_F \times 10^{-3}$ (sec^{-1})	log k_F
54.9	3.049	0.416	2.97	3.473
57.7	3.023	0.737	5.26	3.721
60.3	3.000	1.21	8.64	3.936
62.2	2.983	2.08	14.8	4.170
64.0	2.967	3.02	21.6	4.334
64.0	2.967	2.75	19.7	4.494
66.0	2.949	4.15	29.6	4.471
67.5	2.937	9.15	65.3	4.815
67.5	2.937	8.32	59.4	4.774
68.3	2.930	6.73	48.1	4.682
70.0	2.915	10.1	72.1	4.858
71.5	2.902	13.9	98.6	4.994
73.0	2.890	11.0	78.5	4.895
73.2	2.888	13.8	98.5	4.993
75.2	2.871	18.1	129	5.111
77.5	2.853	18.0	129	5.111

Table V ctd.

Set c - λ = 460 mμ , (Mb) = 1.17×10^{-4} M

T (°C.)	$10^3/T(^oK)$	Initial slope x 10^3 (sec^{-1})	$k_F \times 10^{-3}$ (sec^{-1})	log k_F
54.9	3.049	0.62	4.43	3.646
57.7	3.023	1.21	8.64	3.936
60.1	3.002	2.11	15.1	4.179
62.2	2.983	2.40	17.1	4.233
64.0	2.967	2.88	20.6	4.314
66.0	2.949	4.65	33.2	4.521
68.3	2.929	7.50	53.5	4.728
68.9	2.924	10.0	71.4	4.854
70.0	2.915	14.2	101	5.004
71.5	2.902	16.0	114	5.057
73.5	2.886	15.8	113	5.053
75.2	2.871	21.6	189	5.276
77.5	2.853	35.4	310	5.491

TABLE VI

ACTIVATION VALUES AT 280 AND 430 mμ

λ mμ	ΔH^* (Kcal/mole)	ΔS^* e.u.	ΔF^* (Kcal/mole)	A
280	45.6	17.4	39.8	6.9×10^{32}
430	48.0	20.6	41.2	3.5×10^{36}

The number of hydrogen bonds broken in the activation step (C $\rightarrow$ I transformation of Fig. 4) was calculated by using equation (15)

$$\Delta H^* = - \frac{n K_{ij}}{1 + K_{ij}} \Delta H^o_{ij}$$

making the assumption that the broken bonds are all equivalent and of the ij type. Arguments supporting a value of $K_{ij} = 4$ and $\Delta H_{ij} = 6$ Kcal/mole are given by Scheraga (1961). Inserting these values in the above equation leads to a value of 10 for n, the number of bonds broken in the activation step.

b) Thermodynamic Results: Plots of the equilibrium absorbance increments against temperature are shown in Fig. 29, 30 and 31, for the three wavelengths studied. Two transitions were observed at both 280 and 430 mμ and three transitions at 460 mμ. Below 50°C. the denaturation process is very slow and above 80°C precipitation sets in rapidly. Hence, equilibrium measurements were confined to the temperature range 50 - 80°C. A set of thermodynamic properties was calculated for each transition.

Considering that the native myoglobin molecule consists of eight helical and eight non-helical regions (page 12), and assuming the denatured state pertaining to the last transition to be perfectly coiled, one may write, in analogy to Flory's terminology (page 26)

$$H_8C_8 \xrightleftharpoons{K_1} H_nC_{(16-n)} \xrightleftharpoons{K_2} H_{(n-i)}C_{(16-n+i)} \xrightleftharpoons{K_3} C_{16}$$

for a sequence of three transitions. Accordingly, the equilibrium constants K_1, K_2 and K_3 for the first, second, and third transitions are given by

$$K_1 = \frac{H_nC_{(16-n)}}{H_8C_8} = \frac{\text{Coil}_1}{\text{Helix}_1} \qquad (41a)$$

$$K_2 = \frac{H_{n-i}C_{(16-n+i)}}{H_nC_{(16-n)}} = \frac{\text{Coil}_2}{\text{Helix}_2} \qquad (41b)$$

$$K_3 = \frac{C_{16}}{H_{(n-i)}C_{(16-n+i)}} = \frac{\text{Coil}_3}{\text{Helix}_3} \qquad (41c) .$$

Note that the coiled form for any transition corresponds to the helical form of the transition directly following it.

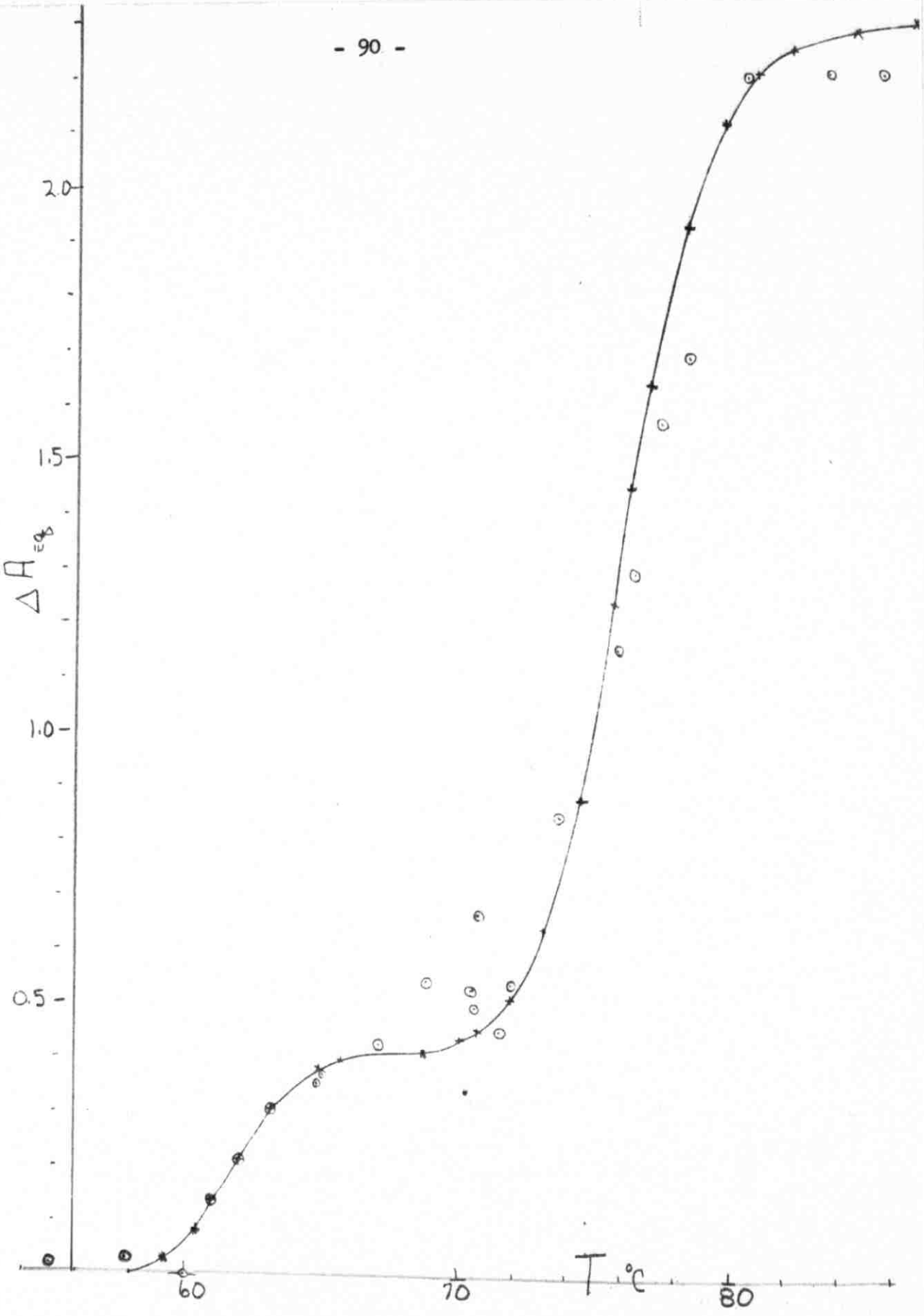

Fig. 29 - Equilibrium absorbance increments as a function of temperature at 280 mμ. ⊙ Experimental points × points obtained from the van't Hoff plot. (c.f. Table VIIa).

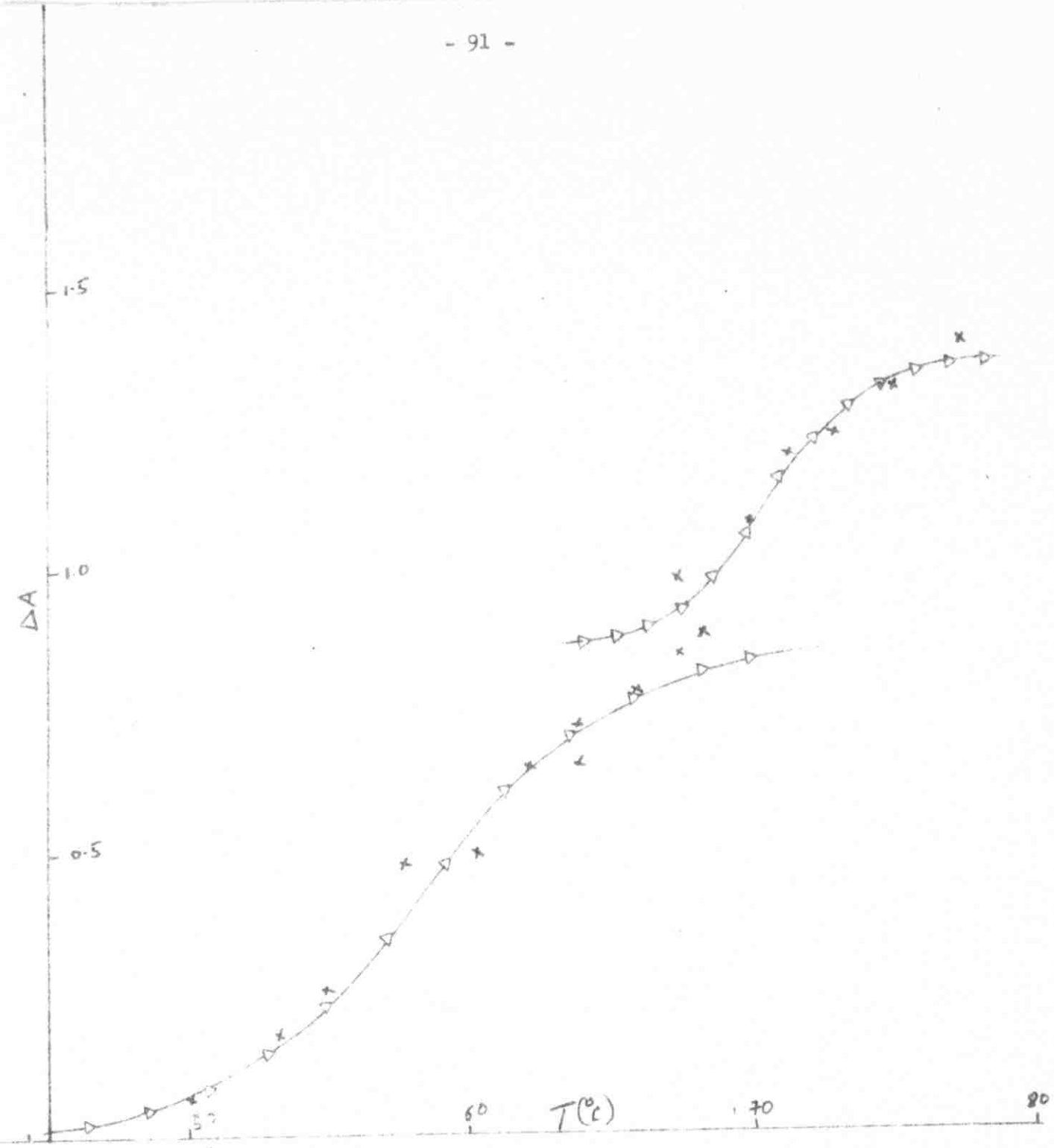

Fig. 30 - Equilibrium absorbance increments as a function of temperature at 430 mμ. × Experimental points O points obtained from the van't Hoff plot. (c.f. Table VIIb).

Fig. 31 - Equilibrium absorbance increments as a function of temperature at 460 mμ. ○ Experimental points × points obtained from the van't Hoff plot. (c.f. Table VIIc).

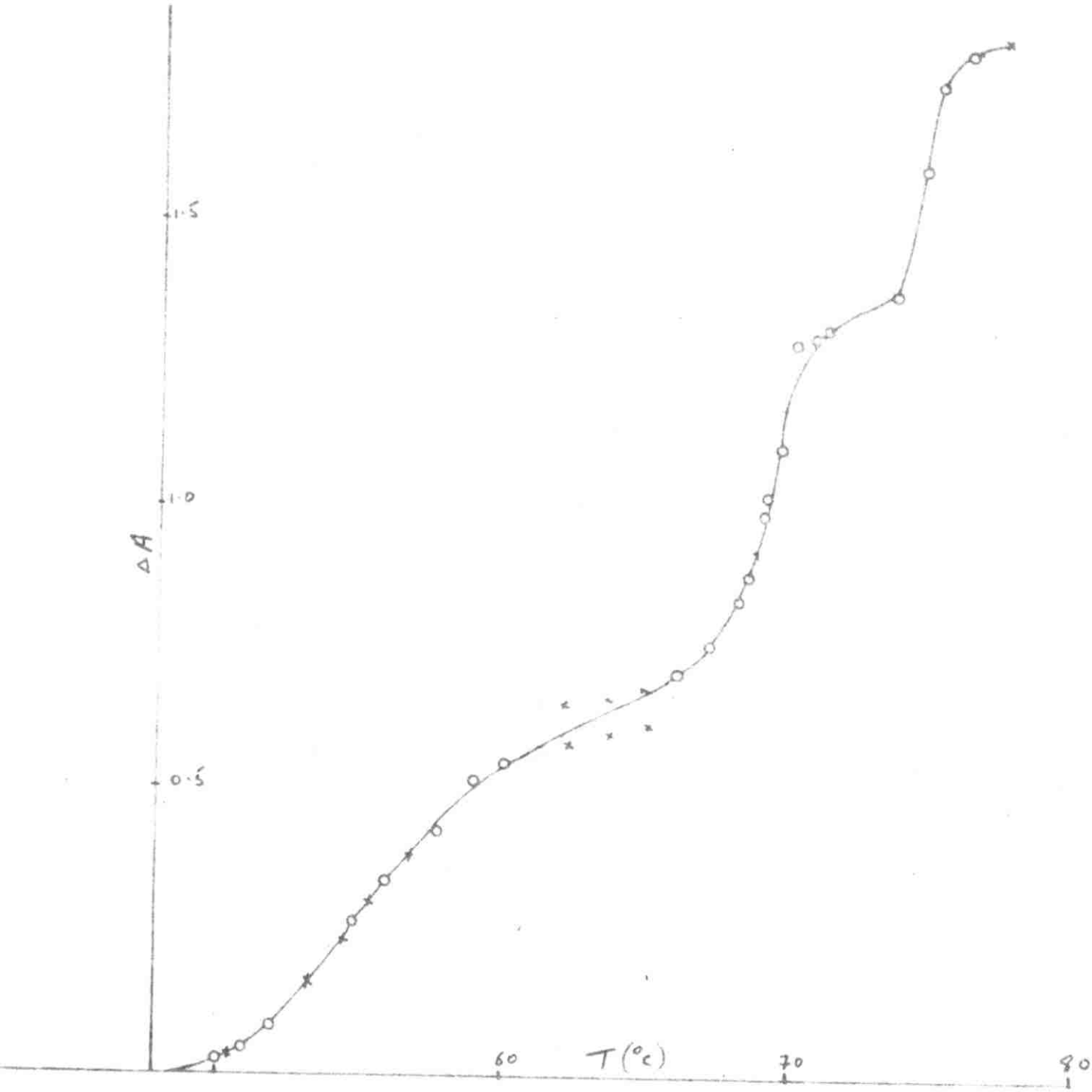

Fig. 31 - Equilibrium absorbance increments as a function of temperature at 460 mμ. o Experimental points x points obtained from the van't Hoff plot. (c.f. Table VIIc).

The above equilibrium constants were calculated from the observed ΔA values as follows: when $\Delta A = 0$ the molecule is in the native state and when ΔA becomes insensitive to temperature following the end of each transition, the molecule is in any one of the coiled states, $H_nC_{(6-n)}$, $H_{(n-i)}C_{(6-n+i)}$, etc. The equilibrium constants K_1, K_2 and K_3 are therefore given by

$$K_1 = \frac{\Delta A_{t_{(1)}}}{\Delta A_{t\alpha_{(1)}} - \Delta A_{t_{(1)}}} \qquad (42a)$$

$$K_2 = \frac{\Delta A_{t_{(2)}}}{\Delta A_{t\alpha_{(2)}} - \Delta A_{t_{(2)}}} \qquad (42b)$$

$$K_3 = \frac{\Delta A_{t_{(3)}}}{\Delta A_{t\alpha_{(3)}} - \Delta A_{t_{(3)}}} \qquad (42c)$$

where $\Delta A_{t_{(n)}}$ and $\Delta A_{t\alpha_{(n)}}$ are equilibrium absorbance increments for the nth transition at temperature t and at infinite temperature, respectively. ΔA and K values for the transitions at 280, 430 and 460 mμ are found in Table VII.

To treat each transition independently, all ΔA values of equation (42) were obtained by subtracting the sum of the corresponding values (at the same temperature) for the preceding transitions from the observed values. This may be illustrated as follows: (p. 97)

TABLE VII

THERMODYNAMIC DATA

(for van't Hoff plot)

pH = 6.87, I = 0.100

Set a - λ = 280 mμ , (Mb) = 3.57 x 10^{-5} M , A_{native} = 1.31

$T^{\circ}C$	$10^3/T^{\circ}A$	ΔA_{eq}(obs)	ΔA_{eq}(corr)	K = coil/helix	log K
50.0	3.095	0.000	0.000	0.000	--
55.0	3.048	0.020	0.020	0.0516	-1.287
57.9	3.022	0.030	0.030	0.0789	-1.103
61.0	2.994	0.135	0.135	0.491	-0.309
62.0	2.985	0.212	0.212	1.07	0.029
63.0	2.976	0.305	0.305	2.91	0.464
64.8	2.960	0.355	0.355	6.46	0.810
65.0	2.958	0.375	0.375	10.7	1.029
67.0	2.941	0.430	0.430	--	--
68.7	2.926	0.545	0.545	--	--
70.4	2.912	0.530	0.120	0.068	-1.170
70.5	2.911	0.560	0.090	0.050	-1.301
70.6	2.910	0.670	0.260	0.159	-0.799
70.7	2.909	0.455	0.045	0.024	-1.620
71.8	2.900	0.540	0.130	0.074	-1.131
73.5	2.886	0.850	0.410	0.277	-0.558
75.5	2.873	1.16	0.750	0.658	-0.182
76.1	2.864	1.30	0.990	1.10	0.041
77.0	2.857	1.58	1.17	1.62	0.210
78.0	2.849	1.70	1.59	5.30	0.724
80.0	2.832	2.22	1.81	22.6	1.354
83.0	2.848	2.27	1.86	60.3	1.780
85.0	2.793	2.30	1.89	--	--

Table VII ctd.

Set b - λ = 430 mμ , (Mb) = 1.17×10^{-4} M, $A_{native} = 0.935$

$T^{\circ}C$	$10^3/T^{\circ}A$	ΔA_{eq}(obs)	ΔA_{eq}(corr)	K = coil/helix	log K
50.0	3.095	0.068	0.068	0.085	-1.071
53.2	3.065	0.185	0.185	0.270	-0.569
54.9	3.049	0.255	0.255	0.415	-0.382
57.7	3.023	0.480	0.480	1.23	0.090
60.3	3.000	0.500	0.500	1.35	0.130
62.2	2.983	0.650	0.650	2.95	0.470
64.0	2.967	0.730	0.730	5.21	0.717
64.0	2.967	0.680	0.680	3.58	0.554
66.0	2.949	0.780	0.780	8.67	0.938
68.2	2.930	0.814	0.814	14.4	1.158
68.3	2.930	0.880	0.020	0.042	-1.768
70.0	2.915	1.08	0.220	0.786	-0.105
71.5	2.902	1.20	0.340	2.12	0.326
73.0	2.890	1.23	0.375	3.00	0.477
73.2	2.888	1.25	0.390	3.55	0.550
75.2	2.871	1.32	0.460	11.5	1.067
77.5	2.853	1.40	0.540	--	--
78.4	2.845	1.36	0.052	89.1	1.949

Table VII ctd.

Set c - λ = 460 mμ , (Mb) = 1.17×10^{-4} M, A_{native} = 2.99

T^0C	$10^3/T^0A$	ΔA_{eq}(obs)	ΔA_{eq}(corr)	K = coil/helix	log K
50.0	3.095	0.030	0.030	0.053	-1.276
51.0	3.086	0.045	0.045	0.081	-1.090
52.0	3.076	0.086	0.086	0.166	-0.780
54.9	3.049	0.270	0.270	0.819	-0.087
56.0	3.039	0.339	0.339	1.31	0.117
57.7	3.023	0.430	0.430	2.53	0.403
59.0	3.012	0.520	0.520	6.50	0.813
60.1	3.002	0.550	0.550	11.2	1.045
62.2	2.983	0.630	--	--	- --
64.0	2.967	0.630	--	--	--
66.0	2.949	0.710	0.110	0.172	-0.765
67.0	2.941	0.760	0.160	0.265	-0.577
68.0	2.932	0.840	0.240	0.490	-0.310
68.3	2.930	0.880	0.310	0.699	-0.156
68.9	2.925	0.990	0.390	0.964	-0.016
69.0	2.923	1.02	0.420	1.47	0.168
69.5	2.920	1.11	0.508	3.17	0.500
70.0	2.915	1.29	0.668	10.0	1.000
70.6	2.910	1.30	0.702	31.6	1.500
71.0	2.906	1.31	0.715	35.7	1.553
73.0	2.890	1.36	--	--	---
73.5	2.886	1.38	0.025	0.048	-1.314
74.0	2.881	1.45	0.120	0.304	-0.517
74.5	2.877	1.60	0.265	0.757	-0.121
75.0	2.873	1.75	0.415	4.15	0.618
75.2	2.871	1.82	0.485	16.2	1.209
75.5	2.869	1.83	0.495	24.7	1.393

$$\Delta A_{t_{(n)}} = \left(\Delta A_{t_{(n)}}\right)_{obs} - \sum_{1}^{n-1} \Delta A_{t_{(n-1)}} \qquad (43a)$$

and

$$\Delta A_{t\alpha_{(n)}} = \left(\Delta A_{t\alpha_{(n)}}\right)_{obs} - \sum_{1}^{n-1} \Delta A_{t\alpha_{(n-1)}} \qquad (43b)$$

Plots of the logarithm of the equilibrium constant against the reciprocal of the absolute temperature (van't Hoff plots) were fairly linear and yielded enthalpy values from the slopes (Fig. 32). Using these plots the symmetry of the ΔA vs. temperature curves (Figs. 29 - 31) were improved by calculating ΔA values from the equilibrium constants. Entropy values were obtained by using equation (26). The transition temperatures were taken as those of half conversion, i.e. $K = 1$ or α of equation (36) $= \frac{1}{2}$. At the transition temperature $\Delta F = 0$. The sharpness of the transition was calculated from equation (37) by equating $\left[(n-4)\ \Delta H^{0}_{res} + \Delta H^{0}_{h}\right]$ to $(\Delta H)_{obs}$. Values for the enthalpy, transition temperature, and sharpness of the transition are found in Table VIII.

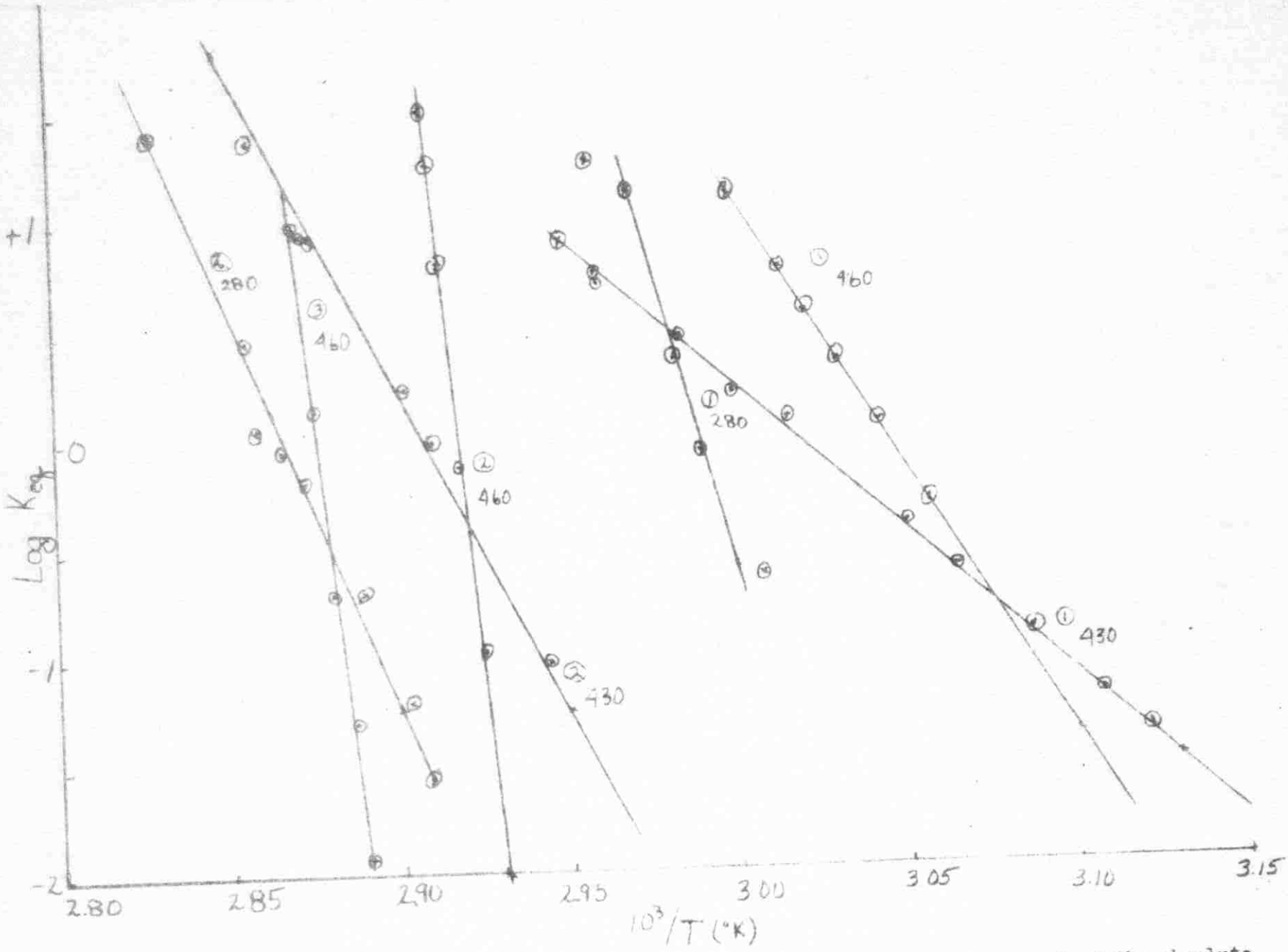

Fig. 32 - Plots of the logarithm of the equilibrium constant against the reciprocal of the absolute temperature. Wavelengths (mu) and the numbersof the transition steps are indicated. (c.f. Table VIII)

TABLE VIII

THERMODYNAMIC VALUES

at 280, 430 and 460 mμ

λ mμ	Step	ΔH Kcal/mole	ΔS e.u.	T_{tr} (°C)	$\left(\frac{d\alpha}{dt}\right)^{\neq}_{T_{tr}}$
280	1	197	588	61.8	0.222
	2	172	493	75.5	0.179
430	1	61.2	183	58.4	0.062
	2	139	405	70.7	0.148
460	1	114	347	55.4	0.133
	2	456	1330	68.8	0.493
	3	684	1970	74.4	0.715

Sharpness parameter

$\neq$ see equation (37) page 37

CHAPTER V

DISCUSSION

A. Spectral Changes

No alterations were observed in the spectrum of native myoglobin after heating to temperatures below 50°C then re-equilibrating at 25°C (Section A, 1). Two possibilities present themselves to interpret this behaviour (a) myoglobin solutions can withstand prolonged heating below 50°C. (b) some completely reversible changes have taken place. Evidence in favour of the second alternative is furnished by measurements at the elevated temperature (Section B). These measurements indicated small increments in absorbance below 50°C, for example 6 - 15% at 47°C.

With temperatures above 50°C, profound spectral changes take place. Their magnitude is a function of temperature, period of heating and the wavelength region studied. That complete reversibility is not achieved after equilibration at 25°C is probably due to the following factors:

a) The entropy of the denatured state is larger by several hundred entropy units (Table VIII) than that of the native state. The process of crossing the activation barrier in the reverse direction is of high steric requirements and is therefore improbable.

b) Whereas the process of heating results in the rupture of hydrogen and hydrophobic bonds, the process of cooling leaves many sites

on the myoglobin molecule with unsatisfied potential. As a result, bond formation begins to take place between these sites, intermolecularly as well as intramolecularly, leading to the formation of short helical segments interspersed within huge molecular species. A reverse transition is extremely improbable in such a system.

The small blue shift observed at 280 mμ may be attributed to perturbations of the chromophoric groups (3 tyrosine and 2 tryptophane residues) which result from changes in environment. These perturbations may originate from any, or from a combination of, the following factors:

a) The chromophores are brought from a medium of high refractive index (the interior hydrophobic region of myoglobin) to a medium of low refractive index (the exterior polar environment).

b) The rupture of tyrosyl-carboxylate hydrogen bonds. This was suggested by Leach and Scheraga (1960) to account for the blue shift in the denaturation of ribonuclease.

c) Interaction of the phosphate ion of the buffer with the pi electron system of the aromatic rings.

The small blue shift at 630 mμ, due to perturbations in the absorption of the heme chromophore is probably due to factor (a) above, together with the destruction of hydrophobic bonds and the modification of pi electron interactions between the side-chains of the porphorin ring and the hydrophobic groups in the interior of the molecule.

The optical density changes are much more profound than can be attributed solely to environmental changes. They are mainly due to the liberation of chromophoric groups that were masked in the interior of

the native molecule. The peak at 240 mu in the difference spectrum is due to increments in the peptide bond absorption. At 260 mμ, the absorption maximum of phenylalanine, the optical density of the denatured species at $\sim 70^{\circ}C$ is nearly double that of the native species (Tables II & IV). If the process of denaturation is taken to be complete at this temperature it may be concluded that, of the six phenylalanine residues, three are buried in the molecule and three are exposed on the surface. The changes in the absorption of the heme group vary from nearly 0% at 409 mμ to 350% at 650 mμ (Fig. 22). The large magnitude of these changes suggests that the heme group comes nearer to the surface as the molecule unfolds and that the location of heme in the native molecule severely diminishes its normal extinction. The variation in the magnitude of these changes with wavelength implies that the participating chromophores are embedded to different extents within the native molecule.

B. Kinetic Behaviour

The first two steps at 280 mu and the first step at 240 mμ (p. 77), being too fast to be followed by our instrument, are probably due to instantaneous re-equilibration of the system to meet the thermal stress. The first step at 280 mμ, involving a small increase in absorbance, is possibly due to the melting of icebergs (p. 18) in the vicinity of the exterior tyrosine and tryptophane residues, thereby causing them to absorb more freely. Another possibility is that these outer residues are distributed over a range of conformations in the native state and

that thermal perturbation of the system changes this distribution, thereby modifying their environment and consequently their absorptive behaviour.

The observed transition order of 1.39 with respect to myoglobin concentration suggests that the process is essentially unimolecular but that moderately strong intermolecular forces operate between the myoglobin molecules.

The initial rate with respect to time indicated a zero order transition. This suggests that certain species of very minute concentrations are rate determining. These may be hydrogen ions, phosphate ions of the buffer, or impurities in the protein. The variation of the transition order with time and temperature leads one to conclude that the general transition is the sum of several processes, which may be in the forward or reverse direction. Furthermore, these processes should have different activation energies and therefore several transition paths. It is also possible that these paths lead to different denatured states so that the emperical rate equation may be written in the form

$$\frac{dC_N}{dt} = -\sum_i \frac{dC_D}{dt} = \frac{kT}{h} \sum_i K_i C_i^* \qquad (44)$$

in which K_i is the transmission coefficient for the ith path, this equation is of a form analogous to equation (10).

The temperature dependences of the rate constants for the transitions at 280 and 430 mμ are in fair agreement with the Arrhenius law. However,

the transitions as followed at 460 mμ do not obey this law. This anomalous behaviour may be accounted for in three ways:

1) If several simultaneous processes produce the same product, the Arrhenius plots are not expected to be linear, either as the result of different activation energies or changes in the distribution of species with temperature.

2) Flory's treatment of the gambler's ruin problem (pp. 26 - 29) predicts that in the vicinity of the transition temperature the rate is dominated by ΔT of equation (19) and not by the rate constant. The rapid decrease in rate with lower temperatures is simply a reflection of the term $\left(1 - \frac{1}{r}\right)$ of equation (18) which gives the probability that a succession of steps would ultimately lead to complete denaturation.

3) If it is assumed that hydrogen bonds as well as hydrophobic bonds participate in the activation process, then the rate constant, k_F, is expected either to decrease or increase with increasing temperature. This is because hydrogen bonds tend to weaken but hydrophobic bonds to become stronger with increasing temperature (p. 17).

The entropies of activation for the transitions at 280 and 430 mμ, as calculated from the Arrhenius plots, were 17.4 and 20.6 e.u., respectively. These values are less than the observed net entropy values (Table VIII) by a factor of a few tens. This result is consistent with the model for thermal denaturation shown in Fig. 4, which requires that the activated state be somewhat more relaxed than the native state due to the rupture of a few side-chain hydrogen bonds (10 bonds in our experiments - see p. 88). It further requires that the denatured state

be one of maximum liberational entropy, due to the collapse of the helical arrangements, and hence considerably more relaxed than either Fors C or I. If the thermal transition were to involve an activated state of ruptured backbone hydrogen bonds but inact side-chain hydrogen bonds, then the expected entropy of activation should be about ten times the magnitude of that observed.

C. Thermodynamic Behaviour

We now wish to estimate a few thermodynamic parameters for the unfolding of each of the eight helical units in myoglobin to an isotropic random coil, in the absence of side-chain interactions, cooperation between helices, and other stabilizing factors. Comparison of the values obtained in this manner with the experimental values should yield a qualitative estimate of the degree of mutual stabilization and cooperation within the native molecule.

The net free energy of unfolding, ΔF^{0}_{unf}, of equation (35) will therefore be taken as the free energy for unfolding of the backbone hydrogen bonds, ΔF^{0}_{b}, all other terms being neglected. Substituting this result in equation (28) and solving for T, one obtains

$$T = \frac{(n-4)\ \Delta H^{0}_{res} - \Delta F^{0}_{b}}{(n-1)\ \Delta S^{0}_{res}} \qquad (45)$$

Since no covalent cross-links are known to exist in myoglobin ΔS^{0}_{res} should receive no contribution from ΔS^{0}_{x} of equation (29). Furthermore since the assumption of isotropy is made, the contribution of

ΔS^0_{el} of equation (30) to ΔS^0_{res} will be neglected. At the transition temperature $\Delta F^0_b = 0$ and equation (44) becomes

$$T_{tr} = \frac{(n-4)\ \Delta H^0_{res}}{(n-1)\ \Delta S^0_{res}} \qquad (46)$$

The value of ΔH^0_{res} adopted is 1500 cal/mole (Schellman, 1955) and ΔS^0_{res} will be taken as 4 e.u. (Loeb and Scheraga, 1962). Transition temperatures calculated on the basis of the above assumptions are given in Table IX.

To calculate sharpness parameters (p. 37) from the transition temperatures, the term ΔH^0_h of equation (37) (due to side-chain hydrogen bonds) will be dropped. Equation (37) becomes

$$\left(\frac{d\alpha}{dt}\right)_{T_{tr}} = \frac{(n-4)\ \Delta H^0_{res}}{4RT^2_{tr}} \qquad (47)$$

The calculated values are presented in Table IX.

The theoretical transition temperatures for helices D, E_1, E_2, and F require that these helices be intrinsically unstable. Helices A and B are expected to have marginal stability at room temperature. Only helices G and H, which contain the largest number of aminoacid residues, are expected to possess some degree of stability to heat. However, the experimentally determined transition temperatures (Table VIII) are much higher than the theoretical values. This suggests that mutual stabilization between the helices is the dominant factor in preserving the native conformation. That these helices do not behave

TABLE IX

THEORETICAL TRANSITION PARAMETERS

Helix in Myoglobin	n	T_{tr} (°C)	$(d\alpha/dt)_{T_{tr}}$
A	16	27	0.025
B	16	27	0.025
D	7	-86	0.016
E_1	10	-22	0.018
E_2	10	-22	0.018
F	9	-39	0.017
G	19	39	0.029
H	24	53	0.035

as a single unit can be shown by calculating the theoretical transition temperature from equation (45) for a helix of 111 aminoacid residues (the sum of the residues in the eight helical units). This calculation leads to $T_{tr} = 92^{\circ}C$, which is significantly higher than any of the experimental values.

The theoretical sharpness parameters are less than the experimental values of Table VIII by a factor of 10. Even for the hypothetical helix of 111 aminoacid residues, the theoretical sharpness of 0.150, as calculated from equation (47), is less than most of the experimental values. This suggests that the term ΔH_h^0 in equation (37) is of considerable influence in determining the sharpness and must therefore be duly considered. Since this term refers to the standard enthalpy of formation of side-chain hydrogen bonds it is again shown that the bonds exert a considerable influence in maintaining the helical native configuration. Another factor which probably contributes to increasing the sharpness in the decrease in the dielectric constant of water with increasing temperature ($D^{20^0} = 80$; $D^{100^0} = 48$). Since the internal hydrophobic environment of myoglobin is of high dielectric constant, a gradient of this type would be built up between the solvent and the inside of the molecule as the temperature is increased. To diminish the extent of this gradient, the molecule would tend to unfold, thereby bringing the hydrophobic groups into contact with water.

In spite of the fact that helices D, E_1, E_2 and F are of the lowest stability in the independent states (as compared to helices A, B, G and H), it would be too hazardous to conclude that these cooperatively

participate in the first transition. This is because their actual stability in the molecule, due to steric requirements and stabilizing forces might be larger than those of the apparently stronger helices which lie near the extremities and are, in this sense, more susceptible to attack. In the absence of further experimental evidence, it would be difficult to attribute a particular transition to the breakdown of specific helical segments.

We now turn to examine the experimental entropy values and compare them with theoretical values calculated on the assumption of isotropy and independence of helices. Examination of Table VIII reveals that the net entropy change varies between 588 and 3650 e.u. These values indicate a large degree of randomness in the denatured state or, alternately, a very highly ordered native state. If, again, a value of 4 e.u. is taken for ΔS^{0}_{res}, then the expected net entropy change would be 111 x 4 = 444 e.u., much less than the average net values determined experimentally. This calculation leads to the conclusion that the degree of order in the native state is considerably hight than what would be expected if there were no forces to hold the helices in rigid positions relative to each other. The importance of side-chain hydrogen bonds in preserving the configuration of the native molecule is thus again demonstrated. It must be noted that hydrophobic bonds tend to decrease the entropy of the denatured state. This is because, in the process of unfolding, the interior hydrophobic environment of myoglobin comes into contact with the aqueous solvent, thereby leading to a net decrease of $\sim$ 20 e.u. per bond (see page 18). This effect, in addition to increasing the sharpness

of the transition, suggests that the contribution of side-chain hydrogen bonding to the ordered state is even more than that would be expected from calculations based on experimental values.

LIST OF REFERENCES

BLOCK, E.W. (1956), "Order-Disorder Phenomena", John Wiley and Sons Inc., N.Y.

BOEDTKER, H. and DOTY, P. (1956), J. Am. Chem. Soc., 78, 4267.

BRAUNITZER, G., HILSE, K., RUDOLFF, V., and HILSCHMANN, N. (1964). Adv. Protein Chem. 19, 1.

BRESLOW, E., and GURD, F.R.N. (1962), J. Biol. Chem. 237 (2), 371

BUZZEL, A., and STURTEVANT, J. M., (1951), J. Am. Chem. Soc., 73, 2454.

BUZZEL, A., and STURTEVANT, J. M., (1952), J. Am. Chem. Soc., 74, 1983.

COLVIN, J. (1953), Arch. Biochem. and Biophys., 46, 385.

CONN, J.B., GREGG, D.C., KISTIAKOWSKY, G.B., and ROBERTS, R.M., (1940), J. Am. Chem. Soc., 63, 2080.

CRICK, F.H.C., and KENDREW, J.C. (1957), Adv. Protein Chem., 12, 169.

DECHEV, G., (1961), Izvest. Inst. Biol., 11, 67, C.A. 22406i, 55 (1961).

EDMUNDSON, A.B., (1965), Nature, 205, 883.

Elliot, D.F., Biochem. J., (1952), 50, 542.

EVANS, M.G., and GEGLEY, J., (1949), Biochim. et Biophys. Acta, 3, 188.

FLORY, P.J., (1956), Science, 124, 53.

FLORY, P.J., (1961), J. Polymer Sci., 49, 105.

FOSS, J.G., and SCHELLMAN, J.A., (1959), J. Phys. Chem. 63, 2007.

FOSS, J.G., (1961), Biochim. et Biophys. Acta, 47, 569.

FRANK, H.S., and EVANS, M.W., (1945), J. Chem. Phys., 13, 507.

FRANK, H.S., and WEN, W.Y., (1957), Discussions Faraday Soc., 24, 133.

FRENSDORFF, H.K., WATSON, M.J., and KAUZMANN, W., (1953), J. Am. Chem. Soc. 75, 5157, 5167.

GIBBS, R.G., BIER, M., and NORD, F.F. (1952). Arch. Biochem. and Biophys., 35, 216.

HANANIA, G.I.H., YEGHIAYAN, A., and CAMERON, B.F., (1965), Biochem. J., 98, 189.

HARRISON, S.C., and BLOUT, E.R., (1965), J. Biol. Chem. 240(1), 299.

HARTMAN, K.A., Jr., (1966), J. Phys. Chem., 70, 270.

HAUROWITZ, F., DiMOIA, F., and TEKMAN, S., (1952), J. Am. Chem. Soc., 74, 2265.

HERMANS, J., Jr., and SCHERAGA, H.A., (1961), J. Am. Chem. Soc., 83, 3283.

HILL, T.L., (1959), J. Chem. Phys., 30, 383.

KAUZMANN, W., and SIMPSON, R.B., (1953), J. Am. Chem. Soc., 75, 5154.

KAUZMANN, W., (1954), In "the Mechanism of Enzyme Action" (W.D. McELORY and B. GLASS, eds.), John Hopkins Univ. Press, Baltimore, Maryland, p. 70.

KAUZMANN, W., (1959), Adv. Protein Chem., 14, 1.

KENDREW, J.C., BADO, G., DINTZIS, H.M., PARRISH, R., and WYCKOFF, H. (1958), Nature, 181, 662.

KENDREW, J.C., DICKERSON, R.E., STRANDBERG, B.E., HART, R.E., and DAVIES, D.R. (1960), Nature, 185, 422.

KENDREW, J.C., WATSON, H.C., STRANDBERG, B.E., DICKERSON, R.E., PHILLIPS, D.C., and SHORE, V.C., (1961), Nature, 190, 666.

KISTIAKOWSKY, G.B., CONN, J.B., and ROBERTS, R.M., (1940), J. Am. Chem. Soc., 62, 1895.

KLOTZ, I.M., (1946), J. Am. Chem. Soc., 68, 2299.

KLOTZ, I.M., (1958), Science, 128, 815.

KLOTZ, I.M., (1960), In "Protein structure and Function", Biol. Dept., Brookhaven National Laboratory, N.Y., p. 25.

LAIDLER, K.J., (1951), J. Am. Chem. Soc., 73, 1455.

LAIDLER, K.J., (1951), Arch. Biochem. and Biophys., 30, 226.

LASKOWSKI, M., Jr., and SCHERAGA, H.A., (1954), J. Am. Chem. Soc., 76, 6305.

LASKOWSKI, M., Jr., and SCHERAGA, H.A., (1956), J. Am. Chem. Soc., 78, 5793

LASKOWSKI, M., Jr., and SCHERAGA, H.A., (1961), J. Am. Chem. Soc., 83, 226.

LEACH, S.J., and SCHERAGA, H.A., (1960), J. Am. Chem. Soc., 82, 4790.

LEVY, M., and BENGALIA, A.E., (1950), J. Biol. Chem., 186, 829.

LINDERSTRØM-LANG, K., (1952), In "Lane Medical Lectures: Proteins and Enzymes", p. 58. Stanford Univ. Press, Standord, California., cited by Kauzmann (1959).

LOEB, G., and SCHERAGA, H.A., (1961), J. Phys. Chem., 64, 134.

LUMRY, R., and EYRING, H., (1954), J. Am. Chem. Soc., 58, 110.

McLAREN, A.D., and PEARSON, S., (1949), J. Polymer Sci., 4, 45.

McMULLAN, R., and JEFREY, G.A., (1959). J. Chem. Phys., 31/1231.

MICHAELSON, A.M., (1958), Nature, 182, 1502.

NEURATH, H., GREENSTEIN, J.P., PUTNAM, F.W., and ERICKSON, J.O., (1944), Chem. Revs., 34, 157.

PAULING, L. (1960), "The Nature of the Chemical Bond", 3rd ed., Cornell Univ. Press, Ithaca, N.Y., p. 500

PEIFFER, S., and LEONIS, J., (1965), Arch. Inter. Physiol. Biochim. 73, 152.

PELLER, L., (1959a), J. Phys. Chem., 63, 1194.

PELLER, L., (1959b), J. Phys. Chem., 63, 1199.

PUTNAM, F.W., (1953), In "The Proteins", (H. Neurath and K. Bailey, eds.), Vol. I, pt. B, p. 807, Academic Press, N.Y.

RIBEIRO, L., and VILLELA, G.G., (1957), Rev. Braz. Biol., 17, 291, cited by C.A. 52, 4769^{e} (1958).

RICH, A., and CRICK, F.H.C., (1955), Nature, 176, 593.

ROSSINI, F.D., (1952), "Selected Values of Chemical Thermodynamic Properties", National Bureau of Standards, Washington, D.C., cited by Kauzmann (1959).

SCHELLMAN, J., SIMPSON, R.B., and KAUZMANN, W., (1953), J. Am. Chem. Soc., 75, 5152.

SCHELLMAN, J., (1955a), Compt. rend. trav. lab. Carlsberg Ser Chim. 29, 233, cited by Scheraga (1961a).

SCHELLMAN, J., (1955b), Compt. rend. trav. lab. Carlsberg ser Chim. 29, 230, cited by Kauzmann (1959).

SCHERAGA, H.A., (1960), J. Phys. Chem., 64, 1917.

SCHERAGA, H.A., (1961a), "Protein Structure", Academic Press, N.Y.

SCHERAGA, H.A., (1961b), J. Phys. Chem., 65, 699.

SCOTT, R.A., and SCHERAGA, H.A., (1963), J. Phys. Chem., 85, 3866.

SIMPSON, R.B., and KAUZMANN, W., (1953), J. Am. Chem. Soc., 75, 5139.

STEIM, J., (1965), Arch. Biochem. and Biophys., 112, 599.

STEINHARDT, J., and ZAISER, E.M., (1955), Adv. Protein Chem., 10, 152.

STURTEVANT, J.M., (1954), J. Am. Chem. Soc., 58, 97.

TANFORD, C., and WAGNER, M.C., (1954), J. Am. Chem. Soc., 76, 3331.

UPENSKY, J.V., "Introduction to Mathematical Probability", McGraw-Hill, N.Y., 1937, Chapter 8, cited by Flory (1961).

WETLAUFER, D.B., (1962), Advances in Protein Chem., 17, 304.

ZIMM, B.H., and BRAGG, J.K., (1958), J. Chem. Phys., 28, 1246.

ZIMM, B.H., and BRAGG, J.K., (1959), J. Chem. Phys., 31, 526.